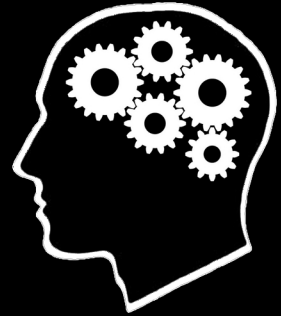


Proceedings of the Master's Programme

COGNITIVE NEUROSCIENCE



Volume 7, Issue 2, July 2012



Table of Contents

Editorials	2
<i>Tom Gijsels</i> Time in the Brain: Neural Evidence for a Space-Time Asymmetry	5
<i>Thomas Gräfnitz</i> Acoustic and Behavioral Modulations of Local Field Potentials in Monkey Auditory Cortex	21
<i>Denise Janssen</i> Neural Underpinnings of Feedback Processing in Toddlers	40
<i>Cătălina Rățală</i> The Social Learning of Trust	52
<i>Anne Rijpma</i> Sex Differences in Synaptic Density and Neurogenesis in Middle-Aged Apolipoprotein E4 and Apolipoprotein E Knockout Mice	64
<i>Rocio Silva Zunino</i> Preverbal Infants' Use of Others' Communicative Signals Depends on Culture	76
Abstracts	87
Institutes associated with the Master's Programme in Cognitive Neuroscience	89

From the Editors-in-Chief of the CNS Journal



Dear Readers,

In your hands lies the latest issue of the Proceedings of the Master's Programme Cognitive Neuroscience. Here, you will find a variety of articles which demonstrate the diversity of our students' work. Two articles reflect the implementation of functional magnetic resonance imaging (fMRI) – a powerful technique that helps us to understand human cognition. One study explored how different types of information influence our trust towards others, while the other investigated the mental representations of space and time. The understanding of human cognition is also aided by the study of animal models. The potential of rat models in clinical research is demonstrated by an article on the genetics and neural changes associated with Alzheimer's disease. In parallel, the relevance of primate research within Cognitive Neuroscience is shown by a study on local field potentials in monkey auditory cortex.

The remaining two articles in this issue focus on the development of cognitive functions. One studied how performance feedback is processed in the toddler brain, while the other illustrated cultural differences in infants' understanding of communicative signals.

Following from last year, we have continued to implement a biannual publication of our student journal. This reflects not only the quality and multi-disciplinary nature of our program, but also the effort and dedication of our journal members and advisors. We all hope that you will enjoy reading this issue. On behalf of the editorial board,

Ricarda Braukmann & Nietzsche Lam
Editors-in-Chief



From the Director of the Baby Research Center

Dear reader,

It is a great pleasure to contribute an editorial to this issue of the *Proceedings of the Master's Programme Cognitive Neuroscience*. Like the previous issues of the Proceedings, the current issue gives a fascinating overview of the research activities of our students, and demonstrates the multidisciplinary nature and broad range of topics within Cognitive Neuroscience.

I am especially delighted that this semester's issue contains two articles featuring research that has been carried out in the Baby Research Center. This nicely reflects the vivid interest and enthusiasm many of our students have for developmental research. At the same time, it shows the important position the area of Developmental Cognitive Neuroscience has gained within the CNS Master's programme.

The rapidly growing interdisciplinary field of Developmental Cognitive Neuroscience is concerned with the development of cognitive functions and their neural bases. Studying how neural and behavioral development synergistically interact is not only interesting for developmental scientists who aim to get to the bottom of what drives and determines the course of human development. It is likewise informative for the rest of the cognitive sciences, as developmental investigations of cognitive skills can be used to help understand the neurocognitive processes underlying those skills.

The curriculum of the CNS Master's now encompasses several courses on developmental topics, such as an introductory Developmental Cognitive Neuroscience course, a course on the clinical aspects of early brain development, and a course on language acquisition. In addition, our students have ample opportunity to gain research experience working with researchers from the field.

I would like to compliment the editorial board on this new issue of the Proceedings, and I hope you enjoy reading about the progress of Cognitive Neuroscience in Nijmegen.

Dr. Sabine Hunnius
Director Baby Research Center

Proceedings of the Master's Programme Cognitive Neuroscience of the Radboud University Nijmegen

Editors-in-Chief

Ricarda Braukmann
Nietzsche Lam

Editor Action, Perception & Consciousness

Ricarda Braukmann

Assistant Editor Action, Perception & Consciousness

Jeffrey Martin

Editor Neurocognition

Sarah Beul

Assistant Editor Neurocognition

Charl Linssen
Yvonne Melzer

Editor Psycholinguistics

Ashley Lewis

Assistant Editor Psycholinguistics

Angela de Bruin

Layout Chief

Claudia Lüttke

Layout Assistants

Katrin Bangel
Matthias Franken
Suzanne Jongman
Jana Krutwig
Nietzsche Lam

Public Relations Chief

Johanna van Schaik

Public Relations Assistant

Dalya Samur

Subeditor

Suzanne Jongman

Assistant Subeditors

Yağmur Güçlütürk
Jana Kruppa

Webmaster

Martine Verhees

Assistant Webmaster

Lies Cuijpers

Programme Director:

Ruud Meulenbroek

Senior Advisor:

Roshan Cools

Cover Image:

T.L.A.

Journal Logo:

Claudia Lüttkes

Photo Editors-in-Chief:

Ilse van Wijk

Photo Sabine Hunnius:

Dick van Aalst

Contact Information:

Journal CNS

Radboud University

Postbus 9104

6500 HE Nijmegen

The Netherlands

nijmegencns@gmail.com

Time in the Brain: Neural Evidence for a Space-Time Asymmetry

Tom Gijsels^{1,2,3}

Supervisors: Daniel Casasanto^{1,2,3}, Shirley-Ann Rueschemeyer^{1,4} Roberto Bottini^{2,3}

¹Radboud University Nijmegen, Donders Institute for Brain, Cognition and Behaviour, The Netherlands

²Max Planck Institute for Psycholinguistics, Nijmegen, The Netherlands

³The New School for Social Research, New York, NY USA

⁴University of York, York, UK

What is the relationship between space and time in the brain and mind? A Theory of Magnitude (ATOM) suggests the relationship is symmetrical, whereas Metaphor Theory (MT) suggests it is asymmetrical. Here we propose a third framework, combining ATOM and MT, which we tested via an interval reproduction task conducted in the functional Magnetic Resonance Imaging (fMRI) scanner. Participants made temporal and spatial judgments on identical visual stimuli (growing lines). In the behavioral data, irrelevant spatial information influenced temporal judgments more than irrelevant temporal information influenced spatial judgments, consistent with previous studies showing the space-time asymmetry predicted by MT. In the Blood Oxygenation Level Dependent (BOLD) data, encoding of both spatial distance and temporal duration correlated with increased activity in overlapping bilateral clusters of the inferior parietal cortex (IPC), consistent with ATOM's proposal that this region functions as a multi-dimensional magnitude accumulator. Region of Interest (ROI) analyses revealed that IPC was activated more strongly during time judgments than during space judgments. This pattern of activation is inconsistent with the predictions made by either ATOM or MT alone, but is consistent with a framework that combines both theories. Because temporal thinking often relies on spatial heuristics, as proposed by MT, people are unable to filter out task-irrelevant spatial information while encoding time (whereas they are relatively successful at filtering out irrelevant temporal information while encoding space). Thus, the IPC magnitude accumulator proposed by ATOM is driven more strongly when people encode time in the presence of irrelevant spatial information than when they encode space in the presence of irrelevant temporal information. Overall, these neural and behavioral data suggest that the relationship between space and time in the brain and mind is better explained by a theory that incorporates core assumptions of both MT and ATOM than by either theory alone.

Keywords: time, space, ATOM, metaphor, inferior parietal cortex, fMRI

Corresponding author: Tom Gijsels; E-mail: gjsselt@newschool.edu

1. Introduction

How do we think about abstract concepts such as love, fairness and eternity? While the field of cognitive neuroscience is still grappling with understanding the neural representation of concrete concepts, matters become even more complicated when it comes to abstract ideas, like time, which cannot be seen, heard or touched. In response to these issues, it has been suggested that representations of abstract concepts are strongly dependent on those that can be experienced more directly. A case in point is the mental representation of the concrete dimension of space and the more abstract dimension of time. Though their exact nature remains elusive, there is substantial evidence that they are closely related. Studies in which subjects perform tasks requiring temporal judgments or estimations consistently observe an influence from task-irrelevant spatial information. Participants are faster to classify visual stimuli as being shorter or longer in duration (Vallesi, Binns, & Shallice, 2008) or auditory stimuli as occurring earlier or later (Ishihara, Keller, Rossetti, & Prinz, 2008) by making left and right hand responses, respectively. Similarly, when classifying words as denoting either past or future events, subjects are faster when responding with the left or right hand, respectively, or when the stimuli are presented in the left or the right hemi-space (Santiago, Lupiáñez, Pérez, & Funes, 2007). This type of spatial influence is not restricted to response speed, but also affects temporal perception more directly. For instance, presenting stimuli in, or directing subjects' attention to, the left hemi-space leads to an underestimation of stimulus duration, whereas right hemi-space focus causes temporal overestimation (Vicario et al., 2008; Vicario, Caltagirone, & Oliveri, 2007).

While these behavioral data demonstrate that time and space interact, they do not explain how this interaction manifests itself on a neural level. One hypothesis is offered by A Theory Of Magnitude (ATOM; Walsh, 2003), which states that space, time, number and all other prothetic dimensions are represented by a common analog magnitude metric. This metric is hypothesized to have arisen out of the need to integrate these dimensions for the successful planning and execution of actions and is proposed to have its neural locus in the bilateral inferior parietal cortices (IPC; Walsh, 2003), and the intraparietal sulcus (IPS) more specifically, with a right-ward lateralization for temporal magnitude encoding (Bueti & Walsh, 2009). Since ATOM assumes that all

prothetic dimensions rely on the same neural metric, Walsh claims that "experiments in which responses are made to two or more magnitudes on successive trials should show cross-domain, within-magnitude priming," (Walsh, 2003: 487). Moreover, ATOM's proposal of a common magnitude system implicitly predicts these relations to be symmetric, as there is no a priori reason to posit that one dimension should depend asymmetrically on another (in the present context: Space should prime time as much as vice versa).

ATOM's predictions are supported relatively well by the available literature. A number of studies have provided evidence for the predicted behavioral interactions across several prothetic dimensions (see Cohen Kadosh, Lammertyn, & Izard, 2008 for an overview), as well as for the predicted overlap of activations in IPC during magnitude processing in various dimensions (Dormal & Pesenti, 2009; Fias, Lammertyn, Reynvoet, Dupont, & Orban, 2003; Fink, Marshall, Weiss, Toni, & Zilles, 2002; Pinel, Piazza, Le Bihan, & Dehaene, 2004). Furthermore, multiple functional Magnetic Resonance Imaging (fMRI) studies have observed right IPC (rIPC) involvement in temporal processing (Basso, Nichelli, Wharton, Peterson, & Grafman, 2003; Beudel, Renken, Leenders, & de Jong, 2009; Bueti, Walsh, Frith, & Rees, 2008; Lewis & Miall, 2003; Macar et al., 2002; Rao, Mayer, & Harrington, 2001), which corresponds to findings showing impaired performance on temporal tasks after Transcranial Magnetic Stimulation (TMS) to the rIPC (Alexander, Cowey, & Walsh, 2005; Bueti, Bahrami, & Walsh, 2008).

Although these data seem to support the notion of a common magnitude metric residing in the IPC, there are some important caveats. First, it is not the case that the IPC is the single locus subserving magnitude processing for a given dimension. Rather, depending on the specific dimension being judged or estimated, a wider system will be recruited (Bueti & Walsh, 2009; Walsh, 2003). This appears to be the case, for instance, for the processing of temporal magnitudes, which has often been noted to recruit a wide range of neural structures, including the cerebellum, the basal ganglia, supplementary motor area, dorsolateral prefrontal cortex (Lewis & Miall, 2006; Macar et al., 2002) and visual areas BA18 (Basso et al., 2003) and V5/MT (Bueti, Walsh, et al., 2008). Second, despite the fact that a common metric implicitly assumes symmetric interactions between all dimensions relying on this system, there have been observations of asymmetric interactions (e.g. space influences numerosity processing more

strongly than vice versa; Dormal & Pesenti, 2007). Not only are these findings hard to account for by the present ATOM proposal, they are also potentially problematic for the theory as a whole. That is, it is difficult to see how prothetic dimensions can have asymmetric interactions at all if they rely on the same neural substrate, a claim that lies at the core of ATOM. Bueti and Walsh (2009) directly address this issue, but hold that it is at present unclear whether there is indeed a specific hierarchy of inter-dimensional connections creating these asymmetries, or whether these effects are just the result of task-specific demands.

Whereas cross-dimensional asymmetries might be problematic for ATOM, they are inherent to a second theoretical proposal for space-time interactions, namely Metaphor Theory (MT). According to Lakoff and Johnson's (1980) MT proposal, our representations and understanding of abstract concepts are crucially dependent on more tangible sensory representations onto which they are metaphorically mapped. These cross-domain mappings are fundamentally asymmetrical, as representations of abstract concepts necessarily rely on concrete experiential representations, but not necessarily the other way around (Lakoff & Johnson, 1980, 1999). In this sense, the observed interactions between space and time are the result of our reliance on concrete spatial representations to be able to understand abstract notions of time. Moreover, as this theory states that the relation between an abstract dimension and the concrete dimension in terms of which it is encoded is asymmetric, the same should hold for space-time mappings. That is, the concrete spatial dimension is hypothesized to influence the abstract temporal dimension more than vice versa.

Evidence for such an asymmetry has indeed been provided. First, linguistic data show that people often talk about time in spatial terms (a short/long trip; the future lies ahead of us/the past is behind us), but rarely recruit temporal terms to express spatial concepts (Lakoff & Johnson, 1999). Second, psycholinguistic (Boroditsky, 2000; Bottini & Casasanto, 2010) and psychophysical studies (Casasanto & Boroditsky, 2008; Casasanto, Fotakopoulou, & Boroditsky, 2010) find asymmetric cross-dimensional interference between space and time. In Casasanto and Boroditsky (2008), subjects saw lines and dots and were required to reproduce their spatial extent or the duration for which they were presented. When reproducing the temporal dimension, participants' judgments were significantly influenced by task-irrelevant variations in the spatial dimension. For instance, longer lines

were judged to be presented for a longer time than shorter lines, even though both were on-screen for the same amount of time. However, when reproducing a stimulus' spatial extent, judgments were not significantly influenced by task-irrelevant manipulations of duration, thereby affirming the asymmetric nature of the space-time relationship. Finally, though MT predicts the interaction between space and time to be asymmetric, it does not state that it is unidirectional. Within this framework it is still possible that temporal information interferes with spatial processing, as long as this interference is not stronger than the effect of spatial information on temporal processing (Casasanto & Boroditsky, 2008). Hence, Merritt, Casasanto, and Brannon's (2010) findings of both spatial interference with temporal judgments and temporal interference with spatial judgments are not problematic for MT, as the former effect was much stronger than the latter one.

At first sight, these behavioral data are inconsistent with ATOM, and consistent with MT. However, they are also consistent with a combination of both theoretical frameworks. More specifically, if both spatial and temporal magnitudes are processed in the IPC, as ATOM claims, then both spatial and temporal information in the stimulus should drive IPC activation. However, according to MT, we are unable to filter out space when encoding time (because we automatically use space heuristically as an index of time) more than vice versa. Hence, the IPC should be activated more when encoding time (because a substantial amount of spatial information is processed along with it) than when encoding space (which doesn't include much irrelevant time).

Importantly, these claims only hold if we assume that the behavioral asymmetry is an indication of asymmetrical encoding. However, since all of the data in support of MT come from behavioral paradigms, it's still theoretically possible that space and time are encoded symmetrically. The observed behavioral asymmetry could then be the result of interactions that occur after the encoding stage (e.g. at the retrieval or response stage).

The current study sets out to directly address these issues. We used fMRI to measure neural activity of subjects engaged in the spatial and temporal reproduction of identical growing lines. First, by looking for areas that are activated during the encoding of both dimensions, we want to establish whether space and time indeed recruit the same neural structure (which is a prerequisite for both theoretical accounts) and whether this structure is located in the IPC (as predicted by ATOM). Second, by defining this area of overlap as a Region of

Interest (ROI) and by directly comparing the Blood Oxygenation Level Dependent (BOLD) response during the encoding stages of both dimensions, we can address the question of whether they are encoded asymmetrically or not. Moreover, by analyzing the precise pattern of activation elicited by each condition, we can disambiguate between the three theoretical possibilities. First, if ATOM alone is correct and time and space are symmetrically related at encoding, then there should be no significant difference between the BOLD signal in both conditions. Second, if MT alone is correct and temporal encoding recruits spatial representations, we should observe a higher BOLD signal for spatial encoding than for temporal encoding. Finally, a combination of both ATOM and MT predicts a higher BOLD response during temporal encoding than during spatial encoding, because space and time are processed asymmetrically, but both kinds of magnitude are processed by a common metric.

2. Methods

2.1 Participants

Eighteen participants (16 right-handed, 1 ambidextrous, 1 left-handed; male = 9; M = 23.7 years, range: 20-31 years) took part in the current experiment. No participant mentioned having any neurological or psychiatric disorder and all had normal or corrected-to-normal vision. All participants provided written informed consent and were compensated for their participation (10€/hour). To ensure maximal comparability with previous behavioral data (Casasanto & Boroditsky, 2008) and because language-effects on the specific type of space-time interactions have been noted (Casasanto, 2010), only native English speakers were recruited as participants. However, due to difficulties in finding monolingual English speakers in the Netherlands, 4 participants were included who were raised bilingually (i.e. 4 participants indicated on our language questionnaire that they spoke another language before the age of 6). Inclusion of these early bilinguals did not affect the results, however, as the predicted behavioral effects replicate other experiments (cf. below).

2.2 Stimuli

Lines of varying lengths were presented for varying durations. Durations ranged from 1000 ms to 4000 ms in 600 ms increments. Displacements

ranged from 100 to 400 pixels in 60 pixel increments. The six durations were fully crossed with the six displacements, producing 36 unique lines. Half of the lines were red and half were blue. Color was randomly assigned and counter-balanced across conditions and participants. Lines grew horizontally across the screen, one pixel at a time, from left to right, along the vertical midline. The starting position of the lines was, on average, at 337 pixels from the left border of the screen, though the exact point was randomly jittered (± 25 pixels) so the monitor could not be used as a reference frame for spatial estimations.

Responses were given with an MR-compatible joystick device (Current Designs, Philadelphia, USA; model: HHSC-JOY-1). Participants used their right hand to control the joystick for cursor movement and their left index finger for button responses.

2.3 Experimental procedure

In this experiment, participants engaged in four different tasks: Spatial reproduction, temporal reproduction and two color identification tasks. Each trial started with a white iconic task cue that was presented for 1 second and indicated the relevant dimension ('X' for the space condition, an hourglass for the time condition and two types of empty squares for the two color conditions). This cue was followed by a single growing line that stayed on the screen until it reached its maximum displacement and was then replaced by a blank screen. After a period of 4 seconds (+ random jitter; range = 0-2 seconds), a response cue and a cursor appeared and remained on screen until participants performed the required task or until a time-out period of 12 seconds had elapsed.

In the space condition (S), an 'X'-icon appeared in the upper- or lower-left corner of the screen (the position of the cue remained constant for a single participant, but was counterbalanced across participants). Participants moved the cursor from the center of the screen to the center of the icon, clicked once, moved the cursor rightwards in a straight line and then clicked a second time, so the distance between both clicks accurately represented the displacement of the line (Fig. 1A). In the time condition (T), an hourglass-icon appeared in the lower- or upper-left corner of the screen (i.e. in the corner opposite to the space cue). Participants again moved the cursor to the center of the icon, clicked once, waited for the amount of time the line had been on the screen and clicked a second time in the same spot, so the time between both clicks accurately

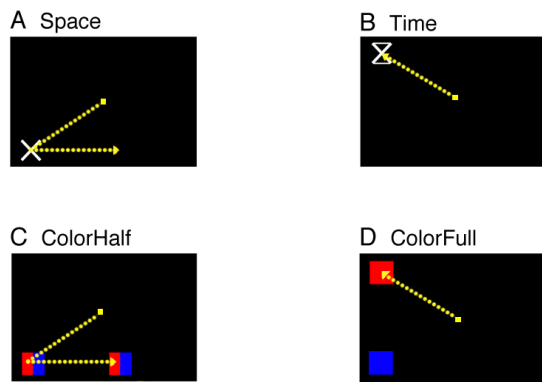


Fig. 1 Examples of the tasks for each of the conditions. The yellow dotted lines illustrate the movements required for each response and were not shown during the experiment. **A.** In the Space condition participants moved the cursor from the center of the screen to the center of the X-icon, clicked once, moved the cursor rightwards in a straight line and then clicked a second time, so the distance between both clicks accurately represented the displacement of the line. **B.** In the Time condition participants moved the cursor to the center of the hourglass icon, clicked once, waited for the amount of time the line had been on the screen and clicked a second time in the same spot, so the time between both clicks accurately represented the duration of the line. **C.** In the Color-Half condition, participants saw two squares appear, each consisting of a red and a blue half. Participants first moved the cursor to the half of the left square that matched the color of the line, clicked once, moved the cursor rightwards in a straight line to the half of the right square that matched the color of the line and clicked again. **D.** In the Color-Full condition participants saw a blue and a red square appear in the upper- and lower-left corners of the screen and clicked twice on the square that had the color of the presented line (see section 2.3 for further descriptions of the tasks and counterbalancing procedures.).

represented the duration of the line (Fig. 1B).

Finally, two color identification conditions were included as control conditions. In the color-half condition (CH), participants saw two squares appear, each consisting of a red and a blue half. The left square was presented in the same corner in which the spatial response cue was presented for that participant and the second square was presented 250 pixels to the right of the left one. Participants first moved the cursor to the half of the left square that matched the color of the line, clicked once, moved the cursor rightwards in a straight line to the half of the right square that matched the color of the line and clicked again. Both squares were identical within a given trial (e.g. two red-blue squares), but the order of the colored halves was counter-balanced across trials (red-blue squares for 50% of the CH trials and blue-red squares for the other 50%) (Fig. 1C). In the color-full condition (CF), participants saw a blue and a red square appear in the upper- and

lower-left corners of the screen (square position was counterbalanced across trials) and clicked twice on the square that had the color of the presented line (Fig. 1D).

By including these two color conditions and subtracting them from the target conditions during analysis, we can control for two potential confounds to our main effects of interest. First, they provide a low level visual baseline for the target conditions, so activations caused by the perception of the lines can be filtered out. Second, they offer a way of ruling out that any potential BOLD asymmetry between the space and time conditions is caused by motor response preparation. That is, if the encoding of space and time coincides with the preparation of the ensuing response, then an observed difference in BOLD signal between both conditions could be caused by the difference in the size of the prepared movement rather than by the difference in the encoding of the relevant dimensions per se. However, because each of the color conditions requires a response that is matched in terms of motor movement (and thus in preparation) with its respective target condition (S & CH; T & CF), subtraction of these controls from the targets should cancel out differential activations between space and time due to motor preparation. Third, since color is a metathetic dimension rather than a prosthetic one, activations elicited by color judgments can be subtracted from those elicited by the target dimensions without affecting the pattern of activity in magnitude-related areas.

Before entering the scanner, participants engaged in a short practice round. They read the task instructions and performed 3 trials of each condition. All participants performed all four tasks correctly at the end of practice. While in the scanner, the participants performed each of the four tasks for each of the 36 unique lines (i.e. $4 \times 36 = 144$ trials in total). Trials were presented randomly within condition and pseudo-randomly across conditions (i.e. no more than 3 trials of the same condition could follow each other).

2.4 fMRI data acquisition

Functional data were acquired on a Siemens Avanto 1.5 T MRI system (Siemens, Erlangen, Germany) using a standard birdcage head-coil for RF transmission and signal reception. T2*-weighted BOLD-sensitive images were acquired using a gradient EPI sequence (Echo Time = 40 ms; Repetition Time = 2.280 s; 32 axial slices in ascending order; voxel size = $3.3 \times 3.3 \times 3.0 \text{ mm}^3$). For each subject we also acquired a T1-weighted

high-resolution anatomical scan (Echo Time = 2.950 s, Repetition Time = 2.250 s, voxel size = 1.0 x 1.0 x 1.0 mm³, 176 sagittal slices, field of view = 256).

2.5 fMRI data analysis

Functional data were preprocessed and analyzed with SPM8 (Statistical Parametric Mapping, Wellcome Department of Cognitive Neurology, London, UK). Preprocessing involved the removal of the first 5 volumes to allow for T1 equilibration effects. To correct for head movements, images were spatially realigned with rigid body registration along three translational and three rotational axes. Then, images were temporally realigned to the middle slice (slice 17) to correct for slice timing acquisition delays. Images were co-registered to each subject's structural scan and normalized to a standard EPI template in Montreal Neurological Institute space and resampled at an isotropic voxel size of 2 mm. To remove baseline-drifts and low frequency signal changes, a 1/128 Hz temporal high-pass filter was applied. The normalized images were then smoothed with an isotropic 8 mm FWHM Gaussian kernel.

These preprocessed data were analyzed on a subject-by-subject basis using an event-related approach. The time series were entered into a General Linear Model with separate regressors for the encoding and response phase of each of the conditions (modeled as the stimulus and response onsets for S, T, CH and CF), which were then convolved with a canonical hemodynamic response function (HRF). Though response phase regressors were added to the model for completeness, they were not further analyzed and will not be discussed in the following pages. Finally, nuisance regressors were added to the model to account for disturbances caused by small head movement.

To single out neural activity specific to spatial and temporal encoding, we computed two contrast images for each participant individually ([S-CH] and [T-CF]). These contrast images were then entered into separate second level random effects analyses to compute the Space- and Time-specific activations on the group level. Each of these two analyses consisted of a one-sample t-test to reveal activations that were significantly different from zero across the contrast images from all participants. A double threshold was applied to protect against Type I errors: Only voxels with a $p < .001$ (uncorrected) and a volume exceeding 41 voxels (328 mm³) were considered (volume sizes were defined by the Monte Carlo Simulation approach described by Slotnick, 2011).

Since our main point of interest is the neural overlap between spatial and temporal encoding, a conjunction analysis was performed on the two second level contrast images ($[S\text{-}CH] \cap [T\text{-}CF]$). Based on our a priori hypothesis, bilateral clusters of IPC activity that emerged from the conjunction were extracted and defined as our ROI's. From these ROI's, we extracted the contrast values for the [S-CH] and the [T-CF] contrasts for each subject, using the MarsBaR SPM package (Brett, Anton, Valabregue, & Poline, 2002; <http://marsbar.sourceforge.net/>, version 0.42).

3. Results

3.1 Behavioral results

To begin with, we tested whether spatial and temporal reproduction was affected by variation in the task-irrelevant stimulus dimension. First, the spatial and temporal extents of the stimuli as well as each participant's spatial and temporal responses were normalized. Then, we calculated the normalized slopes of the effect of spatial variation on temporal reproduction (ST) and the effect of temporal variation on spatial reproduction (TS) for each participant separately (see Fig. 2 for the group averages of the normalized slopes). The results showed significant cross-dimensional effects: The spatial extent of stimuli predicted the variation in the temporal responses (Wald X₂₍₁₎ = 23.55, $p = .001$) and the duration of stimuli predicted the variation in spatial responses (Wald X₂₍₁₎ = 12.21, $p = .001$). Importantly, although these effects were found for both dimensions, they were also strongly asymmetric: Spatial variation affected temporal reproduction significantly more than vice versa (ST > TS, Wald X₂₍₁₎ = 8.00, $p = .01$).

Next, to investigate within-dimensional performance, we used the normalized stimulus and response values to calculate the normalized slopes of the effect of spatial variation on spatial reproduction (SS) and temporal variation on temporal reproduction (TT), for each participant separately (see Fig. 2 for group averages). Though the results show significant within-dimension effects for both Space and Time reproduction (SS: Wald X₂₍₁₎ = 10139.17, $p = .001$; TT: Wald X₂₍₁₎ = 1465, $p = .001$), they also demonstrate a significant difference between both types of within-dimension performance: Participants were significantly better at spatial than at temporal reproduction (SS > TT, Wald X₂₍₁₎ = 20.41, $p = .001$).

The previous pattern of results is confirmed by a regression analysis of all the normalized slopes, testing for main effects of Target Dimension (Space; Time), Dimensionality (Within; Between) and their interaction, with Subjects as a repeated measure. While the within-dimensional slopes are significantly higher than the cross-dimensional slopes (main effect of Dimensionality: Wald $X^2(1) = 907.36$, $p = .001$), there is no significant effect of Target (Wald $X^2(1) = 0.35$, $p = .56$). We did observe a significant interaction between Target and Dimensionality (Wald $X^2(1) = 24.18$, $p = .001$), showing significantly higher within-dimension slopes for space than for time and higher between-dimension slopes for time than for space (Fig. 3A).

This difference in within-dimension performance between space and time hasn't been observed in other studies (e.g. Casasanto & Boroditsky, 2008) and is potentially problematic for the interpretation of the between-dimension asymmetry. Indeed, if performance in one dimension is near perfect,

it is arguably less susceptible to interference from other dimensions, whereas a dimension with lower performance is more susceptible to simultaneously presented information in another dimension (Bottini & Casasanto, 2010). In this sense, the aforementioned difference between the cross-dimensional effects could be a consequence of participants being less accurate on the temporal task and thus being more susceptible to interference from the spatial dimension. The asymmetry, then, would be an artifact of this difference rather than a fundamental property of the way time and space are encoded.

To test this scenario, we re-ran the regression model after equating for within-dimension performance. To do this, we excluded the data from participants with low TT-slopes until the within-dimension performance was the same for both Space and Time (i.e. until $SS = TT$; $N = 7$). After doing this, the difference in between-dimension slopes persisted: The spatial extent of stimuli predicted the

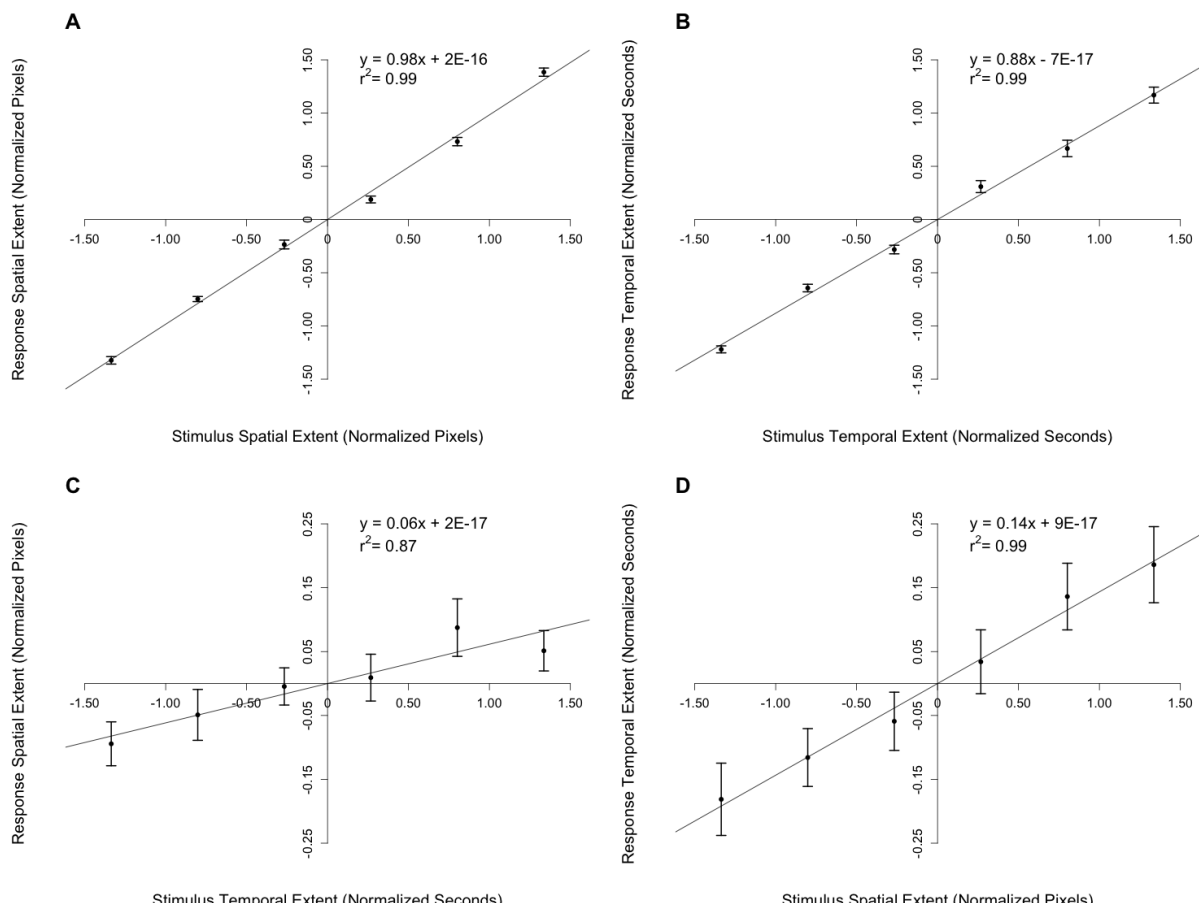


Fig. 2 Grand averages of displacement and duration estimates, based on the normalized stimulus and response values. **A.** Within-dimensional effects for Space, showing the effect of actual line displacement on reproduced displacement. **B.** Within-dimensional effects for Time, showing the effect of actual line duration on reproduced duration. **C.** Cross-dimensional effects for Space, showing the effect of actual line duration on reproduced displacement. **D.** Cross-dimensional effects for Time, showing the effect of actual line displacement on reproduced duration. Error bars indicate SEM.

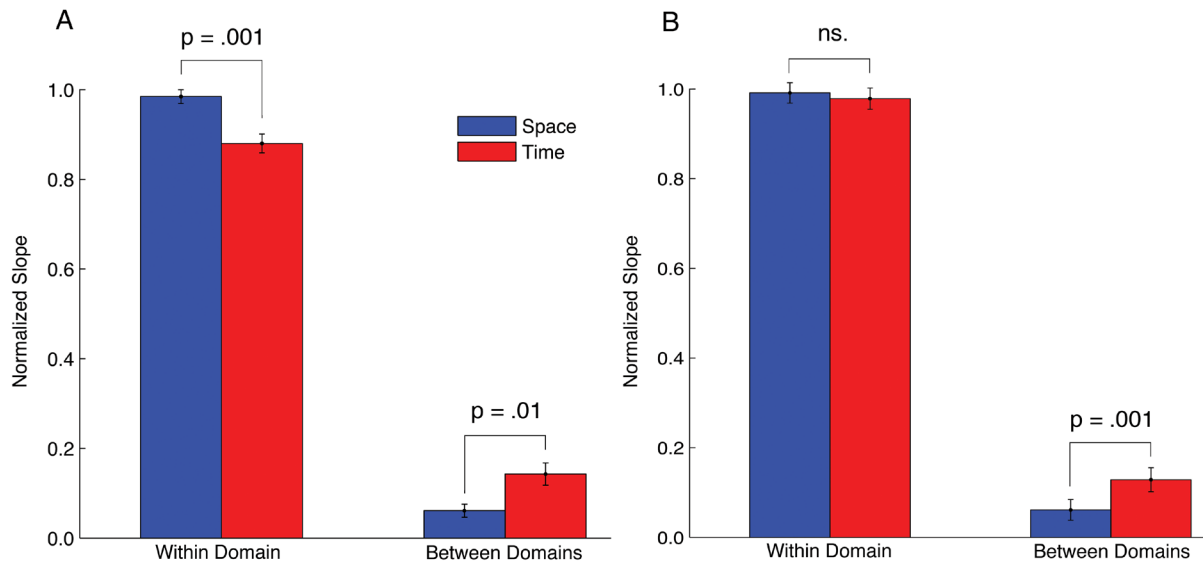


Fig. 3 Group averages of the normalized slopes calculated on the basis of the normalized stimulus and response values. Blue: Space; Red: Time. **A.** Data of all subjects. Left: a significant difference between the within-dimensional slopes of space and time (space within > time within; Wald $X^2 = 20.41$; df = 1; p = .001). Right: a significant difference between the cross-dimensional slopes of space and time (time between > space between; Wald $X^2 = 8.00$; df = 1; p = .01). **B.** Data after removing participants to equate for within-dimension performance (N = 7). Left: non-significant difference between the within-dimensional slopes for space and time. Right: significant difference between the cross-dimensional slopes of space and time (time between > space between; Wald $X^2 = 12.56$; df = 1; p = .001). Error bars indicate SEM.

variation in the temporal responses more than vice versa (ST>TS, Wald $X^2(1) = 12.56$, p = .001) (Fig. 3B). Thus, even after equating within-dimension performance, we still observed the space-time asymmetry, demonstrating that it is a robust effect and not an artifact.

3.2 Neuroimaging results

3.2.1 Patterns of activation

A list of areas showing significantly more activation for space and time encoding than for their respective color control-conditions can be found in Tables 1 and 2. During spatial encoding ([S-CH]), increased bilateral activation was observed extending posteriorly and superiorly from the lateral inferior parietal lobe (IPL) (including the right supramarginal gyrus) along the intraparietal sulcus (IPS) into the posterior reaches of the superior parietal gyrus (Fig. 4A). These parietal clusters were connected to bilateral activation sites in the extrastriate visual cortex, comprising part of the superior and middle occipital gyrus (putative V3A). Additional extrastriate activity was observed bilaterally, but in more ventral regions, spanning the inferior and middle occipital gyrus and extending into the posterior inferior

temporal gyrus. Furthermore, bilateral activations were also found in the precentral gyrus (both dorsally, extending into adjacent parts of the middle and superior frontal gyrus, and ventrally, extending into the superior part of the pars opercularis of the inferior frontal gyrus), in the anterior insula and in a ventral part of the middle frontal gyrus extending anteriorly. Finally, medial frontal activations were observed in the SMA and a posterior part of the medial superior frontal gyrus.

For the temporal encoding contrast ([T-CF]), activations were revealed in bilateral parietal regions, including the supramarginal gyrus and the lateral IPL, extending posteriorly along the IPS and into the angular gyrus in the right hemisphere (Fig. 4B). Furthermore, a left-lateralized cluster was observed in the extrastriate visual cortex, including a part of the inferior and the middle occipital gyrus, just anterior to the cuneus. This contrast also showed broad bilateral activations of the precentral gyrus, extending dorsally into the posterior middle and superior frontal gyrus and ventrally into the IFG pars opercularis and triangularis, the anterior insula and across the sylvian fissure into the bordering region of the superior temporal gyrus. Bilateral activity was also observed in dorsolateral prefrontal cortex and medially in the SMA, a posterior part of the medial superior frontal gyrus and the anterior cingulate.

Table 1. Regions showing significantly more activation for Space than for ColorHalf ($p < .001$, voxel cluster size > 41).

Brain region	Zmax	Extent (voxels)	x	y	z
Frontal lobe					
Left precentral gyrus		3608			
Supplementary motor area	5.95		-12	0	60
Left precentral gyrus	5.14		-56	4	40
Left middle frontal gyrus		151			
Left middle frontal gyrus	3.73		-40	48	4
Left inferior frontal gyrus		129			
Left inferior frontal gyrus	4.22		-46	32	24
Pars triangularis					
Left anterior insula		173			
Left anterior insula	4.33		-30	22	0
Right middle frontal gyrus		1194			
Right precentral gyrus	5.66		36	-6	56
Right superior frontal gyrus	5.60		26	-2	54
Right inferior frontal gyrus		1198			
Right middle frontal gyrus	4.88		36	36	18
Right anterior insula	4.75		32	28	-2
Right inferior frontal gyrus		1120			
Right inferior frontal gyrus	5.35		58	16	16
Pars opercularis					
Parietal lobe					
Left middle occipital gyrus		4479			
Left middle occipital gyrus	5.71		-30	-76	24
Left superior parietal gyrus	5.68		-14	-64	48
Left superior occipital gyrus	5.34		-26	-80	32
Right inferior parietal lobe		3907			
Right superior parietal gyrus	5.54		22	-68	48
Right supramarginal gyrus	5.53		42	-36	40
Precuneus		47			
Right precuneus	3.88		8	-44	48
Occipital lobe					
Right inferior occipital gyrus		886			
Right inferior temporal gyrus	4.55		46	-68	-4
Right inferior occipital gyrus	4.36		40	-76	-10

The z-scores of the maxima, the cluster extent (in voxels) and MNI coordinates are reported.

Temporal lobe activations were restricted to two clusters, a bilateral one in the posterior part of the superior temporal gyrus, just ventral to the sylvian fissure and a second right-lateralized one spanning posterior parts of the inferior and middle temporal gyrus. Finally, this contrast revealed activations in a few subcortical regions, including parts of the thalamus and the putamen bilaterally, the left globus pallidus, the right caudate nucleus and parts of the brainstem close to the superior colliculi.

To reveal neural activations common to spatial and temporal encoding, we performed a conjunction analysis on both aforementioned contrasts ([S-CH] \cap [T-CF]). Overlapping activations were found in bilateral parietal cortex, ranging from lateral IPL into the IPS and including the superior part of the supramarginal gyrus in the right hemisphere (Fig. 4C). A cluster of activity was observed in the left extrastriate visual cortex, including a part of the inferior and the middle occipital gyrus, just anterior

Table 2. Regions showing significantly more activation for Time than for ColorFull ($p < .001$, voxel cluster size > 41).

Brain region	Zmax	Extent (voxels)	x	y	z
Frontal lobe					
Left precentral gyrus		2992			
Left thalamus	4.66		-14	-16	10
Left inferior frontal gyrus	4.33		-46		8
Pars opercularis				8	
Left middle frontal gyrus		345			
Left middle frontal gyrus	3.96		-36		14
Left inferior frontal gyrus		337		54	
Left inferior frontal gyrus	4.73		-40		24
Pars triangularis				28	
Right middle frontal gyrus		8881			
Supplementary motor area	5.91		6	16	46
Right middle frontal gyrus	5.52		40	46	14
Parietal lobe					
Left inferior parietal lobe		1303			
Left intraparietal sulcus	5.18		-44	-52	44
Right inferior parietal lobe		2217			
Right supramarginal gyrus	5.77		56	-30	48
Right intraparietal sulcus	5.22		58	-38	50
Occipital lobe					
Left middle occipital gyrus		358			
Left middle occipital gyrus	4.78		-34	-92	-6
Left inferior occipital gyrus	4.27		-46	-80	-6
Temporal lobe					
Right middle temporal gyrus		292			
Right middle temporal gyrus	4.03		52	-38	-16
Right inferior temporal gyrus	3.65		58		
Right superior temporal gyrus		88		-32	-16
Right superior temporal gyrus	3.78		64		
Right supramarginal gyrus	3.22		58		
				-34	18
Subcortical					
Right thalamus		512		-42	
Right caudate nucleus	4.65		16	4	12
Right thalamus	4.48		12	-14	6
Brainstem		68			
Tegmentum	4.38		-6	-16	-12
Brainstem		63			
Brainstem	3.49		10	-26	-4
Right superior colliculus	3.46		0	-34	-8

The z-scores of the maxima, the cluster extent (in voxels) and MNI coordinates are reported.

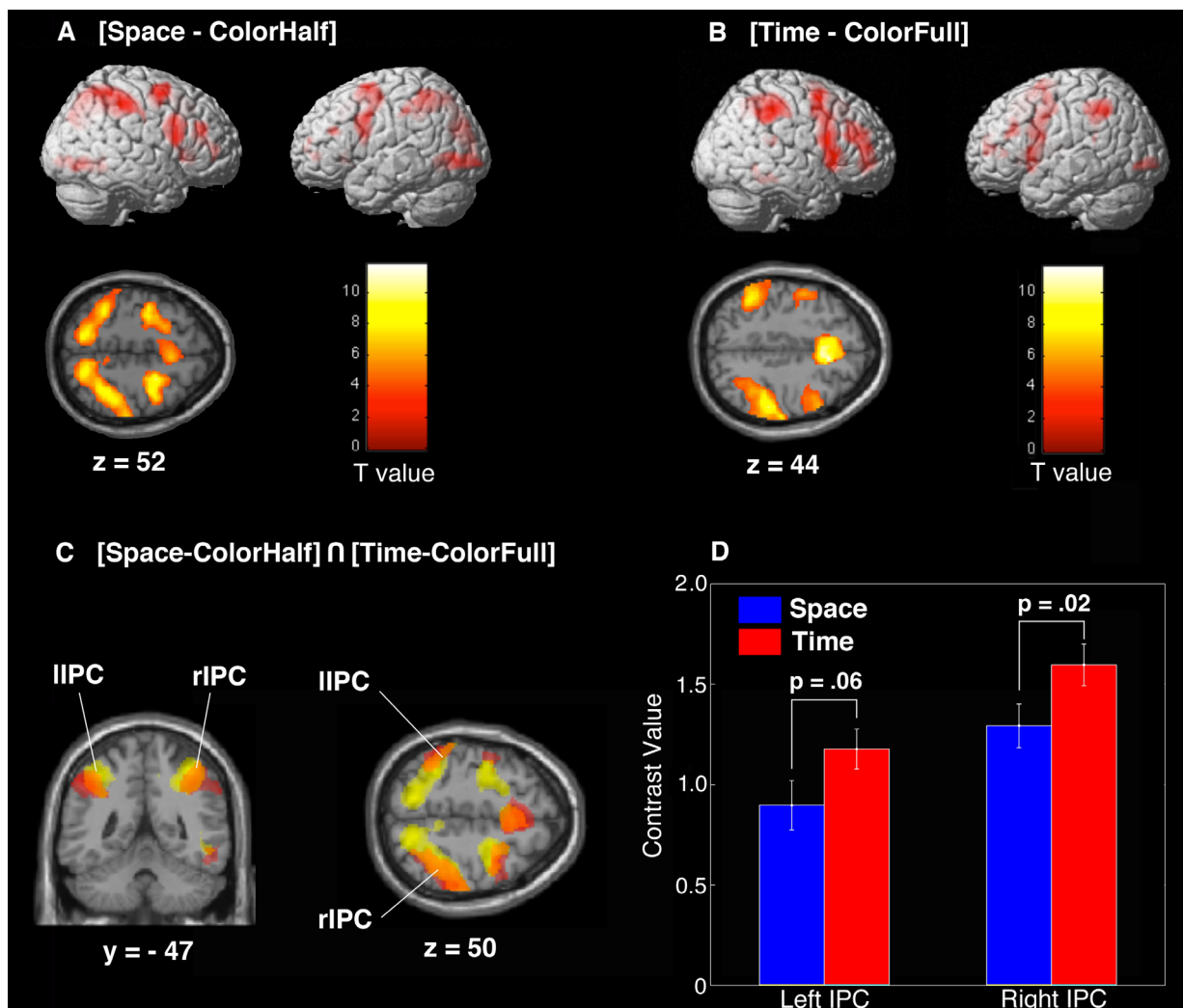


Fig. 4 A. Areas significantly more activated for Space than for ColorHalf ([S-CH]; ColorHalf ($p < .001$; voxel cluster size > 41). Top: Whole-brain view; Bottom: Axial slice showing bilateral Inferior Parietal Cortex (IPC) activity, extending along the Intraparietal Sulcus (IPS). **B.** Areas significantly more activated for Time than for ColorFull ([T-CF]; ColorHalf ($p < .001$; voxel cluster size > 41). Top: Whole-brain view; Bottom: Axial slice showing bilateral Inferior Parietal Cortex (IPC) activity, extending along the Intraparietal Sulcus (IPS). **C.** IPC-clusters emerging out of the conjunction analysis of [S-CH] and [T-CH]. Yellow = Space; Red = Time; Orange = Overlap. **D.** Contrast values extracted for Space and Time for each of the IPC clusters found in the conjunction analysis. Time recruited these clusters more than Space in both the left (Wald $\chi^2 = 3.49$; $df = 1$; $p = .06$) and the right hemisphere (Wald $\chi^2 = 5.14$; $df = 1$; $p = .02$).

to the cuneus. Additionally, a right-lateralized site of temporal lobe activation was found in the posterior part of the inferior temporal gyrus. Frontal overlap occurred in the bilateral precentral gyri, bordering dorsally on the superior frontal sulcus and extending ventrally into the IFG pars opercularis and into the anterior insulae. Separate bilateral clusters of dorsolateral prefrontal cortex activation were found, that included the superior part of the IFG pars triangularis extending into the anterior reaches of the middle frontal gyrus. Furthermore, we observed right-lateralized dorsal activation of the posterior middle and superior frontal gyri, extending into the superior frontal sulcus. Finally, the conjunction revealed medial frontal activations comprising the

SMA, the medial superior frontal gyrus and the middle and anterior cingulate.

3.2.2 ROI analysis

To see whether the bilateral IPC clusters revealed by the conjunction analysis were engaged symmetrically or asymmetrically by space and time encoding, we defined them as our two ROI's and extracted the contrast values per subject for each condition of interest. These contrast values were entered into a regression model, with Condition (Space; Time), Hemisphere (Left; Right) and their interaction (Condition * Hemisphere) as within-subject factors and Subject as a repeated random

effect. As the results indicate, the IPC was recruited more during temporal encoding than during spatial encoding (significant effect of Condition: Wald $X^2(1) = 4.65, p = .03$). Furthermore, the encoding of both dimensions engaged the right IPC more than the left IPC (significant effect of Hemisphere: Wald $X^2(1) = 6.79, p = .01$), but this did not affect the relative difference in activation between space and time in either hemisphere (no significant interaction: Wald $X^2(1) = .073, p = .79$). Notwithstanding the absence of an interaction effect, we performed additional exploratory regression analyses on the data from each hemisphere separately. After doing this, the right hemisphere advantage for temporal processing becomes more pronounced ($T > S$, Wald $X^2(1) = 5.14, p = .02$), while the left-hemisphere effect only reaches marginal significance ($T > S$, Wald $X^2(1) = 3.49, p = .06$) (Fig. 4D).

While these findings demonstrate that the IPC is differentially engaged by spatial and temporal encoding, it still does not necessarily follow that this neural asymmetry is driven by a difference in encoding per se. Indeed, our behavioral results indicated that, for some participants, temporal encoding was more effortful than spatial encoding. Thus, it could be that it is this difference in cognitive effort that drives the BOLD asymmetry, rather than the way these dimensions are encoded. If this is the case, then a measure that reflects this difference in cognitive effort should account for the variation in the BOLD signal more accurately and should thus constrain or even eliminate the main effect of Condition.

To address this issue, the difference between the normalized slopes of within-dimension performance in the space and the time condition (SS-TT) was calculated for each participant and included in the model. Even when cognitive effort was controlled for, we observed the same robust effects. Both IPC clusters were still engaged more by temporal than by spatial encoding (main effect of Condition: Wald $X^2(1) = 4.19, p = .04$), with stronger right hemisphere recruitment (main effect of Hemisphere: Wald $X^2(1) = 4.24, p = .04$). The behavioral measure of cognitive effort, however, did not reach significance (Wald $X^2(1) = 2.42, p = .12$), nor did its three-way interaction with Dimension and Hemisphere (Wald $X^2(1) = 1.60, p = .66$). Including the cognitive effort measure in the exploratory hemi-wise analyses confirms the earlier pattern of observations. Temporal encoding recruits the IPC more than spatial encoding in both hemispheres, as shown by a marginally significant effect of target in the left-hemisphere ($T > S$, Wald $X^2(1) = 3.15, p =$

.08) and a significant effect of target in the right-hemisphere ($T > S$, Wald $X^2(1) = 4.47, p = .04$), whereas the cognitive effort measure did not reach significance in either hemisphere (L: Wald $X^2(1) = 1.23, p = .27$; R: Wald $X^2(1) = 2.85, p = .09$).

4. Discussion

The current study investigated whether the neural structures underlying space and time representations interact at the encoding stage and, if so, whether they do so in the way predicted by ATOM, MT or a combination of both theories. The behavioral results corroborate earlier findings of a space-time asymmetry. When people reproduce a line's duration they are consistently influenced by task-irrelevant spatial variation, more so than their spatial reproduction is influenced by concurrent temporal variation. Furthermore, the widespread neural overlap between both temporal and spatial encoding supports the notion that their interaction already emerges at this stage. Most notably, the conjunction of the spatial and temporal trials revealed shared bilateral clusters of activity in the inferior parietal cortex (IPC), a region proposed by ATOM as being the prime locus for a shared magnitude system. Our ROI-analysis revealed that encoding space and time activated these IPC clusters asymmetrically: Temporal encoding led to a stronger activation than spatial encoding.

While both ATOM and MT predicted overlapping activations for space and time encoding, neither theory by itself predicted the currently observed asymmetrical pattern of activity. First, according to MT, the behavioral asymmetry arises because temporal encoding relies on spatial representations (Casasanto & Boroditsky, 2008). Given ATOM's proposal that these dimensions are encoded by an IPC-based metric (Bueti & Walsh, 2009; Walsh, 2003) that is sometimes speculated to be spatial in origin (Bueti, Walsh, et al., 2008), this region should have been asymmetrically activated by spatial and temporal encoding. That is, if the IPC is indeed originally a spatial representation system, encoding the primary (i.e. spatial) dimension should lead to higher activity than encoding a secondary dimension, such as time. This, however, was not the case, suggesting that this metric is unlikely to have been grafted onto spatial representations and is potentially a-dimensional in nature. Second, the observed asymmetry also runs contrary to ATOM's implicit prediction. If the IPC indeed constituted a fully common analog metric onto which all magnitudes are mapped, then there is

no reason to assume that encoding either dimension would engage this metric more strongly, be it in one direction or the other. Hence, these data suggest that the current ATOM model cannot fully account for the way space and time are neurally encoded.

Though neither theory by itself predicts the observed neural asymmetry, a framework that combines both theories does. More specifically, consider how temporal and spatial magnitudes are processed according to a model that combines the asymmetry predicted by MT and the common accumulator posited by ATOM. At the lowest level, the visual stimulus possesses equal amounts of spatial and temporal information, regardless of the condition it is presented in. Depending on the dimension to be attended to, variation in the target dimension has to be detected and encoded for reproduction, whereas variation in the irrelevant dimension should be filtered out as much as possible. However, as MT states, our temporal reasoning strongly relies on spatial heuristics, more so than vice versa (Lakoff & Johnson, 1999). Hence, even though short events as these could theoretically be represented by purely temporal systems, conceptualizing time in terms of space allows us to mentally manipulate it in a more flexible way. By doing so, we use the tangibility of spatial concepts to import stability into the fluid, evasive dimension of time and can move events forward or backward in time or move ourselves backward or forward in time to relive or predict certain events (Casasanto & Boroditsky, 2008). Because of this, even when spatial information is not immediately relevant for the task at hand, its presence will cause it to be automatically incorporated in the processing of the temporal information of an event. The observations of the behavioral asymmetry seem to support this notion that there is a difference in the extent to which task-irrelevant variation in space and time can be filtered out. Whereas spatial responses are based on mainly the spatial and only some of the temporal information, the temporal responses are substantially influenced by spatial information present alongside the temporal information. Now, if the IPC indeed constitutes a common metric that accumulates these different magnitudes (Walsh, 2003), then differences in their relative contribution to the encoding process should lead to differential activation of this area. That is, if in addition to the task-relevant information there is more task-irrelevant information being encoded in the temporal than in the spatial condition, the former process will cause more information to be accumulated, as reflected by the higher IPC activity (Fig. 5).

Though any arguments about the precise mechanisms causing the asymmetry must remain speculative, the proposed combination of MT and ATOM is also consistent with an attention-gated model of time perception. In standard clock models (e.g. Gibbon, Church, & Meck, 1984), a pacemaker provides a consistent pulse train that is switched to an accumulator, which ‘counts’ the pulses received for the duration of an external event. The attention-gate model (Zakay & Block, 1997) expands on the standard models by adding an attentional gate between the pacemaker and the switch. Depending on the attention devoted to a certain event, the gate can be opened and closed to let the pulses through to the switch, thereby determining the quantity of pulses received by the accumulator and thus the apparent duration of the event. Moreover, the opening of the gate is not hypothesized to be binary but more gradual, so that it can be opened more or less, thereby allowing more or less pulses to reach the accumulator.

If the IPC functions as a magnitude-general accumulator, then it is plausible that it is modulated at a preceding stage by such a magnitude-general attentional gate. The asymmetric activation of the IPC, then, could arise out of the way in which the processes of encoding space and time differently impact on the gate. The current data suggest that during temporal encoding, it is the combined attention paid to not just the temporal but also the

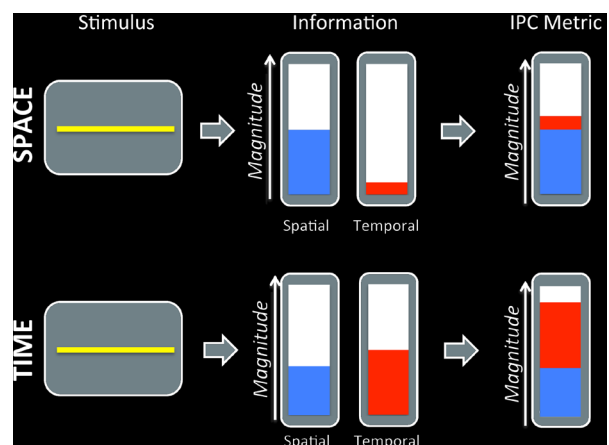


Fig. 5 Schematic representation of the distribution and spread of spatial and temporal information. At the level of the stimulus, each dimension conveys equal amounts of information. The information from the task-relevant dimension is encoded to an equal extent in both dimensions, but the amount of task-irrelevant information encoded differs. Whereas during spatial encoding there is only a limited influence of temporal information, during temporal encoding there is a substantial impact of task-irrelevant spatial information. This differential influence determines the amount of magnitude encoded by the a-dimensional IPC metric.

spatial properties of the event that modulates the opening of the gate. This combined attentional influence on the gate will be higher for temporal than for spatial encoding, due to the inability to ignore the task-irrelevant dimension. Therefore, the increased attentional influence during temporal encoding pushes the gate further open, causing more pulses to be accumulated. This increased amount of pulses is then reflected by higher IPC activation and behaviorally by a substantial impact of the spatial information on the temporal reproduction.

As such, this proposal entails a reconciliation of both Metaphor Theory and ATOM. On the one hand, it posits that the IPC functions as a common magnitude accumulator in a way that is very similar to the one proposed by ATOM. On the other hand, the hypothesis that the putative attention-gating mechanism is modulated differently by spatial and temporal encoding corresponds to the predictions made by Metaphor Theory: People seem to be unable to filter out spatial information when encoding time.

Though unlikely, it is important that we rule out that the current pattern of activity is caused by task-related effects. For instance, it could be argued that the behavioral discrepancy in within-dimension performance indicates that temporal encoding required increased cognitive effort relative to spatial encoding. This difference could then be reflected neurally by the stronger engagement of the IPC during temporal encoding (Cohen Kadosh et al., 2008). Moreover, the lower within-dimension performance during time encoding could expose it to more cross-dimensional influence from the spatial domain, explaining the behavioral asymmetry (Bottini & Casasanto, 2010). However, in previous studies investigating space-time interactions, the cross-dimensional asymmetry was observed even though within-dimension performance was equally high for space and time (e.g. Casasanto & Boroditsky, 2008). Moreover, even when we added extra measures controlling for this difference in cognitive effort, both the behavioral and neural asymmetries persisted. This demonstrates that this cognitive effort account cannot explain the asymmetries.

It is equally improbable that the present data are an artifact of differences in motor preparation between both tasks. First, neural activity caused by motor preparation should have been cancelled out by the subtraction of the activity elicited by the two control conditions. Since each control condition was matched to its respective target condition in terms of motor responses, this procedure should have also removed any differences in motor preparation between conditions. Second, if it were the case

that the IPC asymmetry was driven by differences in response preparation, then it would be expected to occur in the other direction. Because the spatial response was more complex than the temporal one (i.e. it requires more movement planning and coordination), it is precisely the former condition that would be expected to elicit more activation.

A few other theoretically relevant observations flow from the current data. First, they offer some evidence against the alternative claim that the IPC might function as a comparison mechanism. Indeed, some authors have claimed that the common IPC-recruitment by the processing of different magnitudes leaves open the possibility that this area functions as a comparator rather than an accumulator of magnitudes (Cappelletti, Freeman, & Cipolotti, 2009; Cohen Kadosh et al., 2008). However, this interpretation is difficult to sustain given that our task did not include any comparison. Even though it could be argued that reproduction itself has a certain comparison component (i.e. ‘How different is the magnitude of my reproduction to the one encoded?’), this cannot be the case as the current IPC data are based on the encoding process only.

Second, in line with Walsh’s (2003) claims of the hemispheric specialization of the IPC system (lIPC: verbally mediated magnitudes, like number; rIPC: more analog magnitudes, like space and time), we observe a stronger involvement of rIPC for encoding space and time (cf. main effect of Hemisphere). Note, however, that while this lateralization is supported by some studies (e.g. disruption of temporal processing after TMS to right but not the left IPC; Alexander et al., 2005), there appears to be conflicting evidence (see for instance the neuropsychological evidence discussed in Bueti & Walsh, 2009). Likewise, regardless of the stronger rIPC involvement, encoding space and time recruited the IPC bilaterally. Moreover, the three-way interaction between Hemisphere, Condition and Dimension was non-significant in our regression model, showing that the asymmetry did not change between hemispheres. Nonetheless, a tentative further analysis suggests at least a trend towards a stronger rIPC effect (see Fig. 4D).

Third, even though the present experiment mainly investigated the neural relation between spatial and temporal encoding in the IPC, there were many other regions that were commonly recruited by both processes (see Results section for a description). Though a further discussion of these findings is beyond the scope of the present article, it is worth mentioning that these areas comprise some regions that are frequently encountered in

studies of temporal encoding, including the SMA, DLPFC, IFG and the insula (Grondin, 2010; Lewis & Miall, 2006; Wiener, Turkeltaub, & Coslett, 2010). The fact that spatial and temporal encoding commonly activated these regions suggests that they are not necessarily uniquely involved in temporal processing, but may be more general components of a distributed magnitude system.

Finally, a few outstanding questions remain. Though an attentional-gate mechanism accounts for the present findings, future research should try to investigate the neural mechanisms that underlie and directly impact on this gate, both for the spatial and the temporal dimension. Additionally, the majority of the space-time asymmetry studies have been performed with visual stimuli. It is of primary interest to find out whether this asymmetry extends to other modalities. If so, will the asymmetry then occur in the same direction (space influencing time more), or will it change depending on the differences in tangibility or imageability of both dimensions in the other modality (e.g. a reversal in the auditory domain). Furthermore, while our stimuli consist of perceptually simple events, it remains unknown whether the temporal magnitudes of more abstract concepts, such as ‘a party’ or ‘a lifetime’, recruit the same magnitude mechanisms.

5. Conclusion

The current experiment set out to investigate whether time and space are encoded by the same IPC-based mechanism and whether these dimensions neurally interact in a way predicted by ATOM, MT or a combination of both theories. Our fMRI data indicate that encoding both dimensions indeed leads to increased activity in overlapping bilateral clusters of the IPC, supporting ATOM’s proposal of it functioning as a multi-dimensional magnitude accumulator. The ROI analyses, however, revealed that this structure was activated more strongly during temporal encoding than during spatial encoding. This pattern of activation is inconsistent with the predictions made by either ATOM or MT alone, but is consistent with a framework that combines both theories. Because, as proposed by MT, temporal encoding often relies on spatial heuristics people are unable to filter out task-irrelevant spatial information while encoding time (more than vice versa). Since more task-irrelevant information will be present during temporal encoding, the IPC magnitude accumulator proposed by ATOM will be driven more strongly by temporal encoding than spatial

encoding. Not only does this framework account for both the current behavioral and neural data, it is also compatible with the proposal of an attentional gate to the IPC accumulator that is opened more due to the increased attention paid to task-irrelevant information during temporal processing than during spatial processing. As such, the current data suggest that space and time indeed interact at the encoding stage in a way that is predicted by reconciling the proposals made by both MT and ATOM.

References

- Alexander, I., Cowey, A., & Walsh, V. (2005). The right parietal cortex and time perception: Back to Critchley and the Zeitraffer phenomenon. *Cognitive Neuropsychology*, 22 (3), 306-315.
- Basso, G., Nichelli, P., Wharton, C. M., Peterson, M., & Grafman, J. (2003). Distributed neural systems for temporal production: A functional MRI study. *Brain Research Bulletin*, 59 (5), 405-411.
- Beudel, M., Renken, R., Leenders, K. L., & de Jong, B. M. (2009). Cerebral representations of space and time. *NeuroImage*, 44 (3), 1032-1040.
- Boroditsky, L. (2000). Metaphoric structuring: Understanding time through spatial metaphors. *Cognition*, 75 (1), 1-28.
- Bottini, R., & Casasanto, D. (2010). Implicit spatial length modulates time estimates, but not vice versa. In S. Ohlsson & R. Catrambone (Eds.), *Proceedings of the 32nd Annual Conference of the Cognitive Science Society* (pp. 1348-1353). Austin, TX: Cognitive Science Society.
- Brett, M., Anton, J. L., Valabregue, R., & Poline, J. B. (2002). *Region of interest analysis using an SPM toolbox*. 8th International Conference on Functional Mapping of the Human Brain. Sendai, Japan.
- Bueti, D., Bahrami, B., & Walsh, V. (2008). Sensory and association cortex in time perception. *Journal of Cognitive Neuroscience*, 20 (6), 1054-1062.
- Bueti, D., & Walsh, V. (2009). The parietal cortex and the representation of time, space, number and other magnitudes. *Philosophical transactions of the Royal Society of London. Series B, Biological Sciences*, 364 (1525), 1831-1840.
- Bueti, D., Walsh, V., Frith, C., & Rees, G. (2008). Different brain circuits underlie motor and perceptual representations of temporal intervals. *Journal of Cognitive Neuroscience*, 20 (2), 204-214.
- Cappelletti, M., Freeman, E. D., & Cipolotti, L. (2009). Dissociations and interactions between time, numerosity and space processing. *Neuropsychologia*, 47 (13), 2732-2748.
- Casasanto, D. (2010). *Space for Thinking*. In V. Evans & P. Chilton (Eds.), *Language, Cognition, and Space: State of the Art and New Directions* (pp. 453-478). London: Equinox Publishing.
- Casasanto, D., & Boroditsky, L. (2008). Time in the mind:

- using space to think about time. *Cognition*, 106 (2), 579-593.
- Casasanto, D., Fotakopoulou, O., & Boroditsky, L. (2010). Space and Time in the Child's Mind: Evidence for a Cross-Dimensional Asymmetry. *Cognitive Science*, 34 (3), 387-405.
- Cohen Kadosh, R., Lammertyn, J., & Izard, V. (2008). Are numbers special? An overview of chronometric, neuroimaging, developmental and comparative studies of magnitude representation. *Progress in Neurobiology*, 84 (2), 132-147.
- Dormal, V., & Pesenti, M. (2007). Numerosity-Length Interference. *Experimental Psychology*, 54 (4), 289-297.
- Dormal, V., & Pesenti, M. (2009). Common and specific contributions of the intraparietal sulci to numerosity and length processing. *Human Brain Mapping*, 30 (8), 2466-2476.
- Fias, W., Lammertyn, J., Reynvoet, B., Dupont, P., & Orban, G. a. (2003). Parietal representation of symbolic and nonsymbolic magnitude. *Journal of Cognitive Neuroscience*, 15 (1), 47-56.
- Fink, G. R., Marshall, J. C., Weiss, P. H., Toni, I., & Zilles, K. (2002). Task instructions influence the cognitive strategies involved in line bisection judgements: Evidence from modulated neural mechanisms revealed by fMRI. *Neuropsychologia*, 40 (2), 119-130.
- Gibbon, J., Church, R. M., & Meck, W. (1984). *Scalar Timing in Memory*. In J. Gibbon & L. Allan (Eds.), Annals of the New York Academy of Sciences (pp. 52-77). New York: New York Academy of Sciences.
- Grondin, S. (2010). Timing and time perception : A review of recent behavioral and neuroscience findings. *Attention, Perception, & Psychophysics*, 72 (3), 561-582.
- Ishihara, M., Keller, P. E., Rossetti, Y., & Prinz, W. (2008). Horizontal spatial representations of time: Evidence for the STEARC effect. *Cortex*, 44 (4), 454-461.
- Lakoff, G., & Johnson, M. (1980). Conceptual Metaphor in Everyday Language. *Journal of Philosophy*, 77 (8), 453-486.
- Lakoff, G., & Johnson, M. (1999). *Philosophy in the Flesh: The Embodied Mind and Its Challenge to Western Thought*. Chicago: University of Chicago Press.
- Lewis, P. A., & Miall, R. C. (2003). Distinct systems for automatic and cognitively controlled time measurement: Evidence from neuroimaging. *Current Opinion in Neurobiology*, 13, 250-255.
- Lewis, P. A., & Miall, R. C. (2006). Remembering the time: A continuous clock. *Trends in Cognitive Sciences*, 10 (9), 401-406.
- Macar, F., Lejeune, H., Bonnet, M., Ferrara, A., Pouthas, V., Vidal, F., & Maquet, P. (2002). Activation of the supplementary motor area and of attentional networks during temporal processing. *Experimental Brain Research*, 142 (4), 475-485.
- Merritt, D. J., Casasanto, D., & Brannon, E. M. (2010). Do monkeys think in metaphors? Representations of space and time in monkeys and humans. *Cognition*, 117 (2), 191-202.
- Pinel, P., Piazza, M., Le Bihan, D., & Dehaene, S. (2004). Distributed and overlapping cerebral representations of number, size, and luminance during comparative judgments. *Neuron*, 41 (6), 983-993.
- Rao, S. M., Mayer, A. R., & Harrington, D. L. (2001). The evolution of brain activation during temporal processing. *Nature Neuroscience*, 4 (3), 317-323.
- Santiago, J., Lupiáñez, J., Pérez, E., & Funes, M. J. (2007). Time (also) flies from left to right. *Psychonomic Bulletin & Review*, 14 (3), 512-516.
- Slotnick, S. D. (2011). Cluster_threshold (beta) [Software]. Available from <https://www2.bc.edu/sdslotnick/scripts.htm>
- Vallesi, A., Binns, M. A., & Shallice, T. (2008). An effect of spatial – temporal association of response codes : Understanding the cognitive representations of time. *Cognition*, 107, 501-527.
- Vicario, C. M., Caltagirone, C., & Oliveri, M. (2007). Optokinetic stimulation affects temporal estimation in healthy humans. *Brain and Cognition*, 64 (1), 68-73.
- Vicario, C. M., Pecoraro, P., Turriziani, P., Koch, G., Caltagirone, C., & Oliveri, M. (2008). Relativistic compression and expansion of experiential time in the left and right space. *PloS ONE*, 3 (3), 1716.
- Walsh, V. (2003). A theory of magnitude: Common cortical metrics of time, space and quantity. *Trends in Cognitive Sciences*, 7 (11), 483-488.
- Wiener, M., Turkeltaub, P. E., & Coslett, H. B. (2010). Implicit timing activates the left inferior parietal cortex. *Neuropsychologia*, 48 (13), 3967-3971.
- Zakay, D., & Block, R. A. (1997). Temporal cognition. *Current Directions in Psychological Science*, 6 (1), 12-16.

Acoustic and Behavioral Modulations of Local Field Potentials in Monkey Auditory Cortex

Thomas S. E. Gräfnitz¹

Supervisors: Marc M. Van Wanrooij¹, Roohollah Massoudi¹, A. John Van Opstal¹

¹Donders Centre for Neuroscience, Nijmegen, The Netherlands

The primate auditory cortex (AC) occupies a pivotal position within the central auditory pathway. It is still debated whether subdivisions within AC may be primarily involved in the representation of a sound's acoustics or in auditory perception. To study this question we compared neural responses at several sites within the AC, purposely primary auditory cortex (A1), under different task constraints. We reasoned that if the recorded site is concerned with the processing of acoustics only, task-related factors should not modify the neural responses. Here we report on the local field potentials (LFPs) recorded in auditory cortex of a trained macaque monkey. We compared the dynamics of the LFP under two conditions. In the passive listening condition the monkey heard a series of broad-band sounds (dynamic rippled stimuli, with a variety of ripple velocities and ripple densities). The monkey was not rewarded for these sounds, as it was not asked to generate a behavioral response. In the active condition, on the other hand, the monkey initiated a trial by pressing a bar, which started a static flat broadband noise. After a random delay (either 500 or 1000 ms) the noise changed into a dynamic ripple to which the monkey had to respond by releasing the bar. LFPs were measured by low-pass filtering the raw multiunit electrode signal at 300 Hz. Our results indicate systematic modulations of the LFP for specific epochs within the task condition, when compared to acoustically identical events during passive listening. This was found at all recording sites, suggesting a perceptual role for A1. Furthermore, we found behavioral evidence that the monkey learned how to expect later occurring changes in sound. Interestingly, we found that response preparation is also expressed as a specific neuronal correlate in monkey A1.

Keywords: auditory cortex, local field potential (LFP), behavior, top-down, monkey

Corresponding author: Thomas S. E. Gräfnitz, E-mail: thomasgraefnitz@gmail.com

All supplementary material of this article can be found online at <http://www.ru.nl/master/cns/journal/current-issue>

1. Introduction

The ability to quickly recognize the identity and location of sound is often taken for granted. However, auditory processing is highly complex, and distributed across many brain structures in the auditory system, which is characterized by its tonotopic organization. This tonotopy is found immediately at the cochlea, where the location of hair cells on the basilar membrane that transduce sounds into electro-chemical signals depends on their frequency tuning. The cochlea is connected to the cochlear nucleus (CN) via the auditory nerve. The CN projects to the superior olive complexes (SOC) on both sides and to the contralateral inferior colliculus (IC), a midbrain structure, which receives bilateral projections also from the SOC and from the nuclei of the lateral lemniscus, the main input pathway into the IC. The IC projects to the auditory thalamus, composed of the medial geniculate body and other nuclei. The thalamic stations project to primary auditory cortex (A1) as well as to other cortical fields. Pathways originating in A1 project to anterior and posterior fields, which are believed to process different aspects of auditory information, coding respective representations of ‘where’ and ‘what’ information within segregated cortical auditory streams (Miccheli et al., 2007; Rauschecker & Tian, 2000).

Thus, based on the extensive neuroanatomy of the primate auditory system (Kaas, Hacklett, & Tramo, 1999), much of the neural processing necessary for perception of the acoustic surroundings seems to take place subcortically (King & Schupp, 2007). As a result, several neuroscientists wonder which role A1 and surrounding belt areas actually play in auditory perception, more specifically, which aspects of sound these cortical cells are left to compute (Griffiths, Warren, Scott, Nelken, & King, 2004; Nelken, 2008). With regard to cortical areas beyond primate primary auditory cortex (that is, auditory belt areas), several studies have found significant evidence for specific higher-order cognitive processing (Maier & Ghazanfar, 2007; Miccheli et al., 2007; Nelken, 2008). In contrast, the precise role of A1 for auditory perception is still unknown (King & Nelken, 2009). There is currently no agreement whether higher-level cognitive processing occurs at the level of A1. Nevertheless, there certainly exists notable support in favor of A1 being engaged in such processing (Brosch, Selezneva, & Scheich, 2005; King & Nelken, 2009; Riecke, Van Opstal, Goebel, & Formisano, 2007). This study aimed

to investigate whether neural activity in monkey primary auditory cortex solely codes for the physical characteristics (acoustics) of sound, or whether this activity can actually be modulated by context-dependent (non-acoustic) variables, such as ‘task-relevance’ and ‘prediction’. We decided to explore this issue by measuring and comparing the local field potentials (LFPs) from monkey A1, while the animal was engaged in an auditory detection task (active listening), and during passive listening to acoustically identical sounds.

The LFP signal is thought to represent the synchronized (dendritic) input to many neurons, located very close to the recording electrode (Juergens, Guettler, & Eckhorn, 1999; Mitzdorf, 1985; for review, see Logothetis, 2003), while single-unit data represent the output of a single neuron. Frequency modulations in the LFP signal have been linked to specific events. For example in the visual domain, increased LFP power in the gamma frequency band (30–100Hz) facilitates perception and sensorimotor integration in response to visual changes (Womelsdorf, Fries, Mitra, & Desimone, 2006) and is suggested to indicate effective bottom-up and top-down neuronal communication (Fries, 2005, 2009).

We reasoned that if A1 exclusively codes for the acoustic features of sound, such as frequency and intensity, neuronal response patterns as indicated by LFPs, should be identical for active vs. passive listening. On the other hand, differences in neuronal activity during active vs. passive listening to the same acoustic stimuli would strongly argue for a role of monkey A1 in perceptual, context-dependent encoding, such as behavioral relevance of the auditory stimulus and predictive mechanisms of auditory events. Furthermore, we aimed to examine whether specific LFP modulations correlate with conscious, fast perception of auditory changes, indicated behaviorally by the monkey during the active condition.

2. Materials and methods

Neurophysiological recordings were performed in the left auditory cortex (AC) of one adult male rhesus monkey (*Macaca mulatta*, Thor; weight, 8–9 kg; age: 10 years). All experiments were conducted in accordance with the European Communities Council Directive of November 24, 1986 (86/609/EEC) and were approved by the local ethics committee (“dierexperimentencommissie”) of the university for the use of laboratory animals.

2.1 Set-up and animal preparation

The head-restrained monkey sat in a primate chair in a dark and sound-attenuated room (2.45 x 2.45 x 3.5 m). The walls, ceiling, and floor, and every large object present were covered with acoustic foam that eliminated echoes of sound frequencies > 500 Hz (Agterberg et al., 2011). The room had an ambient background noise level of 20 dBA SPL. The monkey was trained to detect a subtle change in sound against small liquid rewards. Shortly before (~24 h) recording periods, the monkey was deprived from his normal ad libitum water supply, and daily water intake was limited to ~200 ml, except for weekends, when it was ~400 ml per day. In a recording session, depending on the experimental condition (see Paradigm), the monkey could earn liquid rewards until he was sated.

2.2 Surgery

After training was completed, three separate surgeries were performed under full anesthesia and sterile conditions. Anesthesia was maintained by artificial respiration (0.5% isoflurane and N₂O), and additional pentobarbital, ketamine, and fentanyl were administered intravenously. In the first surgery, a thin golden eye ring was implanted underneath the conjunctiva. This allowed for precise eye-movement recordings with the so-called double-magnetic induction technique (Bour, Van Gisbergen, Bruijns, & Ottes, 1984; Bremen, Van der Willigen, & Van Opstal, 2007a, 2007b; Bremen et al., 2010; Zwiers, Versnel, & Van Opstal, 2004). However, in the current experiments, the eye movements were not tracked. In the second surgery, one stainless-steel bolt, embedded in dental cement, allowed firm fixation of the head during recording sessions. In the third surgery, a stainless steel recording chamber (12 mm diameter) was placed over a trepanne hole in the skull (10 mm diameter), centered above the midline, and 2 mm posterior of the interaural line. This position of the chamber allowed a vertical approach of the auditory cortex of the left side. The recording sites were assumed to be located in primary auditory cortex (A1), since the stereotaxic coordinates of the recording sites corresponded closely to the coordinates of A1, as previously determined for the monkey by fMRI (in collaboration with dr. H.H. Goossens).

2.3 Recordings

We simultaneously measured single neuron activity and local field potentials (LFPs) by means of one electrode. A glasscoated tungsten microelectrode (resistance: 1–2 MΩ) (Alpha Omega, Ubstadt-Weiher, Germany) was carefully positioned and simultaneously lowered into the brain through two short stainless-steel guide tubes of different thickness by an electronically-driven, custom-made stepping motor (National aperture Inc.). Signals of the electrode were grounded to a contact mounted in the skull bone. The analog electrode signal was amplified (BAK Electronics; model A-1; high-pass filter Fc = 100Hz before 25-02-2010; Fc = 10 Hz after this date) and low-pass filtered (8th order Butterworth filter; 15 kHz cutoff). The LFP signal was obtained from this signal by subsequently low-pass filtering (Krohn-Hite; model 3343; 300 Hz cut-off), and a spike signal was simultaneously obtained by high-pass filtering (Krohn-Hite; model 3343; 100 Hz cut-off). The LFP data were then passed through an A/D convertor (National Instruments) that was controlled by MatLab running on a PC (Windows XP; DELL).

The spike signal was passed through an A/D convertor (TDT-2 system; module AD-1; Tucker-Davis Technologies, Gainesville, FL) and action potentials were detected by an automated algorithm (BrainWare, TDT). Detected spike timings and wave forms were digitally stored on hard disk of a PC (Windows 98). Data recording and stimulus presentation were also monitored by an oscilloscope and by a sound speaker.

2.4 Sound stimuli

Stimulus presentation was controlled by Brainware-software and TDT-2 hardware. A trigger through TG-6 module started sound presentation (DA1, low-pass filtered at 20 kHz through an FT6 module), and data acquisition of both the spike (AD1) and LFP signals. The sounds were presented at the frontal central position at a distance of 100 cm from the monkey by a speaker (Blaupunkt).

Two different types of acoustic stimuli were presented in separate paradigms: (1) pure tones and (2) 500 or 1000 ms of flat broadband noise followed by a spectrotemporally-modulated or dynamic-rippled noise (always lasting 1000 ms). Other stimuli have been presented, but are not analyzed in this thesis (i.e. natural sounds, ripples with varying levels of modulation depths). Pure tones lasted for 150 ms

ranging in frequency from 0.25 to 16 kHz (stimulus spacing: 0.5 x octaves), presented at 4 different sound levels (10, 30, 50, and 70 dB). Those stimuli were each presented at least twice during each experimental session in completely random order. Ripple stimuli were generated according to the study of Depireux et al. (2001) (Fig. 1). The ripples consisted of $n = 126$ simultaneously presented tones with random phase, equally spaced - 20 per octave - along the logarithmic frequency scale, ranging from 250 Hz to nearly 20 kHz:

$$S(t) = \begin{cases} \sum_{n=1}^{126} R(t,x) \cdot \sin(2\pi \cdot f_n \cdot t + \phi_n) & \text{for } -\pi < \phi_n < +\pi \\ \text{with } f_n = f_0 \cdot 2^{(n-1)/20} & \text{for } 1 \leq n \leq 126 \end{cases}$$

Apart from the f_0 component, which had its phase fixed at maximum amplitude ($\Phi_0 = \pi/2$), tonal phase, Φ_n , was randomized between $-\pi$ and $+\pi$. Noise amplitude was modulated by a single sinusoidal envelope, $R(t,x)$:

$$R(t,x) = \begin{cases} 1 & \text{for } 0 \leq t < D \\ 1 + \Delta M \cdot \sin(2\pi(\omega \cdot t + \Omega \cdot x)) & \text{for } t \geq D \\ \text{with } x = \frac{n-1}{20} & \text{for } 1 \leq n \leq 126 \end{cases}$$

Here, t is time in seconds; x is the position on the frequency axis in octaves above f_0 ; ω is the temporal modulation rate, called ripple velocity (RV) (in Hz); Ω the spectral modulation rate, called ripple density (RD) (in cycles/octave, or c/o); ΔM is the modulation depth (MD) of the ripple on a linear scale between 0 and 100%; D defines the duration of the flat — ω and Ω are set to zero — broadband noise at the onset of the stimulus sequence. In the modulated second part ($t > D$), the sign of the ω/Ω ratio sets the upward (>0) or downward (<0) direction with which the amplitude envelope sweeps the spectrotemporal domain. For our ripple stimuli, the modulation depth (MD) was always 100%, and duration D was set to 500 or 1000 ms.

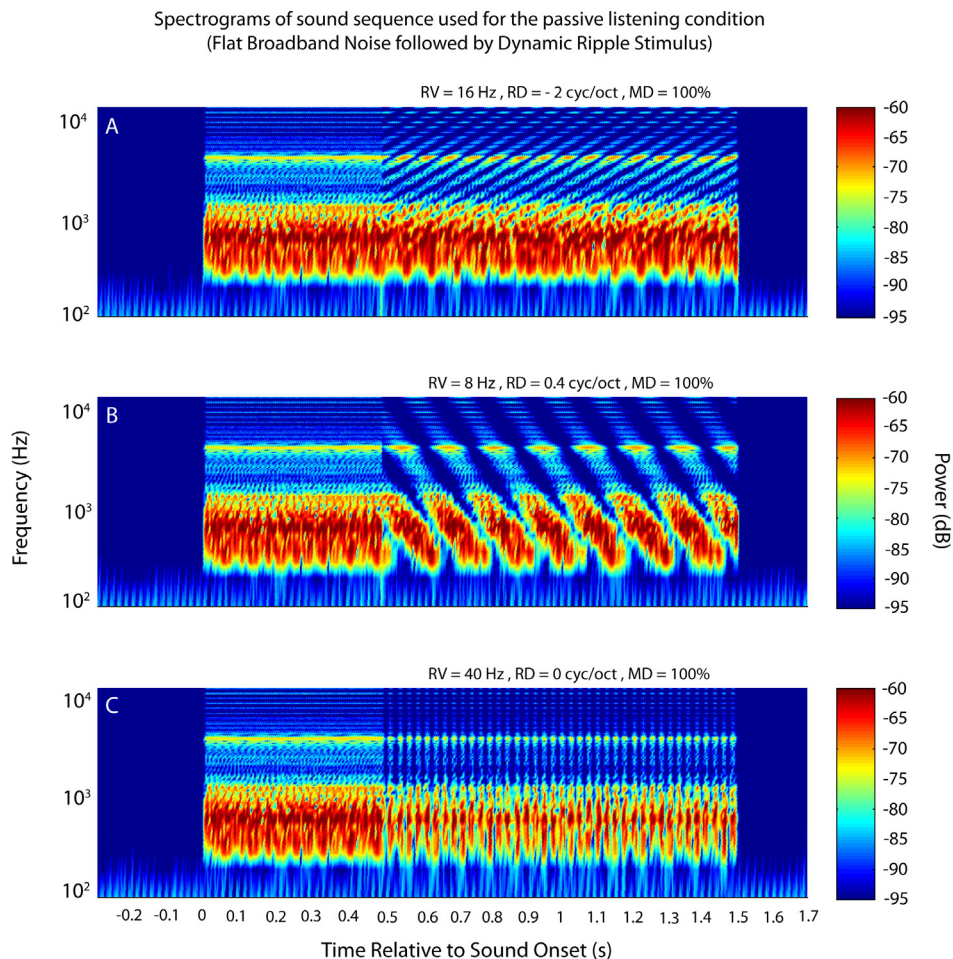


Fig. 1 Spectrograms of sound sequence used for ‘Passive Condition’ and ‘Active 500’. **A.** Spectrogram of Flat Broadband Noise (time: 0 – 0.5 s) and dynamic ripple (time: 0.5 – 1.5 s); RV = 16 Hz, RD = -2 cyc/oct, MD = 100%. **B.** Spectrogram of sound with ripple parameters: RV = 8 Hz, RD = 0.4 cyc/oct, MD = 100%. **C.** Spectrogram of amplitude-modulated noise with ripple parameters: RV = 40 Hz, RD = 0 cyc/oct, MD = 100%. Note that in the Active 1000 trials (not shown), duration of the static period was set to 1000 ms.

2.5 Paradigm

Our experiments consisted of four different paradigms (Fig. 2). These paradigms formed three different experimental conditions: (1) ‘Tone’ (Fig. 2A), (2) ‘Passive’ (Fig. 2B) and (3) ‘Active’ (Fig. 2C, D). During all experimental conditions, the monkey was seated on a primate chair in front of a screen and fixated a straight-ahead fixation light for the entire length of a trial.

In the ‘Tone’ condition (Fig. 2A), we presented a single pure tone, always from 300 to 450 ms recording time, to the monkey with its tonal frequency (0.25 - 0.5 x octaves - 16 kHz) and amplitude (10/30/50/70 dB) varying across trials (see Sound stimuli for details). The monkey passively listened to those pure tones, as its behaviour was not rewarded. Here, each trial lasted 1000 ms.

In the ‘Passive’ condition, after a delay of 300 ms, a flat broadband noise (static sound) was started, which lasted for 500 ms, immediately followed by the presentation of a dynamic ripple, lasting additional 1000 ms (Fig. 2B). As in the ‘Tone’ condition, the monkey passively listened to those sounds, as it had no task and it was not rewarded, nor could it behaviourally influence the initiation of a trial. Each ‘Passive’ trial lasted 2000 ms.

In the ‘Active’ condition (Fig. 2C, D), the monkey had to initiate each trial by pressing a bar. After a

delay of 300 ms, a flat broadband noise (static sound) started, which pseudo-randomly, with equal probability, lasted either 500 ms (Fig. 1; Fig. 2C, ‘Active-500’) or 1000 ms (Fig. 2D, ‘Active-1000’). The static noise was instantly followed by a dynamic ripple of various densities (RD) and velocities (RV) ($RD = -2.0$ to $+2.0$ cyc/oct; $RV = 8 - 40$ Hz), lasting another 1000 ms (see section ‘Sound stimuli’ for details). Note, that in both the ‘Active’ and ‘Passive’ condition, the same acoustic stimuli were used. Yet, in the Active condition, the monkey had the task to intentionally detect the change from flat broadband noise to dynamic ripple, and report his percept by quickly releasing the bar. Whenever the monkey released the bar within 600 ms after ripple onset, it received a reward by a drop of water (Fig. 2C, D). Here, each trial lasted 2500 ms. Trials in which the monkey failed to detect the change in the sound ($RT > 600$ ms) were repeated in the same experiment. During the experiment, the monkey was alert as evidenced by reaction times to the sound change in the Active conditions that were interleaved with the Tone and Passive conditions. Furthermore, the behavior of the monkey was regularly monitored by the experimenter via webcam. The general order of the experiments was “Tone”-“Passive”-“Active”, followed by additional experiments if recording stability was maintained (no effect of order was found in single-unit recordings from two monkeys).

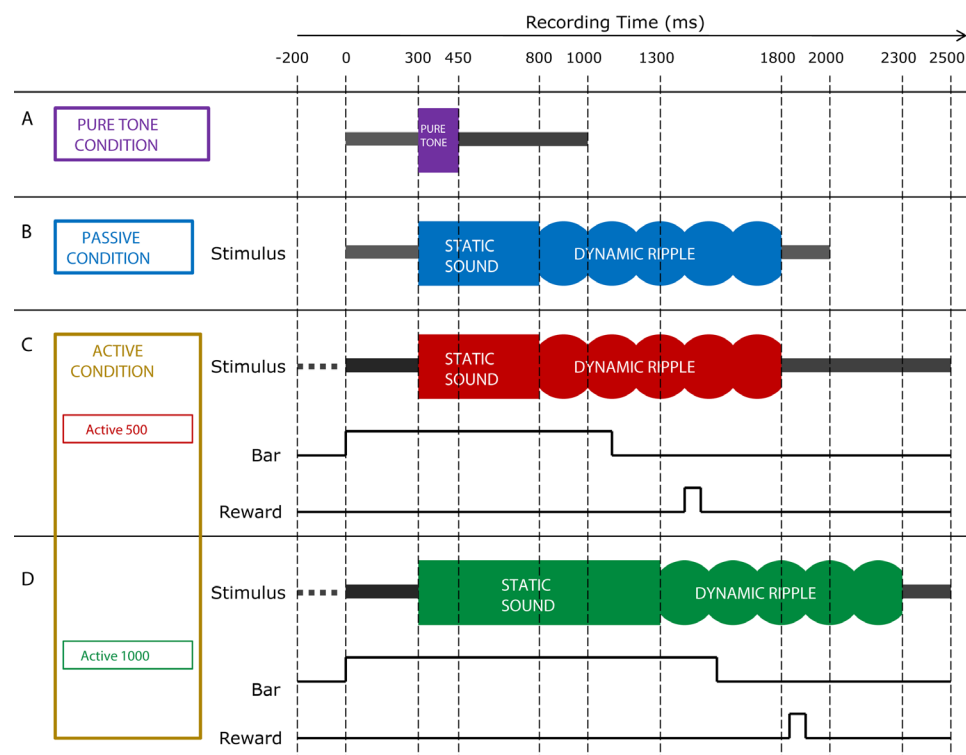


Fig. 2 Experimental paradigms integrated in the three main experimental conditions. **A.** ‘Pure Tone Condition’. **B.** ‘Passive Condition’; duration of static ‘flat broadband noise’ always 500 ms. **C, D.** ‘Active Condition’; here, the static ‘flat broadband noise’ randomly, with equal probability, lasts either 500 ms (‘Active 500’) or 1000 ms (‘Active 1000’).

2.6 Data analysis

All data was analysed in Matlab version 7.6.0 (Natick, MA, USA). A custom-built open-source Matlab toolbox (PandA) was used for specific analysis of the LFP and spike signals (source code can be found at: <http://code.google.com/p/p-and-a/> and tutorials and explanations at: <http://www.mbfys.ru.nl/~marcw/Spike/doku.php>).

2.7 Statistical testing

Statistical testing of the experimental manipulations was conducted by the Statistics toolbox in Matlab and custom-written PandA-routines. We determined 95% confidence intervals around the mean by $\pm 1.96 \times \text{SD} / \sqrt{N}$, with N the number of measurements, and SD the standard deviation in responses across N.

2.8 Line noise removal

Since 50 Hz line noise was a major contributor to the raw LFP data (for illustration see Supplementary Fig. 1), we developed a method to remove those signals from our measurements. First, an algorithm estimated for each LFP trial the magnitude and phase of the 50 Hz line noise on the basis of the raw LFP signal by optimal non-linear fitting for amplitude and phase (Matlab function: *nlinfit*). Subsequently this estimated sinusoid was subtracted from the raw LFP signal (Gieselmann & Thiele, 2008).

3. Results

3.1 Database

We studied the response patterns of monkey auditory cortex (AC) by recording from the left side of the brain of one awake, trained rhesus monkey. The total number of analyzed recording sites for the Tone, Passive, and Active conditions (Fig. 2) were 46, 10 and 10, respectively (Table 1).

3.2 Line noise removal from LFP

Supplementary Fig. 1 shows how effective the line-noise removal method, as assessed in the Methods section for simulated traces, was in removing line noise from one LFP recording. In the example raw trace (Supplementary Fig. 1A, taken from the Tone condition, where the monkey was passively listening to a pure tone of frequency 1 kHz and intensity 30 dB, lasting 150 ms), the LFP is strongly dominated by a line-noise component, which pops up at 50 Hz in its power spectrum (Supplementary Fig. 1B).

After applying the line noise removal method for this trace (Supplementary Fig. 1D, non-linear fitting for amplitude and phase, and assuming exactly 50 Hz frequency), a strong LFP enhancement by pure tone stimulation (Freq: 1 kHz; Intensity: 30 dB) at this A1 recording site is clearly visible (Supplementary Fig. 1C).

Thus, the line-noise removal method works well, removing 50 Hz noise and preserving systematic LFP modulations.

Table 1. Summary of numbers of recorded sites and selection criteria for analysis

Condition	Total number of measurement sites from monkey AC	Number of measurement sites excluded from data analysis	Reasons for removal from data analysis with number of measurement sites concerned	Number of sites effectively used for data analysis
Pure tone condition	51	5	too much remaining 50 Hz line noise (2), Rec. time only 900 ms (2), Just 52 trials recorded (1)	46
Passive condition (ripple)	61	51	comparison file (Active condition) not usable: required stimulus and trial information (e.g. ripple onset) not properly saved (7), too much remaining 50 Hz line noise (1), cell not recorded during Active condition (43)	10
Active condition (ripple)	13	3	too much remaining 50 Hz line noise (1), recording time too short to compute baseline for proper spectrogram computation (2)	10

3.3 Overall enhancement of LFP power during pure tone presentation

Supplementary Figure 2A and B show two example measurement sites. LFP power of one measurement site (Supplementary Fig. 2A) is enhanced by tone presentation while for the other measurement site (Supplementary Fig. 2B) it remains at spontaneous-activity levels. Supplementary Figure 2C shows the average LFP power during tone presentation against the spontaneous activity for all measurement sites (# sites = 46; sites of Supplementary Fig. 1A and B are marked). Most of the points in Supplementary Figure 1C lie above the unity ($x=y$) line, indicating that the average power is higher during tone presentation than during spontaneous activity for most of the measurement sites (42 out of 46). Combined, these recording sites respond significantly to tone presentation (difference in power (tone – spontaneous): $t(45) = 7.1539$; $p < .01$; 95% CI: 1.37 - 2.44 dB).

Furthermore, LFP power (averaged across all sites) was enhanced for the entire LFP frequency range between 1 and 200 Hz (Supplementary Fig.

2D; note that the 95% confidence interval of the mean difference in power between tone presentation and spontaneous activity lies above 0).

3.4 Frequency tuning in LFP signals

In the ‘Tone condition’, tones were presented at various frequencies and intensities. Typically, each tone was presented 4 times during one experimental session, though occasionally a larger number of repetitions was chosen by the experimenter. Figure 3 provides a summary for one representative recording site (“Thor-2010-06-11-0002”) about how LFP modulation depended on tonal frequency. Figure 3A shows that the LFP signal for this site is enhanced during the presentation of a specific 250 Hz, 70 dB tone (red). This enhancement is also evident in the power spectrum (Fig. 3B) at all LFP frequencies when comparing tone-presentation (red) vs spontaneous activity (blue). Figure 3C shows a trial for the same measurement site but a different tone (4 kHz, 70 dB). For this tone, the LFP amplitude does not significantly change ($p > .05$), and LFP power is about equal for almost the entire

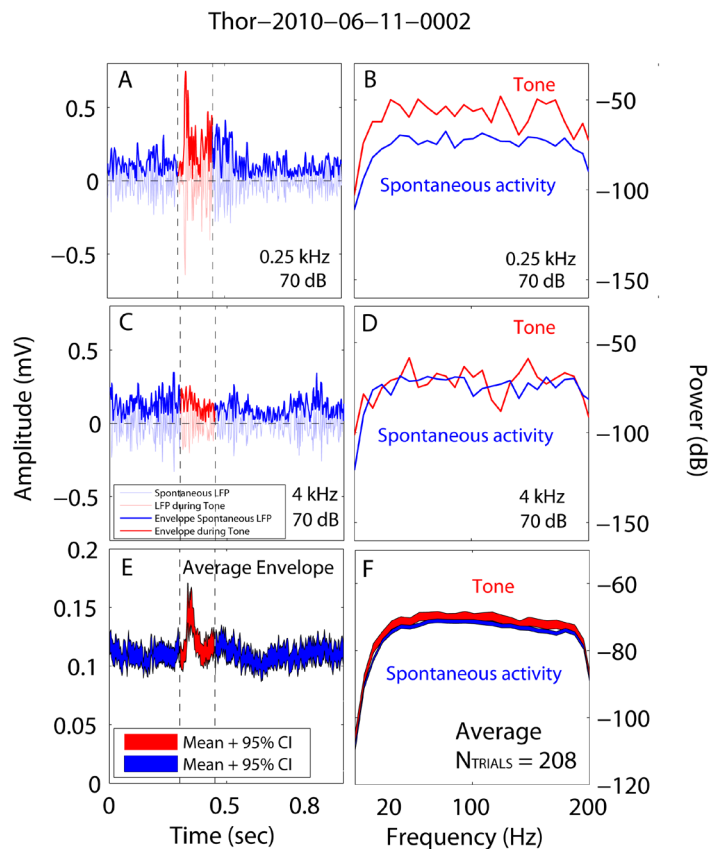


Fig. 3 A. LFP recording that is sensitive to the frequency of a pure tone. Hilbert envelope marked by darker color. **B.** Power spectrum of LFP trial presented in A. **C.** LFP recording that is apparently not responsive to presence of pure tone as indicated by changes in LFP amplitude. Hilbert envelope marked by darker color. **D.** Power spectrum of LFP trial presented in C. **E.** Averaged Hilbert envelope including 95% CI, pooled over all trials (Ntrials = 208). **F.** Average power including 95% CI, pooled over all trials (Ntrials = 208). CI = confidence interval.

LFP frequency range (Fig. 3D).

Figure 3E presents the coarse average Hilbert envelope (representing the average LFP amplitude) over all (208) trials for this recording site, thus neglecting such a tonal-frequency effect. Clearly, for this measurement site, the LFP amplitude is still significantly (indicated by 95% CI) modulated by the presence of a pure tone, and LFP power during tone presentation is noticeably higher than during spontaneous activity for nearly the entire LFP-frequency range (Fig. 3F). This effect is present despite the fact that the LFP signal (e.g. Fig. 3C) is not evidently modulated by presentation of every tone.

In order to quantify the frequency-tuning properties of the recording sites, we computed the root-mean-square (RMS) of the LFP signal (averaging over repetitions), for every unique tone (see Methods section for details) during tone presentation, and during spontaneous activity. By dividing these two RMS values, corrected RMS values (cRMS) were obtained, which indicate the degree of LFP enhancement above spontaneous level resulting from presentation of a specific tone. For instance, a cRMS value of 2 means that the average LFP amplitude computed over the tone period was two times larger than during spontaneous (no-tone) activity.

In Supplementary Figure 3A, we present an LFP tuning curve for one measurement site, obtained by this method. Moreover, the tuning curve of the single-neuron spike data for the same measurement site is also shown. The LFP tuning curve is quite similar to the spike tuning curve. The maximum response (best frequency; BF) lies within the same frequency range (about 0.25 – 1 kHz) for both measurement types. Furthermore, both LFP and spike responses are increasing with growing sound intensities. However, the spike data seems to differentiate more between tonal frequencies at lower sound intensities than the LFP response (compare Supplementary Fig. 3B with D).

Another measurement site is presented in Supplementary Figure 4. Again, frequency tuning is present in both the LFP and the spike data. As in Supplementary Figure 5, the tuning curves are quite similar for both response types. However, here, the LFP response shows sharper frequency selectivity at lower sound levels than the spike response. Moreover, the spike response is more narrowly tuned (BF ~0.75 kHz).

In order to quantify the amount of LFP frequency tuning for all our recordings, we fitted a Gaussian (Supplementary Fig. 5A; blue curve) through

the average cRMS value (indicated by red line in Supplementary Fig. 3A, 4A, 5A for illustration), and determined the amplitude (response magnitude) and width (frequency selectivity; 2 times the standard deviation of the fitted Gaussian, also called sigma, with unit 0.5 octave). This method was invalid for recording sites with a maximum response at the extreme ends of the sound-frequency range (0.25 kHz and 16 kHz). Those measurement sites were therefore excluded from this analysis, as were those sites where the goodness-of-fit of the model (R), was below 0.55. Accordingly, 35 different recording sites were in this tuning analysis. Two of those measurement sites either produced an extreme estimate of amplitude or sigma, and were classified as outliers, and also omitted from the population analysis.

Supplementary Figure 5B depicts the amplitude and tuning width for the remaining 33 recording sites. Amplitudes vary between 0 and 1, while width varies between 0 and 4.2 (octaves). Widths tended to be larger with increasing amplitudes (a linear fit).

3.5 Time-frequency representation of LFPs during active and passive listening

For a more in-depth analysis of the changes in LFP power over frequency and time, we determined the spectrogram or time-frequency representation (Hanning window 64 ms wide; frequency resolution of 3.9063 Hz).

Supplementary Figure 7A-C shows spectrograms of example LFP traces for a single ripple (density 0.8 cyc/oct, velocity 24 Hz and modulation depth 100%), of the recording site in Supplementary Figure 6 ('thor-2009-09-24'), for each of the three ripple paradigms (Supplementary Fig. 7A-C; A – Passive Condition; B – Active-500; C – Active-1000). Furthermore, as a reference, below each LFP trace, we also present the instantaneous firing rate (spikes/s) for those conditions.

In the Passive condition (Supplementary Fig. 7A), LFP power increases notably (red color, about 25 dB) and transiently at frequencies near 12-28 Hz (beta band) and near 50-70 Hz (gamma band), shortly after sound onset. After ripple onset, LFP power again transiently increases for the same frequency bands. Some power increases occur during ripple presentation, again at the same frequency bands. The spike firing rate (Fig. 7G) shows similar patterns, with increases around sound onset and again at about 70 ms after dynamic-ripple onset. For the Active paradigms (Supplementary

Fig. 7B, C), the spectrograms show more variability in LFP power than in the Passive Condition. For the Active-500 trial, the firing rate (Supplementary Fig. 7H) does not seem to be modulated by sound onset, ripple onset or bar release. In contrast, for the Active-1000 trial, the spike firing rate does increase after ripple onset, with only a small sound-onset response (Supplementary Fig. 7I).

Supplementary Figure 8 shows the average spectrograms for all three ripple paradigms (A-C) of the recording site described in Supplementary Figures 6 and 7, while Supplementary Figure 9 shows another example recording site (sites thor-2009-09-24 and thor-2009-10-22, respectively). In addition, the average power across frequency (D-F) and the average power across time over the first 150 ms after ripple onset (J) (normalized to the peak values of the Passive condition) is plotted. Both recordings show an increase (at least 12 dB) in power immediately after sound onset in the Passive conditions (Supplementary Fig. 8/9A, D), which is significantly larger ($p < .05$; 95% CI) than the increase during either Active conditions (Active500, Supplementary Fig. 8/9B, E; Active1000, Supplementary Fig. 8/9C, F). The LFP change for the first 150 ms after the ripple onset is quite similar for the Passive Condition

vs. the Active paradigms (Supplementary Fig. 8/9J), with a pronounced onset peak for site “thor-2009-09-24” (Supplementary Fig. 8D-F) in the beta and gamma bands (Supplementary Fig. 8J), and no onset peak for “thor-2009-10-22” (Supplementary Fig. 9D-F).

However, after the initial 150 ms, the average spectro-temporal response (spectrograms) differs clearly between the Passive and the Active conditions. In the Active paradigms, there is a general increase in LFP activity for “thor-2009-09-24” (Supplementary Fig. 8A-C), and a strong transient LFP increase ~250 ms after ripple onset for “thor-2009-09-22” (Supplementary Fig. 9A-C), which is absent in the Passive condition. Interestingly, the average spike firing rates, shown in Supplementary Figures 8 G-I and 9G-I, differ from their LFP counterparts during these periods (e.g. with strong sound-onset peaks). While in the Passive condition the response pattern of the LFP power almost equals the single-neuron spike data, for the Active paradigms changes in LFP power cannot fully be understood by the single neuron data; for the spike data “thor-2009-09-24” (Supplementary Fig. 8H) now shows a second transient peak, that is no longer present for “thor-2009-10-22” (Supplementary Fig. 9I).

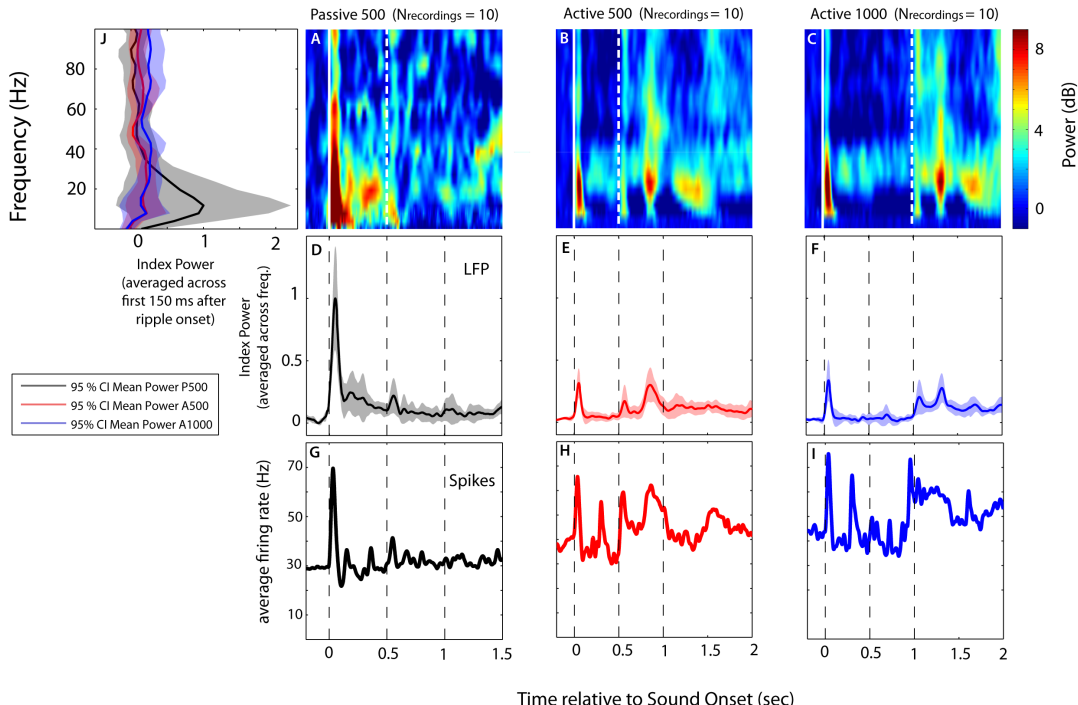


Fig. 4 Spectrogram, average LFP power and Single Neuron Spike data pooled over 10 different pairs of recording sites separately for all three relevant paradigms, aligned to sound onset. **A.** Average spectrogram ($N_{sites} = 10$) for Passive paradigm. **B.** Average spectrogram ($N_{sites} = 10$) for Active 500 paradigm. **C.** Average spectrogram ($N_{sites} = 10$) for Active 1000 paradigm. **D.** Standardized LFP power for Passive paradigm, averaged over LFP frequency (1-100Hz). **E.** Standardized LFP power for Active 500 paradigm, averaged over LFP frequency (1-100Hz). **F.** Standardized LFP power for Active 1000 paradigm, averaged over LFP frequency (1-100Hz). **G.** Average Firing Rate across time for Passive paradigm. **H.** Average Firing Rate across time for Active 500 paradigm. **I.** Average Firing Rate across time for Active 1000 paradigm. **J.** Standardized LFP Power averaged over first 150 ms after Ripple Onset.

LFP modulations were mainly caused by activity in the beta frequency range (12-28 Hz) ($p < .05$). LFP power in the gamma frequency range (30-100 Hz), when observed, tended to be slightly larger in each of the Active paradigms than in the Passive Condition (Supplementary Fig. 8J).

In order to get a better insight into the general effects of our experiments on the LFP and single-neuron signal patterns, we conducted the same analysis as presented in Supplementary Figures 8 and 9, but pooled the data for 10 different pairs of recording sites, as depicted in Figure 4. For the Passive Condition, there is a large LFP increase immediately following sound onset (Fig. 4A, D), mostly driven by beta band activity (Fig. 4J, black), which is significantly higher ($p < .05$; 95% CI) than the transient LFP enhancements of the two Active paradigms (Fig. 4J, red and blue). Furthermore, on average, there is a slight transient LFP increase shortly after ripple onset which is about equal in size for all three conditions (Fig. 4A-F) and not significantly driven by any specific frequency band (Fig. 4J). However, for the Passive condition, beta activity has a relatively higher average LFP power shortly after ripple onset (first 150 ms) (Fig 4A,J). Furthermore, in both Active paradigms, there is a second transient LFP enhancement ~ 250 ms after ripple onset (Fig. 4 Active paradigms, Fig. 5A). This increase has its peak ~ 30 ms earlier for the Active-1000 paradigm compared to the Active-500 paradigm (Fig. 5A). Both transient peaks are primarily driven by increased activity in the beta frequency range ($p < .05$; Fig. 5B). For the Passive Condition, the LFP power pattern across time

resembles the single-neuron (spike) data (compare Fig. 4D with G). For the Active paradigms, however, there are more transient increases in the spike data compared to the LFP data (cf. Fig. 4E,F with H,I). Note also, that due to averaging over sites, we may have lost other differences between conditions (see for example Supplementary Fig. 8 and 9).

3.6 Response times and LFP modulations at bar release

Supplementary Figure 10 shows the response-time distribution, separately for Active-500 (red) and Active-1000 trials (blue), for two different measurements (Supplementary Fig. 10A and B), and for all 10 sites pooled (Supplementary Fig. 10C). In all three graphs, the distribution (peaks representing highest occurrence of response time) of the Active-1000 trials is clearly shifted in the direction of smaller response times, relative to the Active-500 distribution. For the Active-500 trials, there are almost no response times below about 300 ms. In contrast, for the Active-1000 paradigm, a considerable part of the responses might be considered predictive, some being smaller than 200 ms. Consequently, Active-1000 response times were significantly smaller ($t(15.9) = 18.39$, $p < .01$) than Active-500 response times.

We wondered whether LFP modulations can be linked to these behavioral responses (moment of bar release) of the monkey. More specifically, we wanted to investigate whether there is a specific LFP-frequency range wherein LFP changes are related to the moment of bar release. Furthermore,

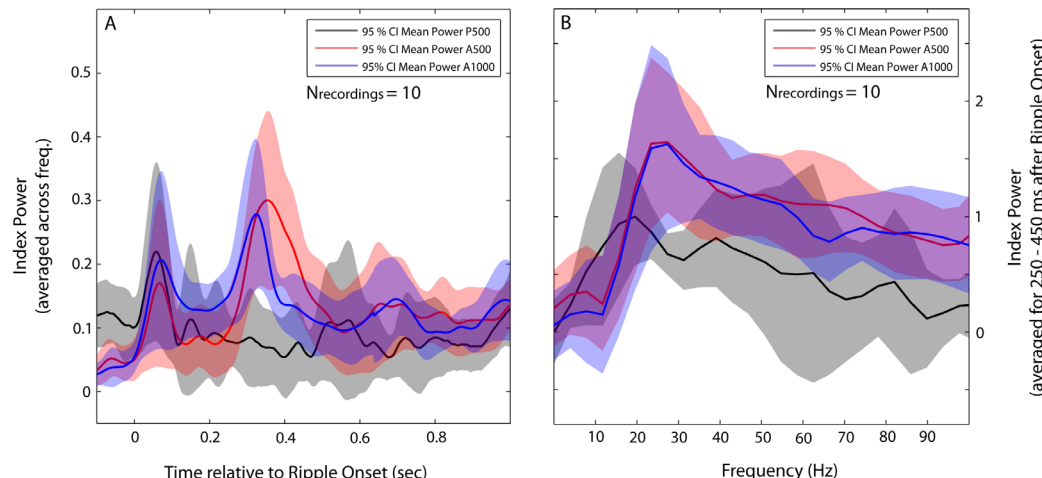


Fig. 5A. Standardized power including 95% CI for the three main paradigms, averaged across LFP frequency (0-100 Hz) pooled over 10 different recording sites, aligned to ripple onset. **B.** Standardized power per LFP frequency (0-100 Hz) including 95% CI pooled over 10 different recording sites averaged over the period 250 ms-450 ms after ripple onset. Note that here, average power was always standardized with respect to the 'Passive Condition', which was scaled to values between 0 (minimum average LFP power Passive Condition) and 1 (maximum average LFP power Passive Condition). CI = Confidence Interval.

we wanted to know whether the learned expectancy during Active-1000 trials, indicated by the behavioral data through significantly shorter response times ($p < .01$), would also have a neuronal correlate in A1, which could be measured by LFPs. We therefore aligned all data to the moment of bar release for further analysis.

Supplementary Figures 11 and 12 show the LFP spectrograms for two recording sites (the same as in Supplementary Figs. 8/9), for the Active-500 and Active-1000 conditions. For the Active-500 paradigm, both examples show a transient LFP increase during the 120 ms prior to bar release (Supplementary Fig. 11/12). This increase is for both sites predominantly in the beta frequency range ($p < .05$), with some minor contribution from the gamma frequency range (Supplementary Fig. 11A, G / Fig. 12A, G). For the Active-1000 paradigm, we observe the same effect (Supplementary Fig. 11 / 12B, G, D). For both paradigms, the single neuron data (Supplementary Fig. 11 / 12E and F) resemble the LFP data (Supplementary Fig. 11 / 12C, D). Note that, given the average reaction time of 300–400 ms, the transient activity increase at ripple onset (Supplementary Figs. 8–9; Fig. 4) representing

exclusively acoustic processing) is still present in our data, at 300–400 ms prior to bar release.

Figure 2.4 depicts the same analysis when pooling the data over 10 recording sites. The transient LFP increase in the 120 ms prior to bar release is evident for both active paradigms (Fig. 6C, D). Again, we find that the transient power enhancement in the beta frequency range is the most important source of the overall power increase in the examined time window (-120 – 0 ms re bar release) for both active paradigms (Fig. 6A, B, G).

At first sight, there also seemed to be a transient LFP increase in higher gamma power (82–90 Hz) in the Active-1000 paradigm relative to the Active-500 paradigm (Supplementary Fig. 13A, B, G) prior to bar release. However, this enhancement in the higher gamma frequency range was not significant ($p > .05$), and was caused by one outlier ('thor-2009-10-07'; Supplementary Fig. 13). Thus, only the beta frequency band of the LFP contributed significantly ($p < .05$) to the observed transient LFP enhancement shortly before bar release. The single-neuron activity pattern (2.4E, F) is quite similar to the LFP data with increasing average spiking activity in the same time window for both active paradigms (Fig. 2.4E, F).

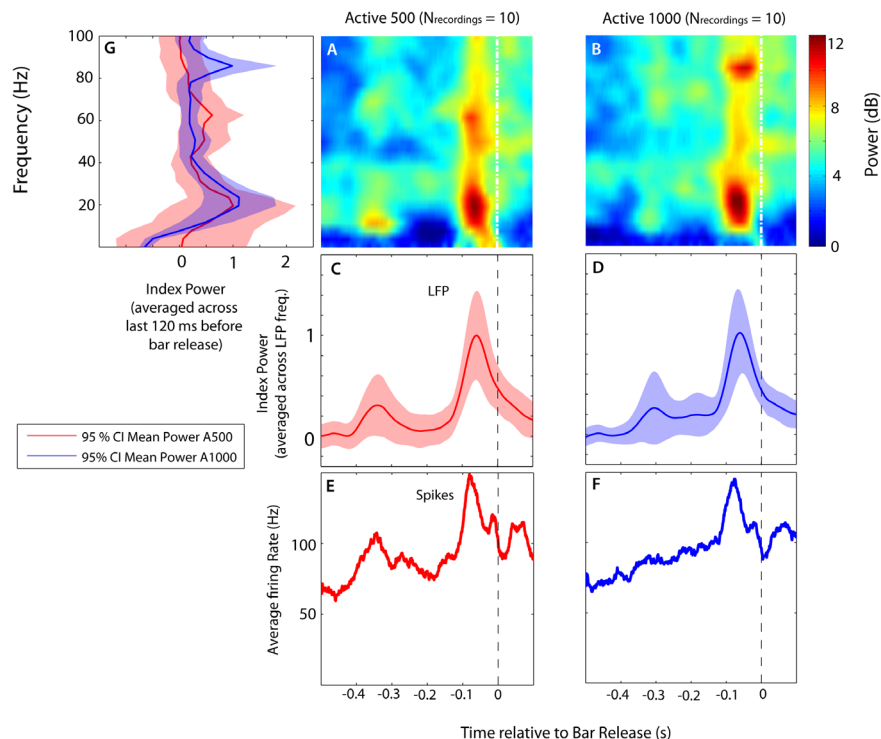


Fig. 6 Spectrogram pooled over 10 different recording sites when data are aligned to time of releasing response bar (here time zero; marked by vertical dashed line!). **A.** Average spectrogram Active 500. **B.** Average spectrogram Active 1000. **C.** Standardized LFP power Active 500, averaged over LFP frequency (1–100 Hz). **D.** Standardized LFP power Active 1000, averaged over LFP frequency (1–100 Hz). **E.** Average Firing Rate (spikes) across time Active 500. **F.** Average Firing Rate (spikes) across time Active 1000. **G.** Standardized LFP power averaged over last 120 ms before bar release, separately for Active 500 paradigm (red) and Active 1000 paradigm (blue). Note that here all data has been first aligned to moment of bar release and time is plotted relative to moment of Bar Release (vertical dashed line).

4. Discussion

This study set out to investigate whether cells in primate primary auditory cortex (A1) are solely coding for the acoustic properties of sound (frequency and sound level), in a bottom-up fashion, or whether those cells are also modulated by task-dependent, top-down, variables. More specifically, we wanted to test whether local field potentials (LFPs) can provide information about these sensory and cognitive processes in auditory cortex. By simultaneously recording single cell activity (spikes) as well as local field potentials from left primate auditory cortex of an awake, trained rhesus monkey, by means of one single microelectrode (1-2 MΩ), we tried to answer those research questions. While measuring, during several experiments, the monkey was either assumed to be in a passive listening state or an active listening state, since it was required to actively respond to specific sound stimuli (Fig. 1, 2; see Methods section for details).

4.1 LFP measurements

The LFP represents the summed activity of synchronous synaptic potentials (Mitzdorf, 1987) and action potentials (Logothetis, 2003; David, Malaval, & Shamma, 2010). It is typically acquired by low-pass filtering the raw multiunit electrode signal at 300 Hz (Delano, Pavez, Robles, & Maldonado, 2008) or lower (cut-off) frequency (up to about 100 Hz) (Chandrasekara, Turesson, Brown, & Ghazanfar, 2010), depending on the LFP frequency range one is interested in. Accordingly, in this study, we extracted LFP traces from single-unit recordings with a single electrode by low-pass filtering the raw multiunit electrode signal at 300 Hz.

As the LFP signal constitutes a low-pass filtered signal, there is the possibility of the spike signal leaking into the LFP signal. More specifically, a strong correlation between single-unit activity and the LFP signal may simply be the result of spiking activity that failed to be removed by low pass filtering (David et al., 2010). This consideration is especially relevant for this study, since our main goal during recording was to obtain a good single-unit signal and both signals were simultaneously acquired by the same electrode. Consequently, we initially tried to remove features correlated with spike events from the LFP recordings by specific linear fitting techniques, in the same way as proposed by David et al. (2010). Yet, due to the relatively high firing rates, this approach removed most of the LFP signal from

our data (not shown).

Interestingly, Sridharan, Boahen and Knudsen (2011) faced a similar problem while recording in the optic tectum of the barn owl. To deal with the high-rate burst-activity of the neurons in this midbrain structure, they developed a new spike removal method (not discussed here in detail). Yet, as this specific method requires a raw signal, bandpass filtered between 2.2 Hz (high-pass cutoff) and 7.5 kHz (low-pass cutoff), we could not apply it on our data, as we had previously segregated the raw electrophysiological data into a low-pass filtered LFP signal and a high-pass filtered spike signal by hardware (see Methods).

Thus, we eventually did not control for potential leaking of spike power into the LFP. Therefore, at least some of the information carried by our LFP signals might be due to spiking activity of a single neuron. Yet, our actual LFP data reveal increases in specific frequency bands (predominantly beta, see Supplementary Figs. 8 and 9; Fig. 4 and Fig. 5B) and the LFP and spike signals are not identical (particularly in the Active condition; e.g. see Supplementary Fig. 8, 9 and 12; Fig. 4).

So, although we did not control for the contribution of spike activity to the LFP signal, we still believe that the LFP signal contains additional information about sensory and cognitive auditory processing.

4.2 Frequency tuning to tones is reflected in LFP activity

In this study, our aim was to measure neuronal activity from primate primary auditory cortex (A1). As it is known from many single-cell recording studies, this area (A1) is characterized by short-latency neuronal responses to tones with narrow frequency tuning and it is organized with a characteristic frequency (CF) gradient from high frequency to low frequency in the caudal to rostral direction (Kosaki, Hashikawa, He, & Jones, 1997; Merzenich & Brugge, 1973; Morel, Garraghty, & Kaas, 1993; Rauschecker, Tian, Pons, & Mishkin, 1997; Recanzone, Guard, & Phan, 2000).

Frequency tuning means that the cell response is maximal for a specific tonal frequency, and becomes smaller as the difference between the tonal frequency and CF increases. In addition, it is also already well established that single-neuron responses in A1 is also modulated by sound intensity (Noreña & Eggermont (2002); Polley, Steinberg, & Merzenich, 2006; Recanzone et al., 2000). Consequently, on the

basis of the spike firing pattern of a neuron one can derive the classical frequency-tuning curve which typically approaches the shape of a Gaussian (see also Supplementary Fig. 5A for an illustration).

A recent study by Lui and Newsome (2006) established LFP tuning curves for speed and direction of a visual stimulus acquired from the middle temporal visual area (MT). Similarly, we computed LFP frequency-tuning curves from A1 sites, acquired during passive listening to tones of various tonal frequencies and intensities (Tone condition; Fig. 2). As shown in figure 3A-D for one measurement site, LFP power is significantly modulated ($p < .05$) by a specific tonal frequency, with constant sound intensity (e.g. compare Fig. 3A with C). This enhancement is observed over the entire LFP frequency range (1-200 Hz) (Fig. 3B).

By computing the average root mean square error (RMS) during tone presentation, separately for each combination of tonal frequency and intensity, frequency tuning curves were successfully constructed from LFP data (Supplementary Fig. 3A, B / 4A, B) for two measurement sites. These tuning curves were similar to the single-neuron tuning curves (Supplementary Fig. 3, 4). The CF appears to be accurately estimated by the LFP data, since it is similar for both LFP and spike measurement. Furthermore, within the specific tonal frequency presented, responses are generally larger with increasing sound level (e.g. Supplementary Fig. 3A). These results are in accordance with a study by Noreña and Eggermont (2002) who have compared the LFP (1-100Hz) with multi-unit cluster activity in auditory cortex of the cat. They have found that the computed CF based on LFP data was not significantly different from the CF based on the multi-unit spike data.

Another corresponding result was their discovery (Noreña & Eggermont, 2002) that frequency tuning curves were significantly broader for the LFP recordings compared to the respective MU recordings. Our data also show that the single neuron is more narrowly tuned (most evident in Supplementary Fig. 4) than the LFP data. This might be because the LFP signal, signifying synchronous activity of groups of neurons around the electrode tip, is expected to give a more blurred output due to differences in response strength and synchrony to a specific tonal frequency between neighboring neurons.

Frequency tuning properties for all our measurement sites were characterized by fitting a Gaussian through the frequency tuning data, pooled over sound level (Supplementary Fig. 5A), thereby

estimating tuning width and strength. We were able to show that tuning width and strength (for 33 sites; see results for details) are moderately correlated ($r = 0.44$; Supplementary Fig. 5B). Furthermore, for most of our recording sites (42 out of 46) LFP power increased by the presence of a tone (Supplementary Fig. 2C) even when averaged across tonal frequency. This average enhancement of about 2 dB was significant ($p < .05$) when examined over all (46) recording sites and was found across the entire LFP frequency range (1-200 Hz; Supplementary Fig. 2D). Thus, even though we averaged over various tonal frequencies and intensities, a significant increase of LFP amplitude was observed.

To summarize, frequency tuning is evident from LFP signals, and resembles those based on the spike data. Sound frequency and level are both important, with frequencies near CF and increasing sound intensities resulting in larger responses for both LFP and spike measurements.

4.3 Active vs. passive listening

In these experiments, the monkey was either passively listening to a sound sequence (Tone condition; Passive condition; Fig. 2A, B) or actively listening (Active condition; Fig. 2C, D). In the Active condition the monkey had to actively respond to a specific sound change (ripple onset) by releasing a bar for which it was rewarded by a drop of water, if it released the bar in time ($RT < 600$ ms). We assumed that the monkey is in a different behavioral state when actively listening compared to when passively listening to sound. Furthermore, the monkey could have learned for the active condition (Supplementary Fig. 10) that the static sound would change certainly into a dynamic ripple at 1000 ms after sound onset, if it did not occur at 500 ms. This greater expectancy of the monkey during the Active-1000 condition was clearly evident from the shorter response times (Supplementary Fig. 10). This anticipation, we reasoned, might also be expressed in A1, observable in the spikes and/or LFPs. In fact, this idea is supported by several recent studies (Atiani, Elhilali, David, Fritz, & Shamma, 2009; Fritz, Shamma, Elhilali, & Klein, 2003; Massoudi et al., in preparation; Roux, Mackay, & Riehle, 2006; Wang, Lu, Snider, & Liang, 2005).

Indeed, our data show that these different behavioral states of the monkey are reflected in the LFPs. More specifically, LFP power is differently modulated in the Passive, Active-500 and Active-1000 conditions (Supplementary Fig. 6). For instance,

when the monkey is actively listening, spiking activity is increased even when no sound is presented (Massoudi et al., *in preparation*). Peak activity is lower after sound onset for the Active conditions. Furthermore, there are remarkable differences in the spectrograms, especially between the Passive and Active conditions (Supplementary Fig. 7, 8 and 9; Fig. 4 and 5). These LFP modulations in time and frequency are complex and dynamic and can, within the two Active listening paradigms, clearly deviate from the Spike response pattern (e.g. compare Fig. 4E and F with Fig. 4H and I). Obviously these patterns suggest top-down modulations due to the behavioral state of the monkey, and are not driven by simple acoustic, bottom-up processes, as these processes were the same in all paradigms.

4.4 Beta activity

In this paper, we considered the beta frequency range to cover LFP frequencies from 12-28 Hz. By means of spectrogram computation, we were able to demonstrate that LFP changes in the beta frequency range are reliably evoked and induced in primate primary auditory cortex in response to task-specific (auditory) events (e.g. sound onset: Fig. 4; bar release: Fig. 6). In fact, transient increases in beta LFP power was found for all conditions after tone onset, sound onset, and in relation to ripple onset. Those effects seem aspecific. How can we understand these transient enhancements of beta power of the LFP in A1?

At present, the functional role of oscillatory neural activity in the beta frequency range, known as the ‘beta rhythm’, is still unclear (Zhang, Chen, Bressler, & Ding, 2008). There have been several studies on the functional role and physiological origin of the beta rhythm (Jensen et al., 2005; Salenius & Hari, 2003; Brovelli et al., 2004). However, there is no accepted, unifying theory on its role for cognitive brain function (Engel & Fries, 2010). Most studies on the beta rhythm have focused on its possible role in sensorimotor functioning, often exclusively measuring from sensorimotor and motor cortex. A huge amount of these studies have been conducted with human subjects by electroencephalography (EEG) or magnetoencephalography (MEG), though there are also some studies employing invasive, electrophysiological methods such as single-cell recording in the awake monkey brain. Research with animals and humans has shown for instance, that beta band activity is particularly evident during steady contractions, is attenuated by voluntary

movements and at maximum during holding periods following movements (Baker, 2007; Baker, Olivier, & Lemon, 1997; Chakarov et al., 2009; Kilner et al., 1999; Klostermann et al., 2007; Riddle & Baker, 2006; Sanes & Donoghue, 1993). The decline of beta power (desynchronization) in sensorimotor and motor brain areas relative to a baseline is considered a reliable marker of the onset of movement preparation, movement execution and even motor imagery (Kuhn et al., 2004; Pfurtscheller & Lopes da Silva, 1999; Pfurtscheller & Neuper, 1997; Pfurtscheller, Neuper, Andrew, & Edlinger, 1997; Zhang et al., 2008).

As far as we know, there are no reports specifically discussing the role of (transient) beta power enhancement of the LFP in primate auditory cortex concerning acoustic and cognitive processing, yet. However, based on a MEG study by Mäkinen and colleagues (2004), we think that the significant beta power increase, immediately following sound onset (e.g. Fig. 4), might be mainly explained by the typical sequence of evoked auditory responses (MEG: P50m, N100m and P200m) reliably following the onset of a tone of fixed frequency following a period of silence. This beta enhancement shortly after sound onset is clearly present in all spectrograms aligned to sound onset and we think that it is mainly driven by acoustic processing, though its average magnitude is significantly higher ($p < .05$) during passive listening (e.g. compare 4D with E,F) compared to active listening. Beta power shortly after ripple onset (first 150 ms) was only notably enhanced in the Passive condition (Fig. 4A,J). Thus, passively listening to the change of an auditory stimulus evokes a brief enhancement of LFP power in the beta frequency range in primate auditory cortex which is in fact absent during active listening, when a behavioral response is required. Hence, we think that beta enhancement due to a sound change can be attenuated by top down factors such as behavioral relevance of an incoming sound change. This might facilitate the efficiency of sensorimotor integration, though a theory supporting this view is not known to us. In addition, we observed a significant temporary enhancement ($p < .05$) of LFP beta power between about 250 to 450 ms after ripple onset (Fig. 4B, C; Fig. 5), which was only present in the Active condition. We are of the opinion that this specific beta power increase is mainly due to the monkey preparing a response (Fig. 6), since the timing of the average increase corresponds quite well with the maxima of the respective response time distributions (Supplementary Fig. 10). By aligning the spectrograms of each LFP trial to the

moment of bar release, we were able to show that average beta power of the LFP acquired from monkey A1 is significantly temporarily enhanced between about 120 ms to 10 ms before bar release (Fig. 6). This particular finding is not in line with results from studies measuring from sensorimotor and motor areas. On the contrary, in our study, we identified LFP beta power enhancement (synchronization) in A1 as a likely indicator for motor preparation whereas studies measuring from sensorimotor and motor cortical areas generally propose beta power attenuation (desynchronization) as a reliable neuronal correlate of the planning of a motor action. On the other hand, of course, these differences could simply be the result of the fact that our and the respective other studies are based on measurements from different, outlying neuronal, cortical structures.

In a recent paper, Engel and Fries (2010) have proposed a new, unifying theory about the functional role of oscillatory neuronal activity in what they considered, the beta frequency range (13-30 Hz). Based on results from earlier experiments with healthy human subjects and animals and with certain human clinical groups (e.g. Parkinson's patients), they suggest that beta band activity and/or coupling in the beta-band range are expressed more strongly if the maintenance of the status quo is intended or predicted, than if a change is expected. Hence, in mechanistic terms, they believe that beta band activity promotes the maintenance of the current sensorimotor set during the next processing step, therefore signaling the status quo. They believe that this mechanism is functional for both, sensory and motor circuits. Our results, however, are opposite to what the hypothesis of Engel and Fries would predict. We identified significant beta band enhancement (synchronization) in primate A1 in a time window (120 ms to 10 ms before bar release) when a change of the status quo is highly likely to be expected by the monkey. For this kind of predictive cognitive state, Engel and Fries predict that higher frequency oscillatory activity and interactions in the gamma frequency range (>30 Hz) would predominate the signal over beta band activity. As can be seen in figure 6, in our study, this clearly was not the case, since there was no significant enhancement of the LFP in the gamma frequency range (30-100 Hz) (Supplementary Fig. 13), while average beta band activity (12-28 Hz) was significantly ($p < .05$) temporarily enhanced around 80 ms prior to bar release (Fig. 2.4).

4.5 Gamma activity

Studies on visual cognitive processing have linked increases in oscillatory neuronal activity in the gamma frequency range (>30 Hz) to several top-down factors, such as perceptual binding, attention and working memory (Kruse & Eckhorn, 1996; Fries, Reynolds, Rorie, & Desimone, 2001; Persaran, Pezaris, Sahani, Mitra, & Andersen, 2002; Siegel & König, 2003; Gail, Brinksmeyer, & Eckhorn, 2004; Henrie & Sharpley, 2005; Rickert et al., 2005; Scherberger, Jarvis, & Andersen, 2005; Taylor, Mandon, Freiwald, & Kreiter, 2005; Womelsdorf et al., 2006). Moreover, Crone, Boatman, Gordon, and Hao (2001) have found, via electrocorticographic (ECoG) recordings in humans, that induced gamma activity in auditory cortex was a significant neuronal correlate of auditory perceptual processing.

Unfortunately, we could only find a few studies that have recorded LFP from primate auditory cortex, examining power changes in the gamma frequency band (>30 Hz). These studies, however, merely focused on quantification of frequency tuning by segregated frequency bands of the LFP (Kayser, Petkov, & Logothetis, 2007), exclusively using the evoked response (Ohl, Scheich, & Freeman, 2000), the lowest frequencies of the LFP (Noreña & Eggermont, 2002), or even not systematically quantified tuning properties at all (Brosch, Budinger, & Scheich, 2002). Thus, our study might be one of the first that systematically examined LFP power changes in the gamma frequency range (30-100 Hz) of the LFP in A1 in relation to cognition and behavior of an awake, trained monkey.

Although there were recording sites that showed visible transient power increases in the gamma frequency range (30-100 Hz) in response to ripple onset (e.g. Supplementary Fig. 8) or relative to supposed level of expectancy (e.g. Supplementary Fig. 11, compare A with B), these effects for ripple onset and level of expectancy were not significant ($p > .05$) when the data were pooled across 10 different pairs of recording sites (see Fig. 4; Fig. 6 and Supplementary Fig. 13, respectively). Besides, LFP power in the gamma frequency range (30-100 Hz) per trial, averaged over the last 120 ms prior to bar release, did not correlate significantly ($p > .05$) at all with the response time data (data not shown). Hence, our study does not provide scientifically convincing evidence for the hypothesis (e.g. Engel & Fries, 2010; Fries, 2009; Womelsdorf et al., 2006) that transiently enhanced neuronal oscillations in the gamma frequency range (>30 Hz) in (auditory)

cortex are a valid indicator of expectancy and/or more effective connectivity between brain areas resulting in faster sensorimotor integration. Yet, it has been reported (Buffalo et al., abstract in Soc Neurosci Abstr 2004, 717.6) that stimulus-induced gamma in awake monkey areas V1, V2 and V4 are exclusively present in superficial cortical layers. On the contrary, it has been proposed that deep cortical layers show stimulus-induced oscillations not in the gamma-band, but exclusively in the alpha-band (8–12 Hz) to beta-range (for preliminary report see Sejnowski & Paulsen, 2006). We did not control for which layer of primate auditory cortex we were recording from. Therefore, the fact that we did not find any evidence for gamma activity in relation to our experimental variables might also be explained by measuring from different, possibly unsuited, cortical layers. Moreover, as mentioned before, most studies supporting theories on the role of the gamma band have been done on visual processing, measuring from different cortical areas (e.g. V4) than auditory cortex. Hence, the area of measurement or possibly also the specific experimental design might also explain for our contradictory findings.

6. Conclusions

Acoustic information is represented in LFP signals recorded from monkey A1. Tuning to sound frequency is evident in these signals, and resembles spike tuning. Width and strength of the frequency tuning are correlated. There is no evidence that sound frequency tuning is represented in specific frequency bands of LFP signals. LFP modulations are related to trial-events (onset sound, onset ripple, reaction time).

LFP beta power (12–28 Hz) dominates the transient response for the Passive condition at sound onset. Beta band modulations are also observed at ripple onset and bar release during Active listening conditions.

In contrast to other studies, our data show no evident specific enhancement in the gamma frequency range (>30 Hz), that might reflect non-acoustic, perceptual, cognitive processing (such as task, prediction and reaction time in the current experiments).

Spike activity and LFP signals are similar, but with notable discrepancies. Thus, LFP signals might contain extra information on auditory processing in A1 that cannot be captured by single neuron recordings.

References

- Agterberg, M. J., Snik, A. F., Hol, M. K., van Esch, T. E., Cremers, C. W., Van Wanrooij, M. M. & Van Opstal, A. J. (2011). Improved horizontal directional hearing in bone conduction device users with acquired unilateral conductive hearing loss. *Journal of the Association for Research in Otolaryngology*, 12, 1-11.
- Atiani, S., Elhilali, M., David, S. V., Fritz, J. B., & Shamma, S. A. (2009). Task difficulty and performance induce diverse adaptive patterns in gain and shape of primary auditory cortical receptive fields. *Neuron*, 61, 467-80.
- Baker, S. N. (2007). Oscillatory interactions between sensorimotor cortex and the periphery. *Current Opinion in Neurobiology*, 17, 649-655.
- Baker, S. N., Olivier, E., & Lemon, R. N. (1997). Coherent oscillations in monkey motor cortex and hand muscle EMG show task-dependent modulation. *The Journal of Physiology*, 501, 225-241.
- Bour, L. J., Van Gisbergen, J. A., Bruijns, J., & Ottes, F. P. (1984). The double magnetic induction method for measuring eye movement--results in monkey and man. *IEEE Transactions on Biomedical Engineering*, 31, 419-427.
- Bremen, P., Van der Willigen, R. F., & Van Opstal, A. J. (2007a). Using double-magnetic induction to measure head-unrestrained gaze shifts. I. Theory and validation. *Journal of Neuroscience Methods*, 160, 75-84.
- Bremen, P., Van der Willigen, R. F., & Van Opstal, A. J. (2007b). Applying double magnetic induction to measure two-dimensional head-unrestrained gaze shifts in human subjects. *Journal of Neurophysiology*, 98, 3759-69.
- Bremen, P., Van der Willigen, R. F., Van Wanrooij, M. M., Schaling, D. F., Martens, M. B., Van Grootel, T. J., & Van Opstal, A. J. (2010). Applying double-magnetic induction to measure head-unrestrained gaze shifts: calibration and validation in monkey. *Biological Cybernetics*, 103, 415-32.
- Brosch, M., Budinger, E., & Scheich, H. (2002). Stimulus-related gamma oscillations in primate auditory cortex. *Journal of Neurophysiology*, 87, 2715-2725.
- Brosch, M., Seleznova, E., & Scheich, H. (2005). Nonauditory events of a behavioral procedure activate auditory cortex of highly trained monkeys. *The Journal of Neuroscience*, 25, 6797-6806.
- Brovelli, A., Ding, M., Ledberg, A., Chen, Y., Nakamura, R., & Bressler, S. L. (2004). Beta oscillations in a large-scale sensorimotor cortical network: directional influences revealed by Granger causality. *Proceedings of the National Academy of Sciences of the United States of America*, 101, 9849-9854.
- Chakarov, V., Naranjo, J. R., Schulte-Mönting, J., Omlor, W., Huethe, F., & Kristeva, R. (2009). Beta-range EEG-EMG coherence with isometric compensation for increasing modulated low-level forces. *Journal of Neurophysiology*, 102, 1115-1120.
- Chandrasekaran, C., Turesson, H. K., Brown, C. H. & Ghazanfar, A. A. (2010). The influence of natural

- scene dynamics on auditory cortical activity. *The Journal of Neuroscience*, 30, 13919-31.
- Crone, N. E., Boatman, D., Gordon, B., & Hao, L. (2001). Induced electrocorticographic gamma activity during auditory perception. *Clinical Neurophysiology*, 112, 565-582.
- David, S. V., Malaval, N., & Shamma, S. A. (2010). Decoupling action potential bias from cortical local field potentials. *Computational Intelligence and Neuroscience*, 2010, 393019.
- Delano, P. H., Pavez, E., Robles, L. & Maldonado, P. E. (2008). Stimulus-dependent oscillations and evoked potentials in chinchilla auditory cortex. *Journal of Comparative Physiology A Neuroethology, Sensory, Neural, and Behavioral Physiology*, 194, 693-700.
- Depireux, D. A., Simon, J. Z., Klein, D. J. & Shamma, S. A. (2001). Spectro-temporal response field characterization with dynamic ripples in ferret primary auditory cortex. *Journal of Neurophysiology*, 85, 1220-34.
- Engel, A. K., & Fries, P. (2010). Beta-band oscillations - signalling the status quo? *Current Opinion in Neurobiology*, 20, 156-165.
- Fries, P. (2005). A mechanism for cognitive dynamics: neuronal communication through neuronal coherence. *Trends in Cognitive Sciences*, 9, 474-480.
- Fries, P. (2009). Neuronal gamma-band synchronization as a fundamental process in cortical computation. *Annual Review of Neuroscience*, 32, 209-224.
- Fries, P., Reynolds, J. H., Rorie, A. E., & Desimone, R. (2001). Modulation of oscillatory neuronal synchronization by selective visual attention. *Science*, 291, 1905-1906.
- Fritz, J. B., Elhilali, M., David, S. V., & Shamma, S. A. (2007). Auditory attention - focusing the searchlight on sound. *Current Opinion in Neurobiology*, 17, 437-455.
- Fritz, J., Shamma, S., Elhilali, M., & Klein, D. (2003). Rapid task-related plasticity of spectrotemporal receptive fields in primary auditory cortex. *Nature Neuroscience*, 6, 1216-1223.
- Gail, A., Brinksmeyer, H. J., & Eckhorn, R. (2004). Perception-related modulations of local field potential power and coherence in primary visual cortex of awake monkey during binocular rivalry. *Cerebral Cortex*, 14, 300 -313.
- Gieselmann, M. A., & Thiele, A. (2008). Comparison of spatial integration and surround suppression characteristics in spiking activity and the local field potential in macaque V1. *European Journal of Neuroscience*, 28, 447-459.
- Griffiths, T. D., Warren, J. D., Scott, S. K., Nelken, I., & King, A. J. (2004). Cortical processing of complex sound: a way forward? *Trends in Neurosciences*, 27, 181-185.
- Henrie, J. A., & Shapley, R. (2005). LFP power spectra in V1 cortex: the graded effect of stimulus contrast. *Journal of Neurophysiology*, 94, 479-490.
- Jensen, O., Goel, P., Kopell, N., Pohja, M., Hari, R., & Ermentrout, B. (2005). On the human sensorimotor-cortex beta rhythm: sources and modeling. *Neuroimage*, 26, 347-355.
- Juergens, E., Guettler, A., & Eckhorn, R. (1999). Visual stimulation elicits locked and induced gamma oscillations in monkey intracortical- and EEG-potentials, but not in human EEG. *Experimental Brain Research*, 129, 247-259.
- Kaas, J. H., Hacklett, T. A. & Tramo, M. J. (1999). Auditory processing in primate cerebral cortex. *Current Opinion in Neurobiology*, 9, 164-170
- Kayser, C., Petkov, C. I., & Logothetis, N. K. (2007). Tuning to sound frequency in auditory field potentials. *Journal of Neurophysiology*, 98, 1806-1809.
- Kilner, J. M., Baker, S. N., Salenius, S., Jousmäki, V., Hari, R., & Lemon, R. N. (1999). Task-dependent modulation of 15–30 Hz coherence between rectified EMGs from human hand and forearm muscles. *The Journal of Physiology*, 516, 559-570.
- King, A. J., & Nelken, I. (2009). Unraveling the principles of auditory cortical processing: can we learn from the visual system? *Nature Neuroscience*, 12, 698-701.
- King, A. J., & Schupp, J. W. H. (2007). The auditory cortex. *Current Biology*, 17, 236-239.
- Klostermann, F., Nikulin, V. V., Kühn, A. A., Marzinzik, F., Wahl, M., Pogosyan, A., Kupsch, A., Schneider, G. H., Brown, P., & Curio, G. (2007). Taskrelated differential dynamics of EEG alpha- and beta-band synchronization in cortico-basal motor structures. *European Journal of Neuroscience*, 25, 1604-1615.
- Kosaki, H., Hashikawa, T., He, J., & Jones, E. G. (1997). Tonotopic organization of auditory cortical fields delineated by parvalbumin immunoreactivity in macaque monkeys. *The Journal of Comparative Neurology*, 386, 304-316.
- Kruse, W., & Eckhorn, R. (1996). Inhibition of sustained gamma oscillations (35–80 Hz) by fast transient responses in cat visual cortex. *Proceedings of the National Academy of Sciences of the United States of America*, 93, 6112- 6117.
- Kuhn, A. A., Williams, D., Kupsch, A., Limousin, P., Hariz, M., Schneider, G.H., Yarrow, K., & Brown, P. (2004). Event-related beta desynchronization in human subthalamic nucleus correlates with motor performance. *Brain*, 127, 735-746.
- Liu, J., & Newsome, W.T. (2006). Local field potential in cortical area MT: stimulus tuning and behavioral correlations. *The Journal of Neuroscience*, 26, 7779-7790.
- Logothetis, N. K. (2003). The underpinnings of the BOLD functional magnetic resonance imaging signal. *The Journal of Neuroscience*, 23, 3963-3971.
- Logothetis, N. K., Pauls, J., Augath, M., Trinath, T. & Oeltermann, A. (2001). Neurophysiological investigation of the basis of the fMRI signal. *Nature*, 412, 150-157.
- Logothetis, N. K., & Wandell, B. A. (2004). Interpreting the BOLD Signal. *Annual Review of Physiology*, 66, 735-769.
- Mäkinen, V. T., May, P. J., & Tiitinen, H. (2004). Human auditory event-related processes in the time-frequency plane. *Neuroreport*, 15, 1767-1771.

- Maier, J. X., & Ghazanfar, A. A. (2007). Looming biases in monkey auditory cortex. *The Journal of Neuroscience*, 27, 4093–4100.
- Merzenich, M. M., & Brugge, J. F. (1973). Representation of the cochlear partition on the superior temporal plane of the Macaque monkey. *Brain Research*, 50, 275–296.
- Micheyl, C., Carlyon, R. P., Gutschalk, A., Melcher, J. R., Oxenham, A. J., Rauschecker, J. P., ..., Wilson, E.C. (2007). The role of auditory cortex in the formation of auditory streams. *Hearing Research*, 229, 116–131.
- Mitzdorf, U. (1985). Current source-density method and application in cat cerebral cortex: Investigation of evoked potentials and EEG phenomena. *Physiological Reviews*, 65, 37–100.
- Mitzdorf, U. (1987). Properties of the evoked potential generators: current source-density analysis of visually evoked potentials in the cat cortex. *International Journal of Neuroscience*, 33, 33–59.
- Morel, A., Garraghty, P. E., & Kaas, J. H. (1993). Tonotopic organization, architectonic fields, and connections of auditory cortex in macaque monkeys. *The Journal of Comparative Neurology*, 335, 437–459.
- Nelken, I. (2008). Processing of complex sounds in the auditory system. *Current Opinion in Neurobiology*, 18, 413–417.
- Niessing, J., Ebisch, B., Schmidt, K. E., Niessing, M., Singer, W., & Galuske, R. A. (2005). Hemodynamic signals correlate tightly with synchronized gamma oscillations. *Science*, 309, 948–951.
- Noreña, A., & Eggermont, J.J. (2002). Comparison between local field potentials and unit cluster activity in primary auditory cortex and anterior auditory field in the cat. *Hearing Research*, 166, 202–213.
- Pfurtscheller G. & Ohl, F. W., Scheich, H., & Freeman, W. J. (2000). Topographic analysis of epidural pure-tone-evoked potentials in gerbil auditory cortex. *Journal of Neurophysiology*, 83, 3123–3132.
- Pesaran, B., Pezaris, J. S., Sahani, M., Mitra, P. P., & Andersen, R. A. (2002). Temporal structure in neuronal activity during working memory in macaque parietal cortex. *Nature Neuroscience*, 5, 805–811.
- Pfurtscheller, G., & Lopes da Silva, F.H. (1999). Event-related EEG/MEG synchronization and desynchronization: basic principles. *Clinical Neurophysiology*, 110, 1842–1857.
- Pfurtscheller, G., & Neuper, C. (1997). Motor imagery activates primary sensorimotor area in humans. *Neuroscience Letters*, 239, 65–68.
- Pfurtscheller, G., Neuper, C., Andrew, C., & Edlinger, G. (1997). Foot and hand area mu rhythms. *International Journal of Psychophysiology*, 26, 121–135.
- Polley, D. B., Steinberg, E. E., & Merzenich, M. M. (2006). Perceptual learning directs auditory cortical map reorganization through top-down influences. *The Journal of Neuroscience*, 26, 4970–82.
- Purves, D., Augustine, G. J., Fitzpatrick, D., Katz, L. C., LaMantia, A., McNamara, J. O., Williams, S. M. (2001). Neuroscience. Sunderland (MA): Sinauer Associates.
- Rauschecker, J. P., & Tian, B. (2000). Mechanisms and streams for processing of "what" and "where" in auditory cortex. *Proceedings of the National Academy of Sciences of the United States of America*, 97, 11800–11806.
- Rauschecker, J. P., Tian, B., Pons, T., & Mishkin, M. (1997). Serial and parallel processing in rhesus monkey auditory cortex. *The Journal of Comparative Neurology*, 382, 89–103.
- Recanzone, G. H., Guard, D. C., & Phan, M. L. (2000). Frequency and Intensity Response Properties of Single Neurons in the Auditory Cortex of the Behaving Macaque Monkey. *Journal of Neurophysiology*, 83, 2315–2331.
- Rickert, J., Oliveira, S. C., Vaadia, E., Aertsen, A., Rotter, S., & Mehring C. (2005). Encoding of movement direction in different frequency ranges of motor cortical local field potentials. *The Journal of Neuroscience*, 25, 8815–8824.
- Riddle, C. N., & Baker, S. N. (2006). Digit displacement, not object compliance, underlies task dependent modulations in human corticomuscular coherence. *Neuroimage*, 33, 618–627.
- Riecke, L., Van Opstal, A. J., Goebel, R., & Formisano, E. (2007). Hearing Illusory Sounds in Noise: Sensory-Perceptual Transformations in Primary Auditory Cortex. *The Journal of Neuroscience*, 27, 12684–12689.
- Roux, S., Mackay, W. A., & Riehle, A. (2006). The pre-movement component of motor cortical local field potentials reflects the level of expectancy. *Behavioural Brain Research*, 169, 335–351.
- Salenius, S., & Hari, R. (2003). Synchronous cortical oscillatory activity during motor action. *Current Opinion in Neurobiology*, 13, 678–684.
- Sanes, J. N., & Donoghue, J. P. (1993). Oscillations in local field potentials of the primate motor cortex during voluntary movement. *Proceedings of the National Academy of Sciences of the United States of America*, 90, 4470–4474.
- Scherberger, H., Jarvis, M. R., & Andersen, R. A. (2005). Cortical local field potential encodes movement intentions in the posterior parietal cortex. *Neuron*, 46, 347–354.
- Sejnowski, T. J., & Paulsen, O. (2006). Network oscillations: emerging computational principles. *The Journal of Neuroscience*, 26, 1673–1676.
- Siegel, M., & Konig, P. (2003). A functional gamma-band defined by stimulus-dependent synchronization in area 18 of awake behaving cats. *The Journal of Neuroscience*, 23, 4251–4260.
- Sridharan, D., Boahen, K., & Knudsen, E. I. (2011). Space coding by gamma oscillations in the barn owl optic tectum. *Journal of Neurophysiology*, 105, 2005–2017.
- Taylor, K., Mandon, S., Freiwald, W. A., & Kreiter, A. K. (2005). Coherent oscillatory activity in monkey area v4 predicts successful allocation of attention. *Cerebral Cortex*, 15, 1424–1437.
- Wang, X., Lu, T., Bendor, D., & Bartlett, E. (2008). Neural coding of temporal information in auditory thalamus and cortex. *Neuroscience*, 154, 294–303.

- Wang, X., Lu, T., Snider, R. K., & Liang, L. (2005). Sustained firing in auditory cortex evoked by preferred stimuli. *Nature*, 435, 341-346.
- Womelsdorf, T., Fries, P., Mitra, P. P., & Desimone, R. (2006). Gamma-band synchronization in visual cortex predicts speed of change detection. *Nature*, 439, 733–736.
- Zhang, Y., Chen, Y., Bressler, S. L., & Ding, M. (2008). Response preparation and inhibition: the role of the cortical sensorimotor beta rhythm. *Neuroscience*, 156, 238-246.
- Zwiers, M. P., Versnel, H., & Van Opstal, A. J. (2004). Involvement of monkey inferior colliculus in spatial hearing. *The Journal of Neuroscience*, 24, 4145-4156.

Neural Underpinnings of Feedback Processing in Toddlers

Denise J.C. Janssen¹

Supervisors: Sabine Hunnius¹, Harold Bekkering¹, Marlene Meyer¹, Ellen R.A. de Brujin²

¹Radboud University Nijmegen, Donders Institute for Brain, Cognition and Behaviour, The Netherlands

²Leiden Institute for Brain and Cognition, Leiden University, Leiden, The Netherlands

From early childhood, feedback plays an essential role in the learning of action-outcome contingencies. However, the neural source of the feedback processing system – the anterior cingulate cortex – is known to show a protracted structural maturation, which continues into adolescence. The aim of the present study was to investigate feedback processing in young children, and to relate its electrophysiological correlate (the feedback-related negativity (FRN)) to performance in a feedback-guided task. To this end, toddlers (30-month-olds) performed a simple matching game in which feedback was inherent to the outcome of their actions (i.e. obtaining a matching pair corresponded to a correct outcome and finding a mismatch corresponded to an incorrect outcome). Each trial contained two consecutive phases; first a gambling phase with 50% chance of a correct outcome, and second, an informed phase in which the children could predict the outcome of their choice based on the outcome of the first phase. Analysis of the feedback-locked event-related potentials (ERPs) in the gambling phase revealed a differential electrophysiological response to correct and incorrect outcomes. Moreover, the magnitude of this differentiated response was positively correlated with task performance in the informed phase. We conclude that, in the toddler stage of child development, the neural feedback processing system underlying the FRN has attained the capacity to process the valence of feedback. Furthermore, individual differences in the valence-sensitivity of the feedback-locked ERP accounted for the variability in feedback-guided task performance, demonstrating a close relation between the neural and behavioral correlates of the developing feedback processing system.

Keywords: feedback processing, development, FRN, ACC, early childhood

Corresponding author: Denise Janssen; E-mail: denisejanssen.ru@gmail.com

1. Introduction

From early on in life, we perform many kinds of actions that allow us to interact with our environment. Some actions may lead to the intended outcome, whereas others do not end successfully. In order to learn how to achieve our goals, a cognitive system is required which detects deviances of the actual outcome of our actions with respect to the intended outcome (i.e. error processing). When such information is derived from the environment, rather than elicited endogenously, this cognitive process is more specifically referred to as “feedback processing” (Crone et al., 2003; Müller, Möller, Rodriguez-Fornells, & Münte, 2005; van Meel, Heslenfeld, Oosterlaan, Luman, & Sergeant, 2011). By monitoring action outcomes, appropriate behavioral adjustments can be inferred, which enables us to learn how to handle daily situations. Thus, feedback processing is a pivotal skill from an early age on, guiding the learning process in many aspects of a child’s life – such as playing with toys, adhering to the rules of good manners, and accurately performing educational tasks at school.

Over the last two decades, feedback processing has become a frequently studied topic in the field of neuroscience. Previous research has focused predominantly on elucidating its neural underpinnings in adulthood. As a consequence, an interesting aspect of the feedback processing system – namely, its development – has received little attention. In the behavioral literature, several studies have reported that (young) children are less capable of adapting their actions according to feedback than adults, which seems to indicate an immaturity of the feedback processing system on a behavioral level (Crone & van der Molen, 2004; Somsen, 2007; van Duijvenvoorde, Zanolie, Rombouts, Raijmakers, & Crone, 2008). Little is known about the underlying development of the feedback processing system on a neural level. However, from localization studies in adults it is known that its neural source is located in a brain region that develops relatively slowly, namely the anterior cingulate cortex (Bellebaum & Daum, 2008; Debener et al., 2005; Gehring & Willoughby, 2002; Miltner, Braun, & Coles, 1997). More specifically, the anterior cingulate cortex (ACC), which is part of the frontal brain regions, undergoes a protracted structural and physiological maturation, and several of its associated executive functions are still developing in adolescence (Casey et al., 1997; Cunningham, Bhattacharyya, & Benes, 2002; Davies, Segalowitz, & Gavin, 2004; Devinsky, Morrel, &

Vogt, 1995; Hä默er, Müller, & Lindenberger, 2010; Ladouceur, Dahl, & Carter, 2007; Santesso, Segalowitz, & Schmidt, 2006; Segalowitz & Davies, 2004; van Bogaert, Wikler, Damhaut, Szliwowski, & Goldman, 1998; Wiersema, van der Meere, & Roeyers, 2007). With regard to feedback processing, functional Magnetic Resonance Imaging (fMRI) studies have shown that the activation pattern of its associated neural systems changes from childhood to adulthood (Crone, Zanolie, van Leijenhorst, Westenberg, & Rombouts, 2008; van Duijvenvoorde, Zanolie, Rombouts, Raijmakers, & Crone, 2008; van Leijenhorst, Crone, & Bunge, 2006; Velanova, Wheeler, & Luna, 2008).

Importantly, it can be argued that behavioral adjustments on the basis of feedback information are not directly mediated by feedback processing itself. Rather, the processed feedback information could provide the input for a higher level of executive control to adjust behavior (Chase, Swainson, Durham, Benham, & Cools, 2010). Thus, two developmental processes could underlie the improvement of feedback-guided behavior over age: The neural maturation of feedback processing, and the maturation of cognitive control of behavior. Previous developmental research on a related domain has indeed provided support for such dissociated developmental courses of information processing and adjustment of behavior. These studies showed that behavioral evidence of rule knowledge does not always permit its use (Dowsett & Livesey, 2000; Zelazo, Frye, & Rapus, 1996). Developmental research on a neural level could provide a valuable addition to these behavioral findings, offering further insights into the cognitive mechanisms that underlie them. In particular, neurophysiological research could elucidate the role of the developing feedback processing system in the improvement of feedback-guided performance over age. We were interested in investigating whether the immaturity observed for feedback-guided behavior could be proportionally related to the neurophysiological correlate of feedback processing. For this purpose, we performed an event-related potential (ERP) study in which toddlers played a game that involved feedback-guided decision making. As an electrophysiological measure of feedback processing, we measured the feedback-related negativity (FRN), which is known to differentiate between correct and erroneous action outcomes in adults (e.g. Holroyd & Coles, 2002; Miltner et al., 1997; Nieuwenhuis, Ridderinkhof, Blom, Band, & Kok, 2001) and school-aged children (Eppinger, Mock, & Kray, 2009; Hä默er et al., 2010; Holroyd, Baker, Kerns,

& Mueller, 2008; van Meel et al., 2011; van Meel, Oosterlaan, Heslenfeld, & Sergeant, 2005). We considered toddlers to be a particularly interesting age group in the context of feedback processing, for several reasons. In the toddler stage of development, children increasingly engage in interactive activities that guide their learning process. Feedback plays an essential role in such activities, teaching them how – as well as encouraging them – to become proficient. Amongst toddlers, variability exists with respect to proficiency in these early skills. An interesting question pertains to what extent such differences in proficiency are related to feedback processing. Moreover, performing a study with this age group would extend the FRN literature to a larger range in development, since the youngest participants in this field of research so far were 4- to 5-year-olds (Mai et al., 2011). Thus, an FRN study in toddlers would provide new insights into the feedback processing system at a relatively early developmental stage, during which explicit feedback becomes an important part of everyday learning.

Our hypotheses for the present study were threefold. Firstly, based on the general finding in the FRN literature with regard to feedback valence, we expected that the toddlers would show a feedback-locked ERP with a more pronounced negativity following an incorrect outcome, compared to a correct outcome (e.g. Holroyd & Coles, 2002; Miltner et al., 1997; Nieuwenhuis et al., 2001). Furthermore, we were interested in investigating whether the feedback processing system in toddlers already shows the characteristic of flexibly adjusting its processing intensity according to the informative value of the feedback. Based on earlier findings in adults (Bellebaum & Daum, 2008; Hajcak, Moser, Holroyd, & Simons, 2007; Holroyd & Coles, 2002), we predicted that this would be reflected in an attenuated feedback-locked ERP in response to predictable feedback, compared to unpredictable feedback (i.e. the brain dedicates its computational resources to relevant information, and attenuates its processing activity when information is redundant). Thirdly, we aimed to examine whether the electrophysiological responses to feedback are correlated to the performance on the task. We hypothesized that the degree of differentiation between the electrophysiological responses to correct and incorrect outcomes reflects the functionality of the feedback processing system, and hence would be related to the ability to adapt behavioral responses according to the information provided by feedback.

2. Methodology

2.1 Participants

The final sample consisted of twelve toddlers (seven girls; mean age 30.68 months, SD = .19 months). The children were recruited from a database of families that had signed up for participation in child research, and their parents signed an informed consent form after receiving information about the methods and purpose of the present study. The families visited our lab for a session of approximately one hour duration. They received a little present or a monetary compensation for their participation. Another seven toddlers were tested, but had to be excluded from the analysis for the following reasons. One child was unwilling to wear the electroencephalography (EEG) cap, whereas the other six participants did not provide a sufficient amount of EEG-artifact-free and behaviorally valid trials (details about the inclusion criteria are described below).

2.2 Task and stimuli

The toddlers performed a computerized task, which was implemented on a touch screen interface. The task was inspired by the well-known “memory” (or “pairs”) game, with the aim of finding two identical pictures. The stimulus set consisted of 11 different animals, which toddlers are typically familiar with and able to name (e.g. a cow and a lion). Each trial started out with three cards, placed in a vertical configuration, with the middle card always defined as the “example” card. The upper and the lower cards portrayed an animal that was either identical to or different from the animal shown in the middle (see Fig. 1A). In this “familiarization phase”, the toddler was asked to identify the card that was identical to the example card and to indicate the choice by pressing on it. Upon pressing the matching card, both the upper and the lower cards turned face-down, which caused these animal pictures to be hidden from sight. (Note that pressing the mismatching card, example card or any other location on the screen would not trigger any effect.) Once the upper and lower cards were turned face-down, the “shuffle phase” commenced. Here, the upper and lower cards moved in a swift, circular pattern around the stationary example card, for approximately 2 seconds (Fig. 1B). During the shuffle phase, the experimenter explained: “Now the animals will hide”. The speed of shuffling was high

and the shuffling pattern differed across trials, which made it impossible to track the cards' movements and derive predictions about their ending positions. The shuffle phase caused the cards to end up in a horizontal configuration (Fig. 1C). Next, the “first turn (gambling phase)” followed, where the experimenter asked: “Where would the other [animal name] be?”, referring to the identity of the animal shown on the example card. Here, the child's task was to press on either the left or the right card. Upon pressing, the chosen card turned face-up and revealed its picture (Fig. 1D). In case the child had found the correct card (i.e. the card that matched the example card), an auditory stimulus consisting of the corresponding animal sound followed 1000 ms after the appearance of the picture. In contrast, if the incorrect card (i.e. the mismatching picture) had been found, a low-pitched beep sound followed. The duration of the auditory stimuli was approximately 1 second. Simultaneously (i.e. slightly delayed with respect to the picture appearances), the experimenter also gave verbal feedback: “Yes, you've found it”, in case of the matching card and “No, that's not the one” in case of the mismatching card. Note that the auditory and verbal feedback served only for reinforcement purposes. The feedback-locked ERPs were time-locked to the visual feedback, i.e. the appearance of the picture on the chosen card. The outcome of the first turn was defined as “correct” (when the matching card was found) or “incorrect” (when the mismatching card was found). The chance of finding the matching card in the first turn was

50%. Next, the chosen card turned face-down again (independently of its correctness), so that both the left and the right animal pictures were hidden from sight once more. Here, the last phase –the “second turn (informed phase)” – started, which was identical to the first turn (i.e. the experimenter asked where the animal identical to the example picture was hidden and the child could choose either the left or the right card; Fig. 1E,F). The crucial difference between the first turn and the second turn was the predictability of their outcome; i.e. based on the outcome of the first, gamble choice, toddlers could infer the location of the matching card in the second turn. Thus, children's choice behavior in second turns (informed phase) allowed us to investigate whether they adjusted their actions according to the feedback information obtained in first turns. Note that each trial contained a second turn, i.e. the occurrence of the second turn was fixed and independent of the outcome of the first turn.

2.3 Procedure

The experiment took place in an electrically shielded room. Throughout the session, the toddlers sat on the lap of their parent. After preparing the EEG cap, the experimenter shortly explained the goal of the game (finding the matching animal) and demonstrated two trials. The parent was then instructed not to actively engage in the game, since that could influence their child's performance. Following these instructions, the toddlers started

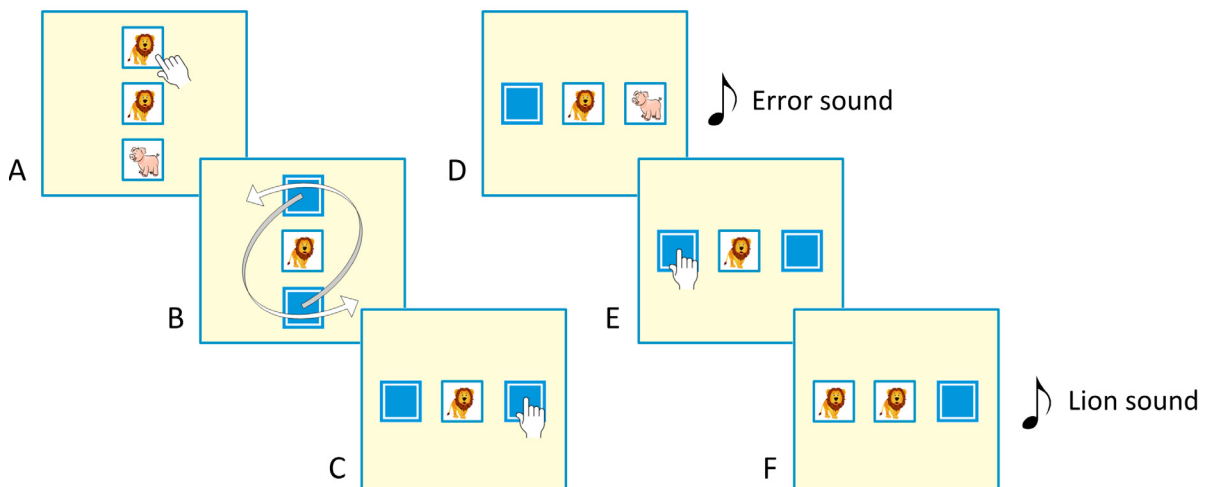


Fig. 1 Exemplar sequence of events in a single trial. **A.** “Familiarization phase”: Participants were instructed to select the matching card, which contained the picture that was identical to the example (middle) card. **B.** “Shuffle phase”: The matching card and mismatching card were shuffled (face-down). **C.** “First turn (gambling phase)”: The participant guessed whether the matching card was located on the left or the right (shown is a situation where the right card was chosen). **D.** The picture of the chosen card was revealed (shown is an example of an incorrect first turn, i.e. the mismatching card was found). The nature of the outcome (correct/incorrect) was unpredictable. **E.** “Second turn (informed phase)”: The participant made a second attempt to find the matching card. **F.** Based on the knowledge gained in the first turn, a correct outcome could, theoretically, be obtained in each second turn.

to perform the task, which contained a total of 55 trials (each consisting of two consecutive turns). This made up approximately 25 minutes of playing time. There were 5 blocks in which each of the 11 different animals appeared on the example card once, while the order of example animals within blocks as well as the identity of the mismatching animal were randomized.

2.4 Electroencephalography recording

The experiment was controlled by Presentation Software (Neurobehavioral Systems; <http://www.neuro-bs.com>). In addition to recording of the card choices and their outcomes by Presentation Software, children's behavior was also videotaped. EEG was recorded with a sampling rate of 500 Hz from 32 scalp sites according to the International 10-10 system, using active Ag/AgCl electrodes, (ActiCAP), Brain Amp DC and Brain Vision Recorder software (Brain Products GmbH, Germany). The data were filtered online with a low cutoff at 0.016 Hz and a high cutoff at 125 Hz. Electrode impedances were kept below 20 kΩ. As the online reference, the left mastoid was used. Offline, the data were referenced to the averaged mastoids.

2.5 Data analysis

Behavioral performance was analyzed in terms of the percentage of correct outcomes on second turns, and thus measured whether toddlers adjusted their actions, based on the information provided by the feedback that was obtained in the first turn. A video analysis was performed in order to exclude invalid trials, which were identified using the following criteria: (1) First or second turns in which the child did not attend the screen during feedback presentation; (2) Second turns which were preceded by a moment of distraction (i.e. when the child was likely to have forgotten the information provided by the first turn).

Feedback-locked ERPs were obtained by creating EEG segments between 200 ms before and 1600 ms after feedback onset (i.e. the appearance of the picture on the card that was chosen in the first or second turn). The 200 ms pre-feedback were used for baseline correction. A 30-Hz low-pass filter was applied, as well as filter padding to prevent edge artifacts. Upon visual inspection of the feedback-locked ERPs, trials containing artifacts were rejected from further analysis. For each participant, an averaged feedback-locked ERP was obtained

per outcome category: (1) Correct first turn, (2) Incorrect first turn, (3) Correct second turn, and (4) Incorrect second turn. The overall low number of incorrect second turns did not allow further analysis of the feedback-locked ERPs belonging to this outcome category (4). The final dataset was restricted to participants that provided at least 10 behaviorally valid, artifact-free trials for each of the other three outcome categories. On average, the total number of excluded trials was 33.78% ($SD = 16.61\%$) for correct first turns, 30.92% ($SD = 15.66\%$) for incorrect first turns, and 45.82% ($SD = 13.47\%$) for correct second turns. The mean number of trials that were included in the statistical analysis were 15.75 ($SD = 5.63$) for correct first turns, 16.17 ($SD = 5.42$) for incorrect first turns, and 20.67 ($SD = 6.60$) for correct second turns.

As a measure of the FRN, we calculated the mean amplitude within a 100 ms time window, centered around its peak. To define the FRN time window, we determined the latency of the peak amplitude in the difference wave, which was calculated by subtracting the grand-average of the activity elicited in response to correct first turns from the activity elicited in response to incorrect first turns (Holroyd & Coles, 2002). The peak of the negative deflection was reached at 372 ms after feedback onset (see Fig. 2). Subsequently, this time window was applied in the analysis of the feedback-locked ERPs for correct and incorrect outcomes, separately.

Statistical analysis was performed using SPSS 15.0 for Windows (SPSS Inc., Chicago, IL). The mean amplitudes of the feedback-locked ERPs were entered in two individual two-way repeated-measures ANOVAs, testing the effect of "feedback valence" (correct first turn versus incorrect first turn) and "predictability" (correct first turn versus correct second turn), respectively. For both ANOVAs, "electrode" (Fz, FCz and Cz) was included as an additional within-subjects factor. The sphericity assumption was checked and corrected values reported if appropriate.

In addition, we performed a correlation analysis between the electrophysiological data and the behavioral performance. As a measure of electrophysiological differentiation, the amplitude for incorrect first turns was subtracted from the amplitude for correct first turns. This produced a larger, positive number for a larger degree of differentiation. Behavioral performance was defined as the percentage of correct second turns. After validating the normality assumption for the Pearson's r , the correlation coefficient was determined for Fz, FCz and Cz, separately.

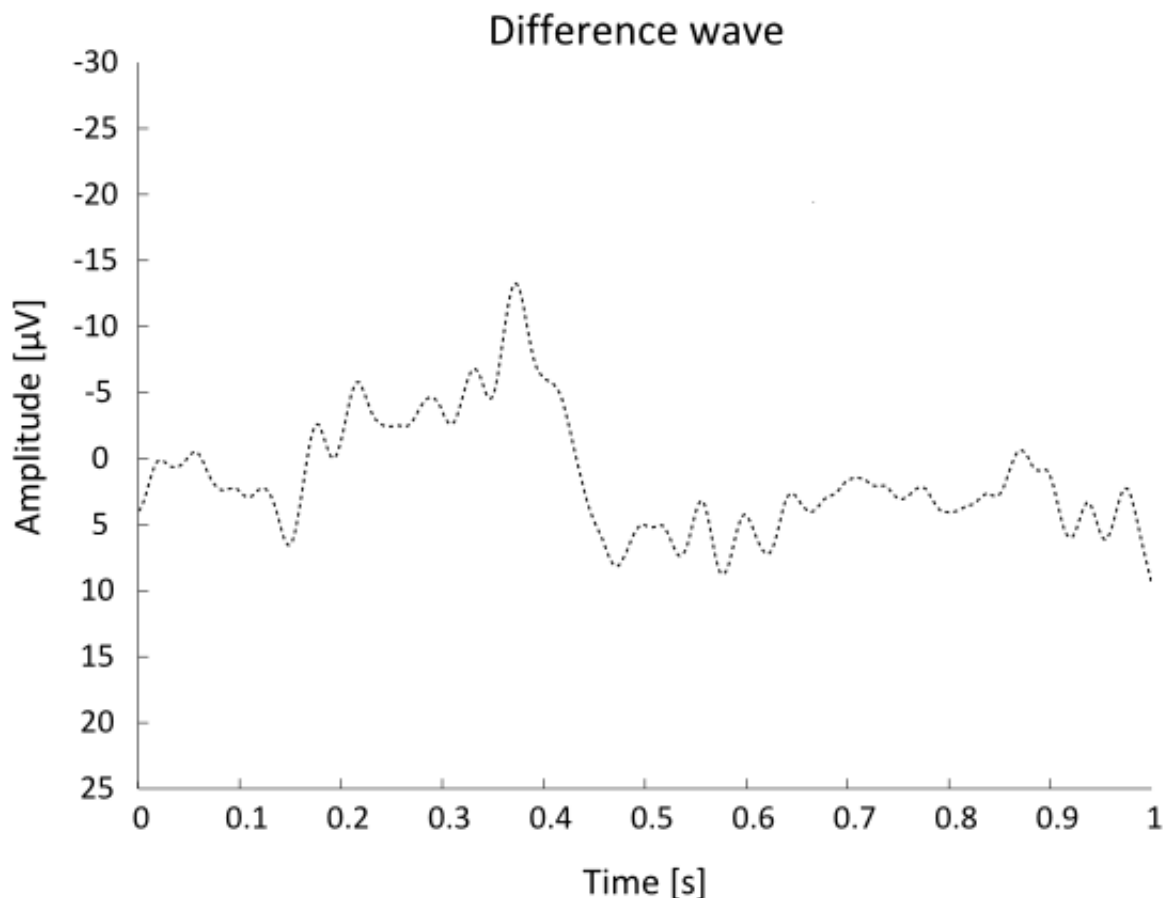


Fig. 2 Difference wave between the feedback-locked ERPs for correct and incorrect first turns, as measured at electrode Fz.

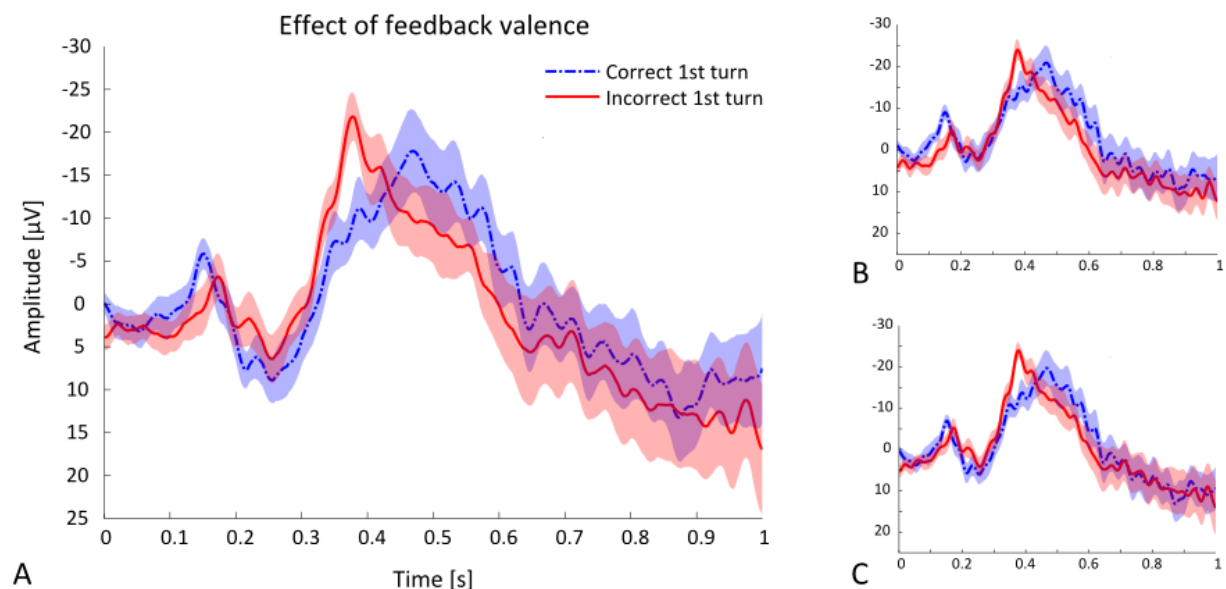


Fig. 3 Feedback-locked ERPs for correct (dashed line) and incorrect (solid line) first turns. Mean \pm one standard errors are plotted for electrode **A**. Fz, **B**. FCz, and **C**. Fc.

3. Results

3.1 Behavioral data

Of the 12 toddlers whose data were included in the statistical analyses, 6 completed all 55 trials, with the number of trials ranging between 26 and 55. On average, the total number of trials was 47.58 ($SD = 10.03$). Given the unpredictable nature of first turns, the mean percentage of correct first turns was 50.42% ($SD = 7.78\%$), as expected. Of the second turns, on average 81.74% ($SD = 12.92\%$) were performed correctly. Although some toddlers did not perform perfectly according to the task instructions, their overall behavioral performance was above chance ($t(11) = 8.51; p < .001$).

3.2 ERP data

In the feedback-locked ERP, a negative deflection started to emerge at approximately 250 ms after the onset of feedback. For feedback representing an incorrect first turn, the negative-going wave reached its peak at approximately 370 ms. In contrast, the negative-going wave for correct outcomes reached its maximum amplitude somewhat later, at approximately 470 ms (see Fig. 3). In effect, the latency difference caused the feedback-locked negativity for correct outcomes to be located outside of the analyzed time window for the FRN. Thus, the shift in latency might have affected the amplitude difference within the FRN time window.

The repeated-measures ANOVA testing the

effect of feedback valence revealed a significant main effect of correctness of outcome ($F(1, 11) = 6.82, p = .024$). More specifically, the amplitude of the negative deflection was more negative for incorrect first turns than for correct first turns. The main effect of electrode was marginally significant ($F(2, 22) = 3.27, p = .057$), while no significant effect was found for the interaction between feedback valence and electrode ($F(2, 22) = 1.58, p = .229$). In a separate repeated-measures ANOVA, we tested the main effect of predictability, which was not significant ($F(1, 11) = .00, p = .992$). Also here, a marginally significant main effect of electrode ($F(2, 22) = 2.90, p = .076$), but no significant interaction between predictability and electrode ($F(2, 22) = 1.04, p = .370$) was found. Closer inspection of the tendency towards statistical significance for the main effect of electrode revealed that amplitudes were most negative for FCz and least negative for Fz, which was the case for both contrasts. Figures 3 and 4 illustrate the feedback-locked ERPs for the feedback valence contrast and predictability contrast, respectively.

3.3 Correlation analysis

Furthermore, we investigated the relation between the differential ERP responses in the gamble phase and the individual task performance in the informed phase. The correlation analysis revealed a statistically significant, positive correlation for each of the three electrodes that were included in the analysis. More specifically, a larger electrophysiological difference between correct and incorrect first turns was

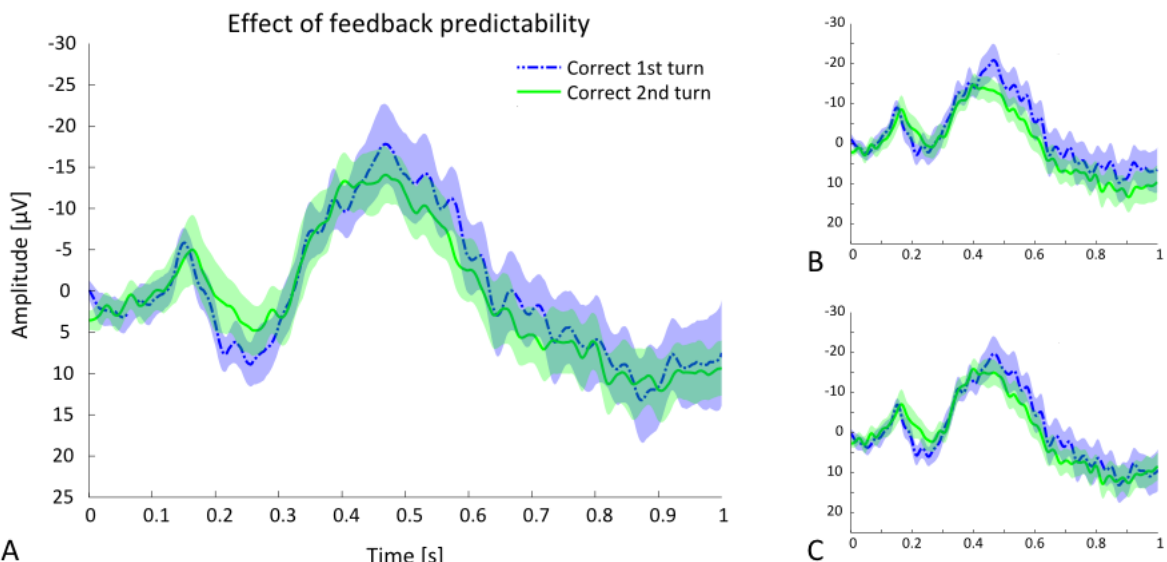


Fig. 4 Feedback-locked ERPs for correct first turns (dashed line) and correct second turns (solid line). Mean \pm one standard errors are plotted for electrode **A**, Fz, **B**, FCz, and **C**, Fc.

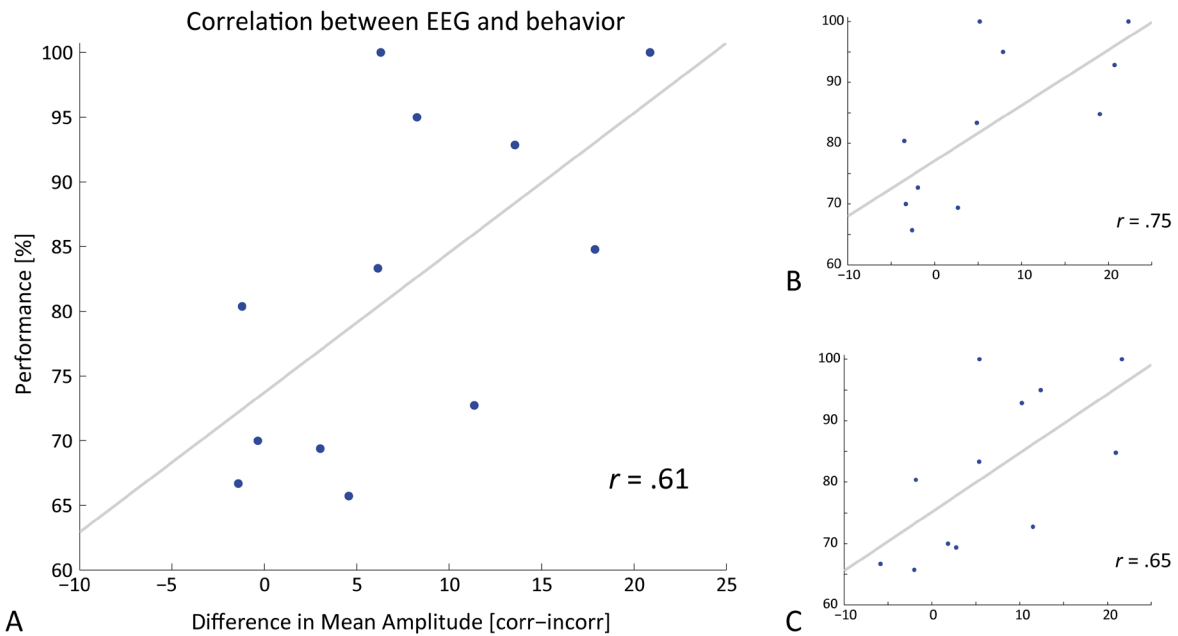


Fig. 5 Correlation between the differential feedback-locked ERP amplitude and behavioral performance on second turns for electrode **A.** Fz, **B.** FCz, and **C.** Fc.

associated with a better behavioral performance on second turns ($r = .61$ for Fz, $r = .75$ for FCz, $r = .65$ for Fc; all p 's $< .05$). The results of the correlation analysis are illustrated in Figure 5.

a neural level accounted for the variability observed in toddlers' behavior.

4.2 Development of the valence effect

Although the FRN in toddlers already showed the characteristic of distinguishing correct and incorrect outcomes, it differed from the typical adult FRN in some respects. First of all, studies in adults have found either no apparent negative deflection for correct outcomes at all (Holroyd & Coles, 2002), or an attenuated peak with a similar latency (Hajcak, Moser, Holroyd, & Simons, 2006). In contrast, in the present toddler study we found an FRN-like negative deflection for correct outcomes that appeared to be similar in amplitude, but shifted in latency compared to the FRN for incorrect outcomes. This finding suggests that the neurophysiological mechanism that processes feedback valence undergoes qualitative developmental changes after toddlerhood. Given that an adult-like effect for feedback valence has been observed for children aged 9 years and older (Eppinger et al., 2009; Hämmeler et al., 2010), it can be inferred that these developmental changes occur within childhood. Further developmental research would be required to obtain a more detailed view of the maturation process of the feedback processing system. In particular, it would be interesting to elucidate the functional significance of these developmental changes. For instance, the emergence of an attenuated ERP response to correct outcomes could reflect a diminished processing intensity, based

4. Discussion

4.1 Summary of the results

The aim of the present study was to elucidate the neural basis of the feedback processing system in young children and its relation to behavior. To this end, we measured the electrophysiological correlate of feedback processing (FRN) in toddlers—the youngest age tested in FRN research so far—while they performed a feedback-guided task. The feedback-locked ERP contained a negative deflection, which was modulated by the valence of the feedback. This finding demonstrates that in toddlerhood—a relatively immature structural stage of frontal brain development—the neural feedback processing system underlying the FRN has attained the capacity to differentiate between correct and incorrect action outcomes. In accordance with this, the task performance was above chance, demonstrating toddlers' ability to adapt their actions according to the information provided by feedback. Interestingly, the degree to which the FRN differentiated between correct and incorrect outcomes in the gamble phase was correlated with the behavioral feedback-guided performance in the informed phase, which illustrates that differences in feedback processing on

on the fact that correct outcomes do not indicate the need of action adjustment (Holroyd & Coles, 2002). In that sense, our finding of comparable amplitudes for correct and incorrect outcomes – though shifted in time – might indicate that toddlers dedicate a relatively large part of their neural resources to the processing of correct action outcomes. It could therefore be suggested that, at a young age, both correct and incorrect action outcomes are processed as though they convey relevant information for future action plans (i.e. performing the similar action or switching to a different action).

The second aspect in which the FRN in toddlers differed from its mature equivalent, was its overall timing. The negative deflection in the difference wave reached its peak amplitude at approximately 370 ms. In adults, the peak of the FRN typically occurs at approximately 250 ms after feedback onset (Holroyd & Coles, 2002; Simons, 2010). This delay in electrophysiological feedback processing is in accordance with the findings of Mai et al. (2011), who studied the FRN in 4-to-5-year-old children and also reported its peak to occur at 370 ms. Altogether, these findings indicate that the FRN undergoes a developmental shift in timing, which has also been found for several other ERP components (Nelson & McCleery, 2008), and is likely a consequence of the structurally immature (e.g. less myelinated) brain. Although our findings were consistent with those of Mai et al. (2011) with respect to the electrophysiological timing of the FRN, these authors did not find an effect of feedback valence, which led them to conclude that the “neural system underlying the FRN may not process feedback valence in early childhood”. In contrast, we have found evidence for differential electrophysiological processing of feedback indicating incorrect action outcomes, compared to correct action outcomes, in even younger children.

4.3 Development of the predictability effect

Earlier studies have established a relation between the FRN and learning, where the amplitude of the FRN was attenuated as feedback became more predictable (Bellebaum & Daum, 2008; Holroyd & Coles, 2002). However, we did not find such an effect of predictability in the current study. Note that we cannot exclude the possibility that a predictability effect was in fact present in our data, though too small to be detected with the amount of trials that we included in our analysis. Thus, this

issue should be investigated more closely in future studies. However, an interpretation of the current finding suggests that the ability of the feedback processing system to fine-tune its activity according to the relevance of feedback develops after toddlerhood. From a theoretical point of view, being able to distinguish relevant and irrelevant feedback is essential for efficient learning. Therefore, it could be hypothesized that the emergence of the effect of predictability – as reflected by the amplitude of the FRN – would be associated with a concurrent developmental improvement in the efficiency of behavioral, feedback-guided learning (e.g. reflected in reaction times or accuracy). It would be interesting to elucidate which mechanism underlies the development of the predictability effect. On the one hand, it could be a direct consequence of the age-dependent structural maturation of the brain areas that are involved in feedback processing. Alternatively, experience could play a role, in the sense that the more the brain is faced with feedback-based learning challenges, the more the feedback-related brain areas will be shaped to optimally process the information. With respect to young children, this issue relates to the following intriguing question: To what extent can a child’s brain be trained to achieve optimal learning capacity?

4.4 Correlation between neural feedback-processing and adaptive behavior

As mentioned in the introduction, two cognitive processes may mediate behavioral performance on a feedback-guided task: The processing of feedback information, and cognitive control of behavior. In the current study, we found a significant correlation between the differential FRN and performance, which demonstrated a close relation between feedback processing on an electrophysiological level and its functional correlate on a behavioral level. In other words, behavioral performance could be explained as a function of neural activity on a feedback processing level, rather than on the level of cognitive control. The correlation supports the hypothesis that action adaptation, according to the information provided by feedback, is determined by the degree to which the neural feedback processing system distinguishes correct and incorrect action outcomes. If this interpretation is correct, the individual differences in task performance and its associated neural responses to feedback reflected a range of developmental differences amongst toddlers. In other words, this would imply that

the toddlers with the most differentiated ERP responses – and hence, the best task performance – possessed a relatively mature feedback processing system. However, as an alternative explanation, it could be suggested that a motivational factor drives the correlation; i.e. the children who were less motivated to perform the task well, might have been less interested in evaluating the outcomes of their actions. On the electrophysiological level, this could be reflected in less differential processing of feedback. Therefore, the suboptimal performance that was observed in the present task might reflect the (negative) influence of motivation, rather than the actual capacity to process feedback. Further research is needed to elucidate to what extent brain development and motivation could account for individual differences in feedback processing. In any case, the close relation between feedback processing on a neural level and a behavioral level provides a promising direction for future research.

It should be noted that the differential processing of correct and incorrect outcomes might have been augmented by the perceptual properties of the feedback stimuli. More specifically, a correct outcome was represented by a picture that was perceptually identical to the example picture, while a mismatching picture indicated an incorrect outcome. Therefore, an early developmental equivalent of the N270 – an ERP component that is elicited when perceptual conflict is perceived (Folstein & van Petten, 2008) – could in principle have contributed to the negative deflection that was observed for incorrect outcomes (see also Jia et al., 2007). Although we cannot determine to what extent a perceptual N270 was present in our ERP data, the correlation with behavior indicated that the FRN accounted for at least a significant part of the electrophysiological difference between correct and incorrect outcomes. In other words, if the differential ERP response reflected processing on a perceptual level only, no correlation with feedback-guided performance would be expected (unless differences in feedback processing could be explained by the ability to detect perceptual differences, which seems like an unlikely explanation).

5. Conclusion

While performing a feedback-guided task, toddlers' brain activity showed an early developmental equivalent of the well-established electrophysiological feedback processing component called FRN. The differential electrophysiological

response to feedback representing correct and incorrect outcomes, respectively, reflects the neural mechanism underlying toddlers' ability to evaluate the outcomes of their actions. Moreover, the magnitude of the differentiation of feedback valence on a neural level was predictive for the degree to which their task performance reflected integration of feedback information into behavior. This demonstrates a close relation between the neural feedback processing system and its functional outcome on a behavioral level.

In contrast, no differential activity was observed for predictable feedback, in comparison with unpredictable feedback. This result might indicate that the feedback processing system has not yet attained the ability to classify feedback according to its relevance (i.e. its informational value), which could have implications for young children's learning capacity in general. Altogether, the neurophysiological and behavioral results obtained in the present study suggest that the feedback processing system underlying the FRN is already functional in toddlerhood – though not yet adult-like, which is in agreement with the early stage of structural development of the frontal brain.

References

- Bellebaum, C., & Daum, I. (2008). Learning-related changes in reward expectancy are reflected in the feedback-related negativity. *European Journal of Neuroscience*, 27, 1823-1835.
- Bellebaum, C., Polezzi, D., & Daum, I. (2010). It is less than you expected: The feedback-related negativity reflects violations of reward magnitude expectations. *Neuropsychologia*, 48, 3343-3350.
- Boksem, M. A. S., Kostermans, E., & de Cremer, D. (2011). Failing where others have succeeded: Medial frontal negativity tracks failure in a social context. *Psychophysiology*, 48, 973-979.
- Casey, B. J., Trainor, R., Giedd, J., Vauss, Y., Vaituzis, C. K., Hamburger, S., ... Rapoport, J. L. (1997). The role of the anterior cingulate in automatic and controlled processes: A developmental neuroanatomical study. *Developmental Psychobiology*, 30, 61-69.
- Chase, H. W., Swainson, R., Durham, L., Benham, L., & Cools, R. (2010). Feedback-related negativity codes prediction error but not behavioral adjustment during probabilistic reversal learning. *Journal of Cognitive Neuroscience*, 23 (4), 936-946.
- Crone, E. A., & van der Molen, M. W. (2004). Developmental changes in real life decision making: Performance on a gambling task previously shown to depend on the ventromedial prefrontal cortex. *Developmental Neuropsychology*, 25 (3), 251-279.
- Crone, E. A., van der Veen, F. M., van der Molen, M.

- W., Somsen, R. J. M., van Beek, B., & Jennings, J. R. (2003). Cardiac concomitants of feedback processing. *Biological Psychology*, 64, 143-156.
- Crone, E. A., Zanolie, K., van Leijenhorst, L., Westenberg, P. M., & Rombouts, S. A. R. B. (2008). Neural mechanisms supporting flexible performance adjustment during development. *Cognitive, Affective, & Behavioral Neuroscience*, 8 (2), 165-177.
- Cunningham, M. G., Bhattacharyya, S., & Benes, F. M. (2002). Amygdalo-cortical sprouting continues into early adulthood: implications for the development of normal and abnormal function during adolescence. *Journal of Comparative Neurology*, 453, 116-130.
- Davies, P. L., Segalowitz, S. J., & Gavin, W. J. (2004). Development of response-monitoring ERPs in 7- to 25-year-olds. *Developmental Neuropsychology*, 25 (3), 355-376.
- Debener, S., Ullsperger, M., Siegel, M., Fiehler, K., von Cramon, D. Y., & Engel, A. K. (2005). Trial-by-trial coupling of concurrent electroencephalogram and functional magnetic resonance imaging identifies the dynamics of performance monitoring. *The Journal of Neuroscience*, 25 (50), 11730-11737.
- Devinsky, O., Morrell, M. J., & Vogt, B. A. (1995). Contributions of anterior cingulate cortex to behavior. *Brain*, 118, 279-306.
- Dowsett, S. M., & Livesey, D. J. (2000). The development of inhibitory control in preschool children: Effects of "executive skills" learning. *Developmental Psychobiology*, 36 (2), 161-174.
- Eppinger, B., Mock, B., & Kray, J. (2009). Developmental differences in learning and error processing: Evidence from ERPs. *Psychophysiology*, 46, 1043-1053.
- Folstein, J. R., & van Petten, C. (2008). Influence of cognitive control and mismatch on the N2 component of the ERP: A review. *Psychophysiology*, 45, 152-170.
- Fukushima, H., & Hiraki, K. (2009). Whose loss is it? Human electrophysiological correlates of non-self reward processing. *Social Neuroscience*, 4 (3), 261-275.
- Gehring, W. J., & Willoughby, A. R. (2002). The medial frontal cortex and the rapid processing of monetary gains and losses. *Science*, 295, 2279-2282.
- Hajcak, G., Moser, J. S., Holroyd, C. B., & Simons, R. F. (2006). The feedback-related negativity reflects the binary evaluation of good versus bad outcomes. *Biological Psychology*, 71, 148-154.
- Hajcak, G., Moser, J. S., Holroyd, C. B., & Simons, R. F. (2007). It's worse than you thought: The feedback negativity and violations of reward prediction in gambling tasks. *Psychophysiology*, 44, 905-912.
- Hämmerer, D., Li, S., Müller, V., & Lindenberger, U. (2010). Life span differences in electrophysiological correlates of monitoring gains and losses during probabilistic reinforcement learning. *Journal of Cognitive Neuroscience*, 23 (3), 579-592.
- Holroyd, C. B., Baker, T. E., Kerns, K. A., & Mueller, U. (2008). Electrophysiological evidence of atypical motivation and reward processing in children with attention-deficit hyperactivity disorder. *Neuropsychologia*, 46, 2234-2242.
- Holroyd, C. B., & Coles, M. G. H. (2002). The neural basis of human error processing: reinforcement learning, dopamine, and the error-related negativity. *Psychological Review*, 109 (4), 679-709.
- Holroyd, C. B., & Krigolson, O. E. (2007). Reward prediction error signals associated with a modified time estimation task. *Psychophysiology*, 44, 913-917.
- Jia, S., Li, H., Luo, Y., Chen, A., Wang, B., & Zhou, X. (2007). Detecting perceptual conflict by the feedback-related negativity in brain potentials. *Cognitive Neuroscience and Neuropsychology*, 18 (13), 1385-1388.
- Ladouceur, C. D., Dahl, R. E., & Carter, C. S. (2007). Development of action monitoring through adolescence into adulthood: ERP and source localization. *Developmental Science*, 10 (6), 874-891.
- Ma, Q., Shen, Q., Xu, Q., Li, D., Shu, L., & Weber, B. (2011). Empathic responses to others' gains and losses: An electrophysiological investigation. *Neuroimage*, 54, 2472-2480.
- Mai, X., Tardif, T., Doan, S. N., Liu, C., Gehring, W. J., & Luo, Y. (2011). Brain activity elicited by positive and negative feedback in preschool-aged children. *PLoS ONE*, 6 (4), e18774.
- Marco-Pallares, J., Cucurell, D., Münte, T. F., Strien, N., & Rodriguez-Fornells, A. (2011). On the number of trials needed for a stable feedback-related negativity. *Psychophysiology*, 48, 852-860.
- Miltner, W. H. R., Braun, C. H., & Coles, M. G. H. (1997). Event-related brain potentials following incorrect feedback in a time-estimation task: Evidence for a "generic" neural system for error detection. *Journal of Cognitive Neuroscience*, 9 (6), 788-798.
- Müller, S. V., Möller, J., Rodriguez-Fornells, A., & Münte, T. F. (2005). Brain potentials related to self-generated and external information used for performance monitoring. *Clinical Neurophysiology*, 116, 63-74.
- Nelson, C. A., McCleery, J. P. (2008). Use of event-related potentials in the study of typical and atypical development. *Journal of the American Academy of Child and Adolescent Psychiatry*, 47 (11), 1252-1261.
- Nieuwenhuis, S., Ridderinkhof, K. R., Blom, J., Band, G. P. H., & Kok, A. (2001). Error-related brain potentials are differentially related to awareness of response errors: evidence from an antisaccade task. *Psychophysiology*, 38, 752-760.
- Oliveira, F. T. P., McDonald, J. J., & Goodman, D. (2007). Performance monitoring in the anterior cingulate is not all error related: Expectancy deviation and the representation of action-outcome associations. *Journal of Cognitive Neuroscience*, 19 (12), 1994-2004.
- Santesso, D. L., Segalowitz, S. J., & Schmidt, L. A. (2006). Error-related electrocortical responses in 10-year-old children and young adults. *Developmental Science*, 9 (5), 473-481.
- Segalowitz, S. J., & Davies, P. L. (2004). Charting the maturation of the frontal lobe: An electrophysiological strategy. *Brain and Cognition*, 55, 116-133.
- Simons, R. F. (2010). The way of our errors: Theme and

- variations. *Psychophysiology*, 47, 1-14.
- Somsen, R. J. M. (2007). The development of attention regulation in the Wisconsin Card Sorting Task. *Developmental Science*, 10 (5), 664-680.
- Van Bogaert, P., Wikler, D., Damhaut, P., Szliwowski, H. B., & Goldman, S. (1998). Regional changes in glucose metabolism during brain development from the age of 6 years. *Neuroimage*, 8, 62-68.
- Van Duijvenvoorde, A. C. K., Zanolie, K., Rombouts, S. A. R. B., Raijmakers, M. E. J., & Crone, E.A. (2008). Evaluating the negative or valuing the positive? Neural mechanisms supporting feedback-based learning across development. *The Journal of Neuroscience*, 28 (38), 9495-9503.
- Van Leijenhorst, L., Crone, E. A., & Bunge, S. A. (2006). Neural correlates of developmental differences in risk estimation and feedback processing. *Neuropsychologia*, 44, 2158-2170.
- Van Meel, C. S., Heslenfeld, D. J., Oosterlaan, J., Luman, M., & Sergeant, J. A. (2011). ERPs associated with monitoring and evaluation of monetary reward and punishment in children with ADHD. *Journal of Child Psychology and Psychiatry*, 52 (9), 942-953.
- Van Meel, C. S., Oosterlaan, J., Heslenfeld, D. J., & Sergeant, J. A. (2005). Telling good from bad news: ADHD differentially affects the processing of positive and negative feedback during guessing. *Neuropsychologia*, 43, 1946-1954.
- Velanova, K., Wheeler, M. E., & Luna, B. (2008). Maturational changes in anterior cingulate and frontoparietal recruitment support the development of error processing and inhibitory control. *Cerebral Cortex*, 18, 2505-2522.
- Wiersema, J. R., van der Meere, J. J., & Roeyers, H. (2007). Developmental changes in error monitoring: An event-related potential study. *Neuropsychologia*, 45, 1649-1657.
- Zelazo, P. D., Frye, D., & Rapus, T. (1996). An age-related dissociation between knowing rules and using them. *Cognitive Development*, 11, 37-63.

The Social Learning of Trust

Cătălina Elena Rățală^{1,2}
Supervisor: Alan G. Sanfey^{2,3,4}

¹*Rotterdam School of Management, Erasmus University, Rotterdam, The Netherlands*

²*Radboud University Nijmegen, Donders Institute for Brain, Cognition and Behaviour, The Netherlands*

³*Radboud University Nijmegen, Behavioural Science Institute, The Netherlands*

⁴*Department of Psychology, University of Arizona, Tucson, USA*

Trust is the lubricant of social interactions (Zak & Knack, 2001). Daily life often confronts us with the decision of whether to trust the people, brands and institutions we come in contact with. As individual experience shows, there is a potential downside associated with trusting: The risk of being betrayed. Given this constraint, how do we decide whom to trust? Several studies demonstrate that people rely on information from previous interactions to assess others' trustworthiness: We learn whom to trust. However, we also have strong prejudice about whom we should trust. Experimental evidence shows that there are in-built mechanisms by means of which we automatically evaluate the trustworthiness of interaction partners. The information used to judge trustworthiness is partially encoded in facial features and emotional expressions. The present study uses functional Magnetic Resonance Imaging (fMRI) to investigate the relationship between automatic judgments of trustworthiness and experience-based judgments in a social decision-making environment (Trust Game). We were able to disentangle the complex relationship between "first impressions" and learning: While left amygdala activation correlates with initial trust based on implicit mechanisms of face evaluation, the subsequent learning of trust is strongly driven by the probability of reciprocation in the latter stages of the interaction.

Keywords: decision making, trust, social learning, trustworthiness, face perception

Corresponding author: Cătălina Rățală; E-mail: c.ratala@donders.ru.nl

1. Introduction

We learn to walk, we learn to read, we learn to play the violin or fly a plane, and we also learn to navigate our social environment. Social learning is one of the bases of human behavior and individuals need to acquire precise and useful information from others, therefore it is critical to decide whom to learn from (Henrich & McElreath, 2003).

Past research on social learning has focused on investigating the impact of direct social interactions. However, more recent research has followed a broader understanding of the concept of social learning that includes decision-making and learning processes influenced by social information obtained from others, not necessarily through a personal contact (Biele, Rieskamp, & Gonzales, 2009). Living in highly social environments and being constantly exposed to other decision-makers, one of the most valuable lessons we can learn is to trust.

Trust is generally defined as a person's willingness to risk potentially negative consequences by relying on another person. It is a highly versatile concept that spans across a wide variety of fields and disciplines. Everyday life confronts us with countless situations that prompt for trusting decisions. From small, inconsequential interactions to potentially life altering situations, from the micro to the macro-level of inter-corporate alliances and economic growth, trust is considered to be a "lubricant", an essential variable for development (Zak & Knack, 2001).

People colloquially refer to trust in terms of a prize: We win the trust of another. While trusting behavior has the potential of leading to highly rewarding outcomes, there is a risk associated with it. Economic research has proposed the so-called "trust as risk" hypothesis: A person's willingness to trust can be shaped by their risk preferences (Eckel & Wilson, 2004; Frank, Seeberger, & O'Reilly, 2004; House, Schunk, & Winter, 2010).

As beneficial as it may be to trust, most of us can attest from experience that not all people are trustworthy, and placing trust in the wrong person can have very unpleasant consequences. Not only because the trust is abused, but also because the faith of the trustee in her own judgment is weakened. Thus, there is a strong incentive for learning to trust the right people. This is crucial in social decision-making, where the uncertainty related to the consequences of our choices is mostly due the fact that we do not know what other decision-makers will do (Sanfey, 2007). Therefore, while making a decision to trust or not, one needs to carefully

consider the underlying risk. But how can risk be evaluated in the social domain?

Tracking the frequency of past positive and negative outcomes is a useful strategy for estimating the probability of a negative event occurring. Similarly, the best predictor of an individual's future behavior is her past behavior (King-Casas et al., 2005; Rilling, King-Casas, & Sanfey, 2008). In fact, this is very well demonstrated by online ratings, which provide information on the past performance of individuals or businesses, such as AmazonTM or E-bayTM. But what happens when prior information is not available? In real-life we are not always aware of a partner's past behavior, such as when interacting with a stranger for the first time. Suppose, for instance, that you want to have your picture taken with a friend, and ask someone passing by if she would be willing to take the picture. How do you know that you can trust this person not to walk away, stealing your camera? Every person possesses innate evaluation mechanisms that use facial features for assessing traits, like attractiveness and aggression, as well as more abstract features, such as competence and trustworthiness. The face is a rich source of information, and it has been proven to play a role in signaling social intentions from which people infer meaning (Amodio & Frith, 2006).

One important brain region for the assessment of trustworthiness is the amygdala. The amygdala is also essential in fear conditioning and consolidation of emotional memories (Adolphs, 2008; Winston, Strange, O'Doherty, & Dolan, 2002; Oosterhof & Todorov, 2008). All these crucial features are evaluated surprisingly fast, within the first 100 milliseconds of an encounter (Willis & Todorov, 2006). The existence of such mechanisms is reasonable from an evolutionary perspective, but the question is: How much do we rely on them? More often than not, people learn that they should not judge a book by its cover. However, when no other information is available, decisions are based on these subtle evaluations (Delgado, Frank, & Phelps, 2005; van't Wout & Sanfey, 2008). Specific facial features account for a trustworthy face and these opinions are present reliably across people (Oosterhof & Todorov, 2008). But how are these automatic evaluations affected by learning?

There are few studies that address this question. Recently, Chang, Doll, van't Wout, Frank and Sanfey (2010) investigated a possible way in which we combine the information from facial features – initial trustworthiness – with the information from the overt behavior in interactions – experienced trustworthiness. The question of interest here is: How

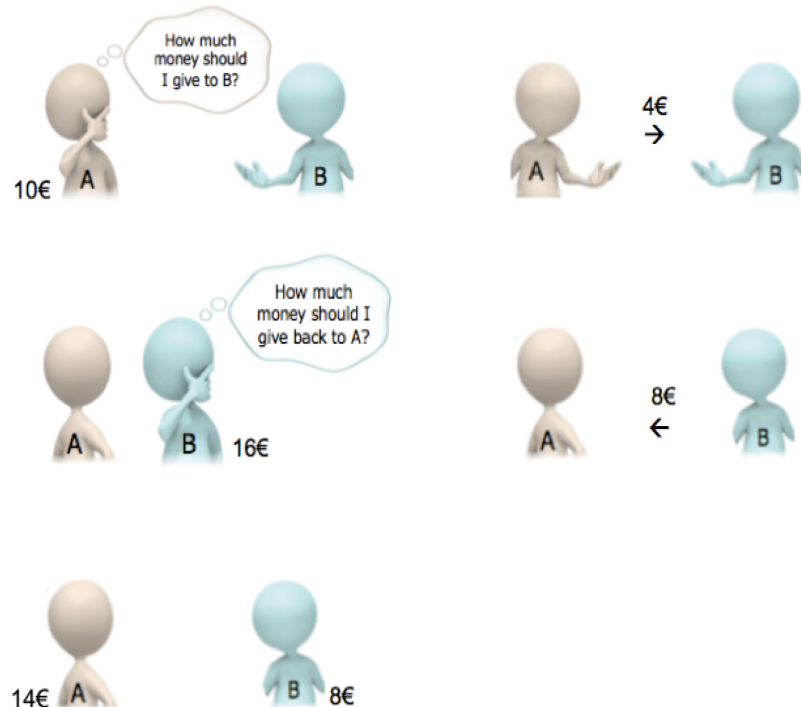


Fig. 1 Task – The Trust Game. The interaction between the investor (player A) and the trustee (player B) is illustrated here. For each player we depicted a hypothetical scenario with the respective amounts of money.

do these mechanisms interact? Chang et al. (2010) used a reinforcement-learning framework to evaluate and classify the learning patterns of trustworthiness. More specifically, their study suggests that we start with automatically generated prior beliefs of trustworthiness and we then update them, as a result of reciprocated and/or unreciprocated trust across repeated interactions. Trustworthiness is referred to as a “dynamic belief system”. The judgments based on facial features serve as an initial belief about how trustworthy a particular person is; very importantly, this belief is continually updated, as a function of experience (Chang et al., 2010).

The modeling approach adopted in Chang et al. (2010) was successful in predicting behavior in a game theoretic environment, thus suggesting that it describes crucial aspects of the process of learning whom to trust. In this work we sought to investigate the neuronal underpinnings of these dynamic beliefs of trustworthiness.

In order to analyze trust-learning behavior we used an iterated version of the Trust Game (Fig. 1). This task represents a simplified version of the Investment Game (Berg, Dickhaut, & McCabe, 1995), extensively used in behavioral economics. Two players are involved in the game, an investor (Player A), and a partner (Player B). Player A is endowed with a certain amount of money by the experimenter. She can decide how much money – if any – she wants to invest in Player B, knowing that

Player B will receive quadrupled amount of money. Then Player B decides if she wants to reciprocate or not, by either sharing half or by keeping the transferred money.

Provided that the investor and the partner interact only once, Game Theory predicts that a rational partner would never reciprocate the trust given by the investor, and would keep the entire amount for herself. The rational investor should be aware of this line of thought, and so she would never send any amount of money to the partner. Thus, by this theoretical view, trust is neither given nor repaid during this game (Berg et al., 1995). However, in most experimental studies conducted with the Trust Game, investors are willing to send some money to the partner, and generally this trust is repaid. Because it captures this pattern of behavior, the Trust Game is a very useful operationalization of trust, that can be thus measured as the amount of invested money (McCabe, Rigdon, & Smith, 2003; Houser, Schunk, & Winter, 2010).

In the present study participants always played the role of the investor. They interacted repeatedly with the same partner. By being exposed to the each game partner multiple times, an environment is created where information about the game partner can be accumulated. This gathering of information leads to a better prediction, and potentially shapes the participant’s trust behavior towards their game partner. We simulated the social context by using

pictures of neutral faces, namely faces that do not display any emotion, to represent the game partners. It has been shown in economic games that emotional expressions – particularly smiling – influence the decision to trust (Scharlemann, Eckel, Kacelnik, & Wilson, 2001). However, these studies focus on the effect of emotional expressions rather than the automatic assessment of trustworthiness of neutral faces. We aimed to show that even with no overt emotional expressions the facial trustworthiness of the game partner impacts the decision-maker. Moreover, as a further control for the effect of the social context, participants played a number of trials with slot machines as partners.

We sought to address three basic questions: (i) Are there brain correlates that distinguish between initial and experienced judgments of trustworthiness? (ii) What effect does the social domain have on trust learning? (iii) What is the effect of reciprocation and betrayal on brain activity?

With respect to the first question, Winston et al. (2002) explored the brain correlates of facial trustworthiness evaluation. They compared implicit and explicit judgments of facial trustworthiness, and showed that activation in the insula is highly related to explicit judgments. Moreover, insula and amygdala activity is correlated with viewing untrustworthy faces. On the basis of this evidence, we expect increase amygdala activation when investors rely on the initial assessment of trustworthiness. Previous literature also shows that the intention to trust a game partner is associated with medial cingulate cortex activity (King-Casas et al., 2005), thus we expect increased medial cingulate activation as a function of the trustworthiness of the face of the opponent.

Activity in the ventromedial prefrontal cortex, in the middle temporal gyrus, the superior temporal sulcus at the medial temporal juncture, in the dorsomedial prefrontal cortex and in the anterior cingulate cortex is associated with predictions based on interaction history and social information (Behrens, Hunt, Woolrich, & Rushworth, 2008). We therefore expect these areas to show increased activation when participants become more experienced. Especially, we expect activity in the caudate nucleus in the high probability of reciprocation conditions as opposed to low probability (King-Casas et al., 2005; Hampton & O'Doherty, 2007).

With respect to our second question – the difference between social and non-social trust – theory of mind areas, for instance the prefrontal cortex, anterior paracingulate and the temporal-parietal juncture, are expected to show higher

activation when participants play with pictures of faces rather than slot machines. Indeed, these areas seem to be related to perspective taking, therefore they should specifically track social learning, and not non-social learning (Amodio & Frith, 2006; Lieberman, 2007).

Finally, we aimed to contrast the neuronal responses between the trials when investments are reciprocated and betrayed. The reinforcement learning literature shows that specific signals in the brain correlate with prediction errors (Daw, O'Doherty, Dayan, Seymour, & Dolan, 2006). These important components of information updating show the difference between the expected and the experienced reward for each given trial. We want to investigate their role in the social domain (Rilling, Sanfey, Aronson, Nystrom, & Cohen, 2004).

2. Methods

2.1 Participants

In this experiment we had 24 (12 males) participants, all students at the Radboud University Nijmegen, with ages between 18 and 27 ($M = 22.00$, $SD = 2.59$). One subject was excluded from fMRI analysis due to technical difficulties with recording. All subjects gave their informed consent, and the study was approved by the Donders Institute for Brain, Cognition and Behaviour.

2.2 Task

In order to measure trust behavior, we used a simplified version of the Economic Trust Game (Berg et al., 1995). The participants received instructions about the nature and rules of the game. They played a multiple trial game (120 trials), always in the role of Player A, the investor. Each Player B represented one of the experimental conditions. We manipulated the partner's level of facial trustworthiness (3 levels: low, high and slot machine) and crossed it with the level of experienced trustworthiness – the level of reciprocation (2 levels: low and high). The experimental manipulations were orthogonalized. Each of the subjects played with six different partners: Two game partners with faces that were rated as highly trustworthy, two game partners with faces that were rated as untrustworthy and two slot machines – as non-social controls.

The high level of reciprocation had an 80% probability of reciprocation while the low level of reciprocation had a 20% probability of reciprocation.

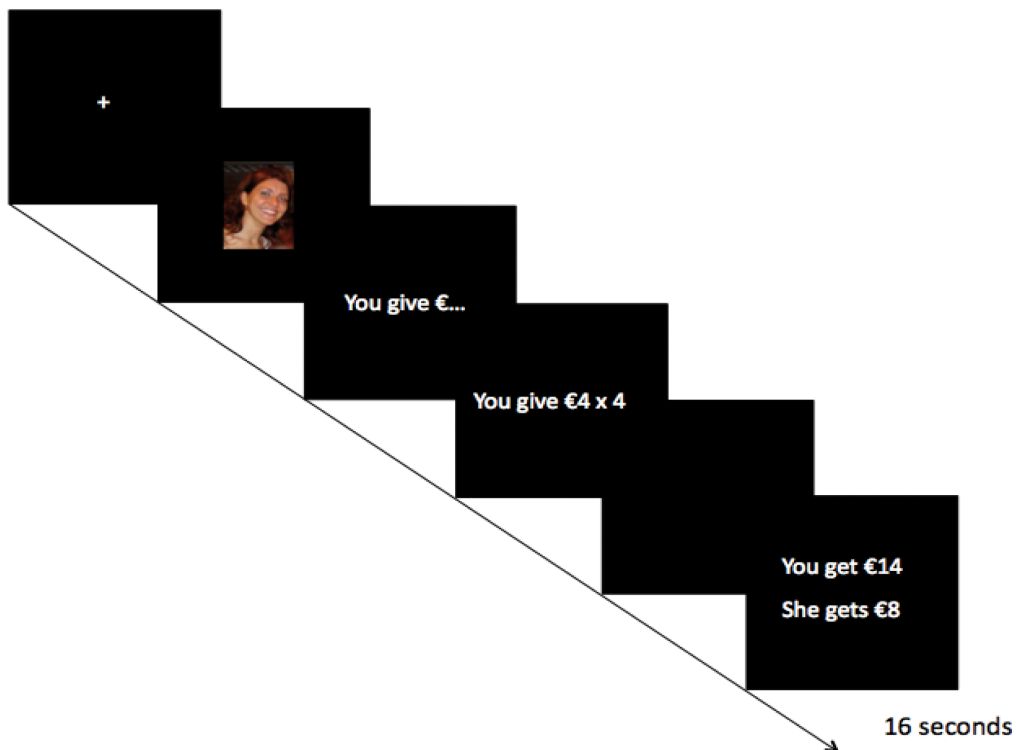


Fig. 2 Trial structure. Each picture corresponds to a screen in the experiment, showing the time course of a single trial of the Trust Game.

The money invested by the participant was multiplied by a factor of 4. If an offer was reciprocated, Player B always reciprocated 50% of the total multiplied amount sent by Player A. When trust was not reciprocated, Player B did not return any money to Player A.

The 120 trials were divided into 5 runs. For each run, the participants played 24 randomly ordered interspersed trials – 4 with each of their 6 game partners (conditions).

Within a trial (Fig. 2), a fixation cross was shortly presented, followed by the face and the name of the game partner (3000 ms). The participant could then decide how much she wants to invest in her game partner. By pressing button “1” the amount showed on the screen increased with increments of 1. The starting value on the screen randomly switched from 0 to 10, to counter any ordering effects. If the participant did not submit an offer in time (8000 ms), she forfeited all of her money for the round. The final screen, the feedback, informed the participant whether her game partner had shared or kept the money. The length of a trial varied between 16 and 19 seconds.

2.3 Stimuli

The stimuli were 8 colored, frontal, photographic images of emotionally neutral faces and 2 pictures of slot machines. Pictures showing faces were selected from a set of 60 images from the psychological image collection of the Psychology Department at the Radboud University Nijmegen. The face stimuli were selected on the basis of trustworthiness ratings given by 98 healthy subjects in a pilot study. Two sets of four faces were matched for trustworthiness levels. Each set consisted of one male and one female with high ratings ($>50\%$, $M = 5.20$) on trustworthiness and one male and female that were rated low ($<50\%$, $M = 3.10$) on trustworthiness on a 7-point Likert scale. Ratings for high and low trustworthiness levels were significantly different. Participants were randomly assigned to play with one of the picture sets, with the other set serving as a control. For each participant the high and low trustworthy pictures were randomly assigned to an experienced trustworthiness condition (high versus low probability of reciprocation). All stimuli were presented via EPrime software (Psychology Software Tools, Inc).

2.4 fMRI data acquisition

Imaging was performed at the Donders Institute for Brain, Cognition and Behaviour with a 3-Tesla head-dedicated MRI system (Magnetom TrioTim; Siemens).

Functional MRI images were acquired using a standard multi-echo imaging pulse T2*-weighted sequence [field of view (FOV), 224 mm; 64 x 64 matrix; repetition time (TR), 2390 ms; echo times (TE), 9.4 ms, 21.2 ms, 33 ms, 45 ms, 56 ms; flip angle, 90°]. Thirty-one ascending slices were acquired (thickness of 3.0 mm; voxel size 3.5x3.5x3.0 mm). The full brain was covered. High-resolution anatomical T1-weighted structural scans (MP-RAGE; 192 slices; voxel size 1x1x1 mm) were acquired for anatomical localization.

The participants had their head lightly restrained within the scanner, in order to limit movement during image acquisition. Each run began with 5 dummy scans (subsequently discarded) to allow T1 equilibration effects.

2.5 Debriefing

After scanning, participants rated both sets of stimuli – those they played against and those they did not – on trustworthiness, attractiveness, competence, aggressiveness, and likeability using a 5-point Likert scale. Participants were also asked to estimate the percentage of the time that each of the players they played with reciprocated their offers, from 0% to 100%, in 10% increments (Chang et al., 2010; van't Wout & Sanfey, 2008).

2.6 Behavioral and fMRI data analysis

All behavioral data analyses were performed using SPSS PASW Statistics 18.0 (IBM, Inc.) with a significance threshold set to alpha = .05. The effects of the facial trustworthiness factor, the reciprocity factor and their interaction on the amount of money invested in the game partner were evaluated.

fMRI analyses were performed using SPM8 (Wellcome Trust Centre for Neuroimaging) running on a Matlab 7 platform (The MathWorks, Inc.). The functional volumes were realigned, slice time corrected, and normalized to the Montreal Neurological Institute (MNI) template. Images were then smoothed using a Gaussian filter of 8 mm full-width at half maximum (FWHM) and high-pass temporal filtering (128 s) was applied. The motion parameters were stored and used as

nuisance variables in the generalized linear model (GLM) analysis. Eight conditions of interest were specified, plus their respective time derivatives. Two time moments were defined as being of particular interest: The presentation of the game partner (picture) and the feedback.

The picture presentation window was 3 seconds long, and we used the six experimental conditions as explanatory variable – low trustworthy partner with low probability of reciprocation (TLPL), high trustworthy partner with low probability of reciprocation (THPL), low trustworthy partner with high probability of reciprocation (TLPH), high trustworthy partner with high probability of reciprocation (THPH), slot machine with low probability of reciprocation (SLPL) and slot machine with high probability of reciprocation (SLPH).

The feedback window was 3 seconds long, and we used the trials when the offer was reciprocated (Reci) and the trials when trust was betrayed (Betray) as explanatory variable.

The t contrasts of interest where specified at the first level analysis, having their significance tested at the second level by means of one-sample t-tests. The specified contrasts were for trust high>trust low, probability high>probability low, for reciprocation>betrayal and for the interaction. We looked at the results across the whole experiment, and we also divided two time windows: the start, comprising of runs 1 and 2 (trials 1 to 8 per condition) and the end, from run 3 on to run 5 (trials 9 to 20 per condition). Moreover, based on coordinates from prior literature we selected regions of interest for the amygdala (Winston et al., 2002; Delgado et al., 2005), the insula (Winston et al., 2002) and the caudate nucleus (Knutson, Adams, Fong, & Hommer, 2001).

3. Results

Using a linear mixed model analysis, we investigated the effects of trustworthiness, reciprocity and their interactions (Baayen, Davidson, & Bates, 2008). There was a main effect of reciprocity $F(1, 23) = 1039.07, p < .001$. Participants learned, over time, to trust – and thus invest – significantly more in the game partners that had a high probability of reciprocation ($M = 5.83, SE = .22$) (Fig. 3), as compared to the ones that had a low probability of reciprocation ($M = 2.82, SE = .22$) (Fig. 4).

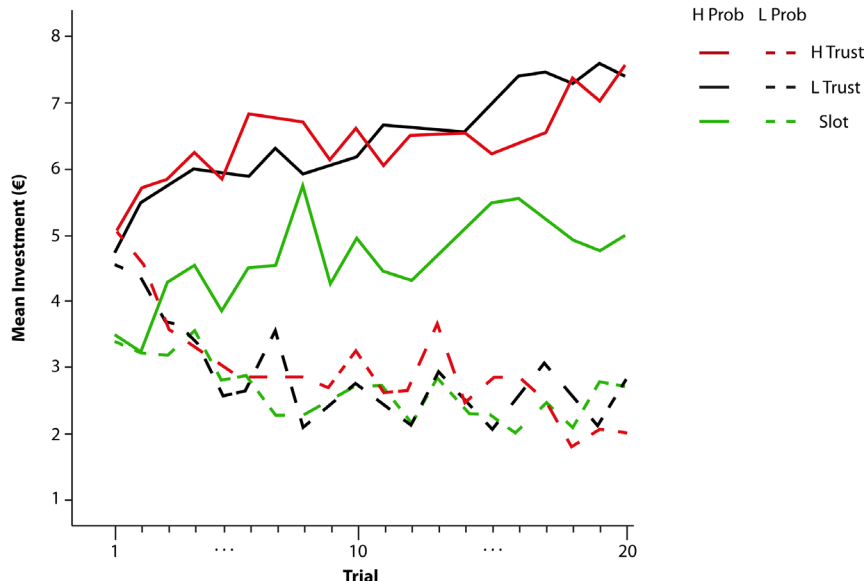


Fig. 3 This figure shows the mean invested amount across subjects for each trial of each condition.

3.1 Behavioral data

The dataset was then divided in two categories: early (the 1st and 2nd sessions, trials 1 to 8 of each condition) and late (from the 3rd session onward). For the early stage, we found that the trustworthiness manipulation was significant ($F(2, 46) = 21.40, p < .001$), the probability of reciprocation manipulation was significant ($F(1, 23) = 177.18, p < .001$), and their interaction was significant ($F(2, 46) = 6.13, p < .003$). As for specific conditions, for the low facial trustworthiness we have no significance ($t(3) = 1.57, p = .12, b = .43$), but there was a significant effect of the partner with the high facial trustworthiness ($t(3) = 2.06, p = .04, b = .56$).

In the late stage, trustworthiness has a lower significance, as expected ($F(2, 46) = 3.51, p < .04$), but the reciprocation was significant ($F(1, 23) = 100.25, p < .001$) and their interaction was significant as well ($F(2, 46) = 4.30, p < .02$). In specific conditions, for the low facial trustworthiness we have no significance, with a much lower value of b as compared to the early stage ($t(3) = .06, p = .95, b = .03$), but there was a significant effect of the partner with the high facial trustworthiness ($t(3) = .36, p = .72, b = .20$).

In the last two trials of the game, for each condition, there was a significant difference in between the investments for the conditions with low, respectively high reciprocation probabilities (high probability conditions, $M = 6.55, SE = .30$; low probability conditions $M = 2.40, SE = .30$).

Finally, we found a non-significant trend for people to invest the smallest amount of money

(even less than in the slot machines low probability condition) in game partners that have high facial trustworthiness but low probability of reciprocation (Fig. 5).

3.2 Post-experiment ratings

Two picture sets were used, each of them entails two sets of stimuli. In order for us to make sure that the pictures used in each of the conditions were viewed accordingly to their designated condition,

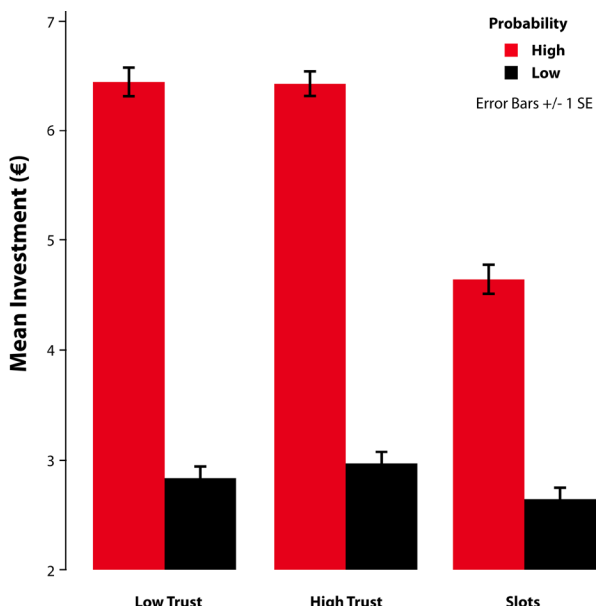


Fig. 4 This figure shows the mean amount of money invested overall, for each of the experimental conditions. Participants learn to invest significantly more in the game partners that have a high probability of reciprocation (depicted here in red).

Mean invested amount for the last trial in each condition

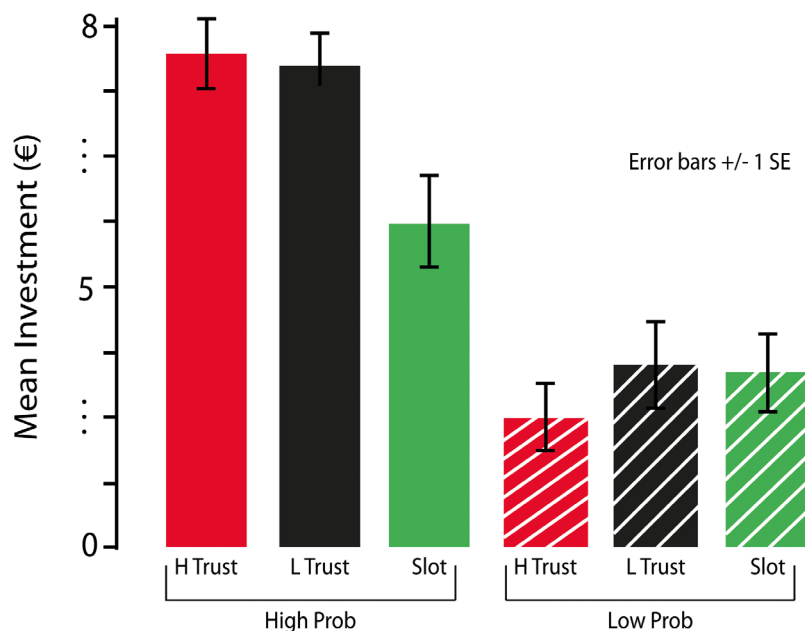


Fig. 5 This figure depicts the mean amount of money invested in the last two trials of each condition. There is a strong effect of probability: Participants invested more in the game partners with high probability of reciprocation. Among the conditions with low probability of reciprocation, there is a trend for investing the least amount of money in the partners who looked trustworthy but had a low probability of reciprocation.

we compared all of the ratings for each participant's control set of the pictures. Using the trustworthiness ratings, an one-way ANOVA $F(1, 24) = 31.42, p < .001$ revealed that the partners who were selected as trustworthy looking ($M = 3.88, SE = .09$) were perceived as such when compared to partners who were selected as low trustworthy looking ($M = 2.83, SE = .15$). We also found strong correlations in between the ratings for trustworthiness and competence, attractiveness and likability, and a negative correlation with aggression.

3.3 fMRI data

The data was initially analyzed overall, and then it was divided in two categories: Early (the 1st and 2nd sessions, trials 1 to 8 of each condition) and late (from the 3rd session onward) (Table 1, Table 2). Contrasting early with late time frames allowed us to better disentangle the brain areas involved in each of the phases of trust learning. All the contrasts presented below were thresholded at a value of $p = .005$ uncorrected. Where small volume correction was applied, contrasts were thresholded at $p = .001$, then after the small volume correction, $p < .05$, FEW.

Overall, we found more activation in the left amygdala (-27, 8, -20) for low as compared to high facial trustworthiness. This effect remained

even when looking at the two time windows, with a stronger activation in the left amygdala (-27, 8, -20) in the late phases of interaction with the game partners (Fig. 6A). We applied small volume correction using a sphere of 10 mm radius centered in -24, -4, -20 (Winston et al., 2002). When looking at the probability factor, we first contrasted all the collapsed high probability versus low probability conditions and found more activation in the posterior cingulate (6, -55, 20). However, for the two time windows we found insula (48, 20, 1) activation in the beginning in the low>high probability contrast. For the high>low probability we found prefrontal and ventromedial prefrontal cortex activation. The same contrast in the late stage of the game yielded activity in the nucleus accumbens (Fig. 6B) and the orbitofrontal cortex.

We found no significant patterns of activation for the interaction of facial trustworthiness with probability of reciprocation.

For the feedback screen, when looking at reciprocation as contrasted with betrayal, we found right caudate activation (9, 17, -8) but also cingulate (12, -4, 28) and orbitofrontal (-15, 47, -17). We applied small volume correction, using a sphere of 10 mm radius, centered in 12, 23, 4 (King-Casas et al., 2005). The corrected cluster was significant and located in the right caudate (9, 20, -5) (Fig. 6C).

Table 1.

Contrast	Side	Coordinates of peak activation			Z scores	Cluster size
Region		X	Y	Z		
TrustLow>TrustHigh						
Amygdala*	left	-27	5	-20	3.53	5
Hypothalamus		0	-1	-8	2.91	17
TrustHigh>TrustLow						
Inferior parietal	right	48	-55	46	3.09	16
Orbitofrontal	right	45	44	-14	2.95	7
Middle temporal	right	66	-40	-5	2.93	9
Prefrontal	right	42	47	1	2.77	9
Start TrustLow>TrustHigh						
Inferior temporal	right	42	-4	-35	3.59	19
Start TrustHigh>TrustLow						
Thalamus	right	12	-19	16	3.03	19
Superior parietal	right	30	-52	37	3.00	16
End TrustLow>TrustHigh						
Amygdala	left	-27	8	-20	3.90	59
End TrustHigh>TrustLow						
Prefrontal	right	45	44	1	2.81	10

4. Discussion

The aim of this study was to gain information about the underlying brain processes associated with initial and experience driven judgments of trustworthiness. Since trust is a central aspect of our daily lives, we are often confronted with questioning our ability to accurately and efficiently evaluate who is trustworthy.

Behavioral results suggest that trust is a dynamic belief (Chang et al., 2010), a belief that is constantly updated based on two essential types of information: Initial evaluations of specific facial features and subsequent experience.

Behaviorally, there was an effect of facial trustworthiness on the amount of money invested in the early stage of the game. As predicted by the model, this effect disappeared in the later stage of the game, suggesting that the initial belief is overwritten, and the investment behavior is mainly driven by experience (Chang et al., 2010). The first type of evaluation – the facial judgment –, is associated with activity in the insula and the amygdala, which is consistent with the existing literature (Winston et al., 2005), and most likely plays a role in associating the visual stimulus to either reward or punishment (Hampton & O'Doherty, 2007). Moreover, when contrasting low to high trustworthy faces we observe more amygdala activation, thus supporting the claim that we have a stronger automatic response

to untrustworthy facial features (van't Wout et al., 2008).

Over time, participants learned to invest more in those game partners that reciprocated and less in the game partners that did not (Fig. 3).

The probability of reciprocity had a significant effect on the investor's strategy across all trials. At the neuronal level, the nucleus accumbens and orbitofrontal activation correlated with higher probability conditions, in the later stages of the game. Ventromedial and lateral areas of the prefrontal cortices were activated as well. When comparing high versus low probability of reciprocity we found increased activation in the left nucleus accumbens and in the orbitofrontal cortex, indicating coding of value and reward. The orbitofrontal cortex plays a role in the evaluation of outcomes and in the integration of information from different sources. The ventromedial prefrontal and orbitofrontal cortices are critical for adaptive decision-making (Wallis, 2007). The medial area is supposed to code for positive values, which is in line with our findings (Gottfried, O'Doherty, & Dolan, 2003).

We also found that within each level of the probability manipulation, the slot machines received significantly less money than the human partners. This pattern of behavior suggests a clear distinction in trusting behavior in social versus non-social interactions.

Finally, brain activation patterns related to

Table 2.

Contrast	Side	Coordinates of peak activation			Z scores	Cluster size
Region		X	Y	Z		
ProbHigh>ProbLow						
Inferior occipital	right	45	-85	-5	3.95	455
Inferior occipital	left	-42	-79	-11	3.58	170
Middle temporal	right	69	-31	-11	3.49	13
Superior occipital	left	-24	-67	49	3.40	32
Superior occipital	right	30	-67	34	3.26	75
Middle occipital	left	-27	-73	31	3.20	26
Posterior cingulate	right	6	-55	-20	3.18	34
Superior occipital	right	21	-64	49	2.79	9
Start ProbLow>ProbHigh						
Insula	right	48	20	1	3.45	31
Start ProbHigh>ProbLow						
Superior occipital	left	-24	-76	28	4.01	201
Middle occipital	right	27	-97	7	3.46	180
Middle occipital	left	-27	-97	4	3.45	116
Prefrontal	left	-36	59	-2	3.40	26
Hippocampus	right	24	-19	-17	3.39	29
VMPrefrontal	left	-6	38	-11	3.31	110
Cerebellum	right	9	-58	-17	3.29	66
Fusiform	right	33	-49	-20	3.28	27
STS	left	-51	-40	13	2.88	6
End ProbHigh>ProbLow						
Inferior orbital	left	-12	8	-20	3.65	35
Middle occipital	right	24	-97	10	3.63	132
Inferior occipital	right	42	-85	-8	3.58	62
Nucleus accumbens*	right	12	14	-11	2.83	5
Orbitofrontal	left	-24	29	-20	3.05	20
Middle occipital	left	-42	-79	-11	3.00	14
Cerebellum	left	-24	-70	49	2.93	20
Reciprocal>Betrayal						
Occipital	right	3	-97	4	4.29	508
Cingulate	right	12	-4	28	4.04	61
Caudate*	right	9	20	-5	3.81	18
Cerebellum	right	33	-43	-26	3.27	29
Prefrontal	left	-27	62	4	3.22	24
Inferior parietal	left	-54	-34	52	3.12	32
Orbitofrontal	left	-33	50	-14	3.12	12
Occipital	right	42	-79	-17	3.10	68
Orbitofrontal	left	-15	47	-17	3.07	27
Betrayal>Reciprocal						
Temporal	right	48	5	-32	3.40	64

reciprocal were found in the head of the caudate and also in frontal medial areas, which can be associated to a social prediction error, as well as in the anterior cingulate cortex. These areas have been previously associated to conflict monitoring (Koch et al., 2008; Pochon, Riis, Sanfey, Nystrom,

& Cohen, 2008), therefore we hypothesize that our conflict conditions – those where probability of reciprocating and facial trustworthiness point toward opposite predictions – explain the significance of the activity.

We expected to be able to fully replicate the

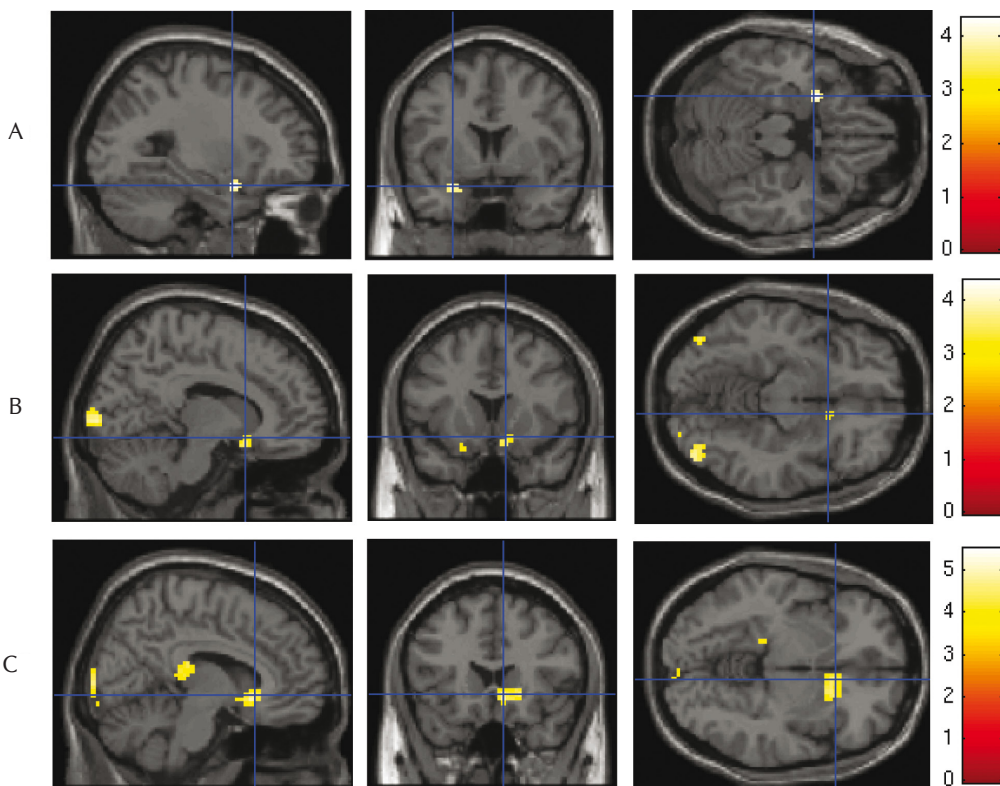


Fig. 6 A. This figure shows activation during the presentation screen. The contrast is between conditions where game partners had low facial trustworthiness and high facial trustworthiness, across the whole experiment. A small volume correction was applied, with a sphere of 10 mm radius, centered at -24,-4,-20 revealing activation in the left amygdala (-27,5,-20), $p < 0.05$, $z = 3.53$, $k = 5$. **B.** This figure shows activation during the presentation screen. The contrast is between conditions where game partners had high probability of reciprocation low probability of reciprocation, in the later stages of the game (trials 3-5). A small volume correction was applied, with a sphere of 10 mm radius, centered at 12, 17, -2, revealing activity in the right nucleus accumbens (12, 14, -11), $p < 0.07$, $z = 2.83$, $k = 5$. **C.** This figure shows activation during the feedback screen. When contrasting reciprocation with betrayal, we found activity in the right caudate (9, 20, -5), $p < 0.05$, $z = 3.81$, $k = 18$. We applied small volume correction, using a sphere of 10 mm radius, centered at 12, 23, 4.

findings of Chang et al. (2010). We did find a main effect of probability over time, where people invest more in game partners that reciprocated. However, we did not find a strong effect of facial trustworthiness on the initial investing behavior, as it was the case for the dataset of Chang et al. (2010). A possible explanation could be the fact that, given the small sample size and the strong effect of probability, the trustworthiness effect gets drowned. However, we did identify a tendency to invest a smaller amount of money even less than in the slot machines with low probability condition in the game partners with high facial trustworthiness that proved to have a low probability of reciprocation (Fig. 6). This may indicate a tendency to be harsher in punishing the betrayal of trust when the expectations on the social outcome are higher.

From our results we can conclude that the pattern identified by Chang et al. (2010) at the behavioral level is correlated with specific brain dynamics that partially address the three questions. First of all, initial and experience based judgments of trustworthiness

are discriminated at the brain level by insula and amygdala activation. Second, probability learning in the social domain is associated with activation in the striatum and in the orbitofrontal cortex. Finally, we found a distinct behavioral difference between social and non-social trust.

As a future direction, we wish to investigate more directly the relation between brain activation and the parameters in the model developed by Chang et al. (2010). To do so, we will integrate the results discussed above with trial-by-trial analysis of brain activity and the latent constructs postulated by the computational model.

Acknowledgements

I would like to thank the Decision Neuroscience group for the great working atmosphere, Filippo Rossi for his critical input, and Marius Zimmermann for the SPM related counseling. In particular, I would like to thank my supervisor, Alan Sanfey, for the support and the inspiration he has provided me with throughout this year!

References

- Adolphs, R. (2008). Fear, faces, and the human amygdala. *Current Opinion in Neurobiology*, 18 (2), 166–172.
- Amodio, D., & Frith, C. (2006). Meeting of minds: The medial frontal cortex and social cognition. *Nature Review Neuroscience*, 7 (4), 268–277.
- Baayen, R., Davidson, D., & Bates, D. (2008). Mixed-effects modeling with crossed random effects for subjects and items. *Journal of Memory and Language*, 59 (4), 390–412.
- Behrens, T. E. J., Hunt, L. T., Woolrich, M. W., & Rushworth, M. F. S. (2008). *Associative learning of social value*. *Nature*, 456 (7219), 245–249.
- Berg, J., Dickhaut, J., & McCabe, K. (1995). Trust, reciprocity, and social history. *Games and Economic Behavior*, 10 (1), 122–142.
- Biele, G., Rieskamp, J., & Gonzalez, R. (2009). Computational models for the combination of advice and individual learning. *Cognitive Science*, 33 (2), 206–242.
- Chang, L., Doll, B., van't Wout, M., Frank, M., & Sanfey, A. (2010). Seeing is believing: Trustworthiness as a dynamic belief. *Cognitive Psychology*, 61 (2), 87–105.
- Daw, N., O'Doherty, J., Dayan, P., Seymour, B., & Dolan, R. (2006). Cortical substrates for exploratory decisions in humans. *Nature*, 441 (7095), 876.
- Delgado, M., Frank, R., & Phelps, E. (2005). Perceptions of moral character modulate the neural systems of reward during the trust game. *Nature Neuroscience*, 8 (11), 1611–1618.
- Eckel, C., & Wilson, R. (2004). Is trust a risky decision? *Journal of Economic Behavior & Organization*, 55 (4), 447–465.
- Frank, M., Seeberger, L., & O'Reilly, R. (2004). By carrot or by stick: Cognitive reinforcement learning in parkinsonism. *Science*, 306 (5703), 1940.
- Gottfried, J., O'Doherty, J., & Dolan, R. (2003). Encoding predictive reward value in human amygdala and orbitofrontal cortex. *Science*, 301 (5636), 1104.
- Hampton, A., & O'Doherty, J. (2007). Decoding the neural substrates of reward-related decision making with functional mri. *Proceedings of the National Academy of Sciences*, 104 (4), 1377.
- Henrich, J., & McElreath, R. (2003). The evolution of cultural evolution. *Evolutionary Anthropology*, 12 (3), 123–135.
- Houser, D., Schunk, D., & Winter, J. (2010). Distinguishing trust from risk: An anatomy of the investment game. *Journal of Economic Behavior & Organization*, 74 (1-2), 72–81.
- King-Casas, B., Tomlin, D., Anen, C., Camerer, C., Quartz, S., & Montague, P. (2005). Getting to know you: Reputation and trust in a two-person economic exchange. *Science*, 308 (5718), 78.
- Knutson, B., Adams, C. M., Fong, G. W., Hommer, D. (2001). Anticipation of increasing monetary reward selectively recruits nucleus accumbens. *Journal of Neuroscience*, 21 (16), RC159(1-5).
- Koch, K., Schachtzabel, C., Wagner, G., Reichenbach, J., Sauer, H., & Schlösser, R. (2008). The neural correlates of reward-related trial-and-error learning: An fmri study with a probabilistic learning task. *Learning & Memory*, 15 (10), 728.
- Lieberman, M. (2007). Social cognitive neuroscience: A review of core processes. *Annual Review of Psychology*, 58, 259–289.
- McCabe, K., Rigdon, M., & Smith, V. (2003). Positive reciprocity and intentions in trust games. *Journal of Economic Behavior & Organization*, 52 (2), 267–275.
- Oosterhof, N., & Todorov, A. (2008). The functional basis of face evaluation. *Proceedings of the National Academy of Sciences*, 105 (32), 11087.
- Pochon, J., Riis, J., Sanfey, A., Nystrom, L., & Cohen, J. (2008). Functional imaging of decision conflict. *The Journal of Neuroscience*, 28 (13), 3468.
- Rilling, J., King-Casas, B., & Sanfey, A. (2008). The neurobiology of social decision-making. *Current Opinion in Neurobiology*, 18 (2), 159–165.
- Rilling, J., Sanfey, A., Aronson, J., Nystrom, L., & Cohen, J. (2004). Opposing bold responses to reciprocated and unreciprocated altruism in putative reward pathways. *NeuroReport*, 15 (16), 2539.
- Sanfey, A. (2007). Social decision-making: Insights from game theory and neuroscience. *Science*, 318 (5850), 598.
- Scharlemann, J., Eckel, C., Kacelnik, A., & Wilson, R. (2001). The value of a smile: Game theory with a human face. *Journal of Economic Psychology*, 22 (5), 617–640.
- Wallis, J. D. (2007.). Orbitofrontal cortex and its contribution to decision-making. *Annual Review Neuroscience*, 30, 31–56.
- van't Wout, M., & Sanfey, A.G. (2008). Friend or foe: The effect of implicit trustworthiness judgments in social decision-making. *Cognition*, 108 (3), 796-803.
- Willis, J., & Todorov, A. (2006). First impressions. *Psychological Science*, 17 (7), 592.
- Winston, J., Strange, B., O'Doherty, J., & Dolan, R. (2002). Automatic and intentional brain responses evaluation of trustworthiness of faces. *Nature Neuroscience*, 5 (3), 277–283.
- Zak, P., & Knack, S. (2001). Trust and growth. *The Economic Journal*, 111 (470), 295–321.

Sex Differences in Synaptic Density and Neurogenesis in Middle-Aged Apolipoprotein E4 and Apolipoprotein E Knockout Mice

Anne Rijpma¹

Supervisors: Amanda J. Kilian¹, Diane Jansen¹

¹Radboud University Medical Centre Nijmegen, Donders Institute for Brain, Cognition and Behaviour, The Netherlands

Apolipoprotein E4 (apoE4) is a major risk factor for Alzheimer's disease (AD) and cardiovascular disease (CVD). It increases plasma cholesterol levels and decreases clearance of amyloid-beta (A β) from the brain. In both AD and CVD sex differences exist in prevalence and in manifestation of the disease. In this study we investigate synaptic density and neurogenesis in different models for AD and vascular disease in both male and female wild type, apoE4 and apoE knockout (ko) mice. Middle-aged female apoE4 mice showed a decrease in synaptic density in the dentate gyrus of the hippocampus. Middle-aged female apoE ko mice showed an increase in neurogenesis in the hippocampus. Middle-aged male apoE mice did not differ from wild type mice on synaptic density nor neurogenesis. Possibly a specific harmful interaction exists between apoE4 and estrogen that is responsible for the decreased synaptic density in these female apoE4 mice. Previous studies have suggested a compensatory mechanism for synaptic failure by temporarily increasing the amount of synaptic contacts and/or neurogenesis. The increased neurogenesis found in female apoE ko mice supports this hypothesis. To our knowledge there are no other studies that investigated synaptic density in female apoE4 or apoE ko mice. Sex specific differences between apoE genotypes could account for some of the sex differences in AD and CVD. Sex differences should be taken into account in any research concerning CVD, AD or apoE.

Keywords: aging, Alzheimer's disease, apolipoprotein E, atherosclerosis, cardiovascular disease, doublecortin, neurogenesis, sex differences, synapse, synaptophysin

Corresponding author: Anne Rijpma; E-mail: rijpma.anne@gmail.com

1. Introduction

Alzheimer's disease (AD) is a neurodegenerative disorder characterized by progressive cognitive decline that accounts for over 60% of all cases of dementia. The most important risk factor for the development of AD is advanced age (Launer et al., 1999; Moreira, Zhu, Smith, Perry, & Larry, 2009). Neuropathologically the disease is characterized by the presence of neuritic plaques and neurofibrillary tangles, as well as neuronal loss, white matter lesions and synaptic changes (Brun & Englund, 1986; Jellinger, 2002; Kim, Basak, & Holtzman, 2009; Moreira et al., 2009). The neuritic plaques consist mainly of amyloid-beta (A β), and the accumulation of this peptide is hypothesized to initiate a pathological cascade that leads to AD (Hardy & Higgins, 1992; Selkoe, 1991). However, A β plaque burden does not correlate with disease severity, as shown by large autopsy studies (Fernando & Ince, 2004; Terry et al., 1991) and PET studies (Klunk et al., 2004), and plaques are found in cognitively normal subjects as well (Davis, Schmitt, Wekstein, & Markesberry, 1999; Fernando & Ince, 2004). From the familial forms of AD (5% of all AD cases), caused by a mutation in the amyloid precursor protein (APP) gene or in presenilin (PS) 1 or 2, we do know however that A β processing is important. Nowadays more and more consensus is reached about A β oligomers, and not the fibrillary A β in plaques, being the neurotoxic forms of A β (DaRocha-Souto et al., 2011; Shankar et al., 2009).

While familial or early onset AD is caused by autosomal dominant genetic mutations, the most important currently known genetic risk factor for sporadic or late onset AD is the apolipoprotein E (APOE) genotype. In the human population the three major alleles that are present are ϵ 2, ϵ 3, and ϵ 4, and the risk for AD is increased in carriers of the ϵ 4 allele (Corder et al., 1993; Strittmatter, Saunders et al., 1993). While in the general population 15% carries one ϵ 4 allele, the occurrence in AD patients is 40-65%. In addition, ϵ 4 allele carriers develop the disease at a younger age than non- ϵ 4 allele carriers (Corder et al., 1993; Farrer et al., 1997). Furthermore, in the non-demented elderly population and in healthy middle-aged people the ϵ 4 allele is also associated with memory decline (Bondi et al., 1995; Flory, Manuck, Ferrell, Ryan, & Muldoon, 2000; Packard et al., 2007; Reed et al., 1994).

The APOE gene codes for apolipoprotein E (apoE) which has several functions in the body and in the brain, including anti-inflammatory and

antioxidant effects (Huang, 2010; Lynch, Morgan, Mance, Matthew, & Laskowitz, 2001; Miyata & Smith, 1996). How the apoE4 isoform exerts its negative effect on the development of AD is not precisely known yet. There are several mechanisms that likely play a role. The first is via its function as a cholesterol transporter. Cholesterol is necessary for the manufacture of bile acids and sterol hormones and for membrane synthesis but excessive levels of cholesterol can be harmful. The apoE4 isoform is a less well functioning cholesterol transporter causing hypercholesterolemia (Davignon, 2005; Mahley, 1988). Because of the altered lipid binding region of apoE4 compared to apoE2 and apoE3, its binding preference is shifted from high density lipoproteins, that are mainly involved in transporting excess cholesterol away from body tissues, to very low density lipoproteins (VLDL) and chylomicron remnants (Huang, 2010; Mahley, 1988; Zhong & Weisgraber, 2009). Down regulation of low-density lipoprotein (LDL) receptors (by increased clearance of VLDL) or competition for LDL receptors then lead to increased plasma LDL levels (Huang, 2010). It is known that in time hypercholesterolemia causes atherosclerosis. Hypercholesterolemia and atherosclerosis, like other cardiovascular risk factors such as hypertension, cardiac disease and diabetes mellitus, are also known risk factors for AD (de la Torre, 2004; Kalaria, 2000). In addition, in the brain it has been shown that less apoE3 is needed in similar sized lipid particles than apoE4, suggesting an impaired or less effective delivery of cholesterol to neurons (Gong et al., 2002).

A second role of apoE in the development of AD is its involvement in the clearance of A β from the brain across the blood brain barrier (BBB) (Bell et al., 2007). ApoE2-A β and apoE3-A β complexes are cleared from the brain at a much faster rate than apoE4-A β complexes (Deane et al., 2008). Increased levels of A β in the brain, especially the toxic oligomers then lead to an increased risk of AD. A β is not only cleared at a slower rate from the brain in APOE4 carriers, it also tends to accumulate more in cerebral blood vessel walls leading to cerebral amyloid angiopathy (CAA). CAA is present in about 10 to 40% of elderly brains but in AD brains the number rises to 80% or more (Jellinger, 2002). The incidence of CAA is higher in APOE ϵ 4 AD patients and non-AD ϵ 4 carriers compared to non- ϵ 4 carriers (Greenberg, Rebeck, Vonsattel, Gomez-Isla, & Hyman, 1995; Trembath et al., 2007) and is associated with cognitive decline (Arvanitakis et al., 2011; Attems, Quass, Jellinger, & Lintner, 2007). The deposition of A β in cerebral

blood vessel walls leads to smooth muscle cell degeneration and weakening of the vascular wall (Iadecola, Park, & Capone, 2009), which can result in micro- or macro- intracerebral bleedings. These aggravate the neurodegenerative process and inflammatory response (micro bleedings) or may lead to hemorrhagic stroke (macro bleedings) (Bell & Zlokovic, 2009).

Like apoE can interfere with A β , by reducing its clearance from the brain, the other way around, A β can also interfere with apoE. A β can decrease the ability of apoE to bind lipids (Strittmatter, Weisgraber et al., 1993) and effective functioning of apoE as a cholesterol transporter is dependent on its lipid binding ability. Possibly this is a mechanism by which AD pathology and apoE genotype interact in the brain to have a detrimental effect on the severity and onset of the disease.

A shared mechanism by which these risk factors could increase the risk for AD is that they can all lead to cerebral hypoperfusion. Normal functioning of all tissues depends on an adequate blood flow but the brain is especially sensitive with its high demand for glucose and inability to store energy. Aside from the obvious energy and nutrient deficiency that cerebral hypoperfusion causes, it also reduces the flow-dependent clearance of byproducts of brain activity (Iadecola et al., 2009). For instance, a decreased blood flow also decreases the clearance of A β from the vasculature (Iadecola, 2004), thereby increasing CAA. In addition, hypoperfusion reduces neuronal protein synthesis, important for synaptic plasticity (Klann & Dever, 2004). It has been shown that cerebral blood flow (CBF) is reduced in AD patients (Johnson et al., 2005) and CBF reductions are predictive of conversion to AD in patients with mild cognitive impairment (Hirao et al., 2005). Evidence for cerebral hypoperfusion is also found in animal models of AD. We have shown that APP/PS1 mice have a decreased cerebral blood volume at 15 months of age in the cortex (Hooijmans et al., 2009) and at 13 months of age in the microvasculature of the hippocampus (Zerbi et al., submitted).

In both AD and cardiovascular disease (CVD) sex differences exist. While women have a higher risk for AD, men are generally more affected by CVD (Pilote et al., 2007). For instance, men are more prone to develop high cholesterol serum levels and have so at a younger age than (premenopausal) women (Maas & Appelman, 2010; Maas et al., 2011). Atherosclerotic apoE knock out female mice have lower total cholesterol serum levels than males, while they have larger atherosclerotic plaques (Smith et al., 2010). Most of these sex differences

disappear however after women reach menopause, when they catch up with and even surpass men in the prevalence of CVD (Abbey, Owen, Suzakawa, Roach, & Nestel, 1999; Pilote et al., 2007). Besides differences in prevalence and age of onset, CVD can manifest itself differently in men and women. For example, while men have thicker atherosclerotic plaques that are localized in the large coronary arteries, women tend to have more diffuse plaques that also impair the smaller microvasculature (Maas & Appelman, 2010; Maas et al., 2011; Villablanca, Jayachandran, & Banka, 2010). And while men have higher death rates due to acute myocardial infarctions, more women die of stroke and cardiac arrest (Netherlands, 2009, Statistics Netherlands, The Hague/Heerlen). Also the effect of APOE genotype is not equal across sexes. The increased risk for AD and cognitive deficits in the non-demented population in e4 carriers is higher in women (Bartres-Faz et al., 2002; Bretsky et al., 1999; Mortensen & Hogh, 2001) and especially female apoE4 mice show spatial memory deficits (Bour et al., 2008; Raber et al., 1998).

So far, it is unknown by which mechanism apoE is influenced by sex. Possibly an interaction with estrogen plays a role, as is suggested by the postmenopausal increase in the incidence of CVD in women. The aim of the current study is to investigate these sex differences in aging, and we focus on parameters that are important for cognitive functioning. Therefore we look at synaptic density and neurogenesis in different models for AD and vascular disease in both male and female mice.

2. Materials and methods

2.1 Animals

Homogenous apoE-deficient (B6.129P2-Apoe^{tm1Unc}/J) mice were originally obtained from Jackson Laboratories (Bar Harbor, ME, USA) and subsequently bred in the Central Animal Laboratory (CDL; Radboud University Nijmegen Medical Centre, RUNMC). The mice for this specific study were bred from male and female apoE knockout (apoE ko) animals, generating homogenous apoE ko offspring. Homogenous human apoE4 transgenic mice were originally obtained from Taconic Transgenic Models (Hudson, NY, USA). In this strain the murine apoE gene is replaced with the human apoE4 alleles (4/4). The animals for the current study were bred at the CDL (RUNMC) by using both male and female apoE4 mice, generating

homogenous apoE4 offspring. Both apoE4 and apoE ko transgenic mice have C57BL6/J mice as background strain. C57BL6/J wild type (WT) mice were originally obtained from Harlan Laboratories, Inc. (Horst, the Netherlands) and subsequently bred in the CDL (RUNMC).

In total, 22 male mice and 21 female mice of the 3 different genotypes (WT, apoE4, and apoE ko) aged 9-15 months (males: 9-12 months, $M = 10.7$; females: 12-15 months, $M = 13.2$) were used in this study. The mice were housed in standard cages (Makrolon type 3, 42.5x26.5x15.5 cm, animals per cage: max 11) at 21°C on a 12h light/dark cycle (lights on at 7 a.m.) and were fed rodent lab chow. Water and food was administered ad libitum. There were no differences in brain or body weight between the genotypes in males or in females.

The experiments were performed according to Dutch federal regulations for animal protection and were approved by Veterinary Authority of the Radboud University Nijmegen Medical Centre.

2.2 Tissue preparation

Mice were anesthetized with Isoflurane (3-3.5% in a mixture of oxygen and N_2O (2:1)) and transcardially perfused, first with phosphate buffered saline (0.1 M PBS), then with 4% paraformaldehyde. Brains were removed immediately after perfusion fixation, postfixed overnight in 4% paraformaldehyde at 4°C and transferred the next day to 0.1 M PBS with 1% sodium azide. Brains were transferred to 30% sucrose in 0.1 M phosphate buffer 24 hours before cutting the brains in 40 μ m coronal sections on a sliding microtome (Microm HM 440, Walldorf, Germany) equipped with an object table for freeze sectioning at -60°C. Sections were divided into 6 complete series (1 out of every 6 sections) while cutting. Sections were stored in 0.1 M PBS with 1% sodium azide at 4°C until being used for immunohistochemistry.

2.3 Immunohistochemistry

All stainings were done according to standard protocols and all steps were performed at room temperature on a shaker table. Males and females were stained separately. Free-floating brain sections were first rinsed (rinsing of sections always with 0.1 M PBS), after which endogenous peroxidase was blocked with 0.3% H_2O_2 in 0.1 M PBS, rinsed again and pre-incubated with 0.1 M PBS-BT (0.1 M PBS with 1% Albumin Bovine Serum and 0.3% Triton-X-100). Sections were then incubated

overnight with a primary antibody (monoclonal rabbit-anti-synaptophysin clone EP1098Y, 1:20000 in PBS-BT for males, 1:10000 in PBS-BT for females, Abcam Inc., Cambridge, UK; goat-anti-Doublecortin (C18): sc-8066, 1:3000 in PBS-BT, Santa Cruz Biotechnology, Inc., Santa Cruz, CA, USA). After another rinse, sections were incubated for 90 min with a secondary antibody (donkey-anti-rabbit biotinylated IgG, 1:1500 in PBS-BT, Jackson ImmunoResearch, West Grove, PA, USA; donkey-anti-goat biotinylated IgG, 1:1500 in PBS-BT, Jackson ImmunoResearch, West Grove, PA, USA), rinsed again, and incubated with Vector ABC-Elite (A and B, 1:800 in PBS-BT, Vector Laboratories, Burlingame, CA, USA). Finally, sections were rinsed, pre-incubated with DAB-Nickel solution, incubated with Dab-Nickel solution with 0.3% H_2O_2 , and rinsed to stop the reaction. Sections were mounted on gelatin-coated object glasses (0.5% gelatin and 0.05% Chrome aluminium sulphate), dried overnight at 37°C, dehydrated in alcohol series, cleared up in Xylol and enclosed in Entellan.

2.4 Quantification

All quantifications were performed independently by two investigators and blind to experimental groups.

2.4.1 Synaptophysin

To determine the amount of synaptophysin-immunoreactive presynaptic boutons (SIPBs), appropriate sections were digitized and photomicrographed using the Zeiss Axioskop microscope, equipped with a 100 \times oil immersion objective and a 10 \times projection lens and software of Microbrightfield (Williston, VT, USA). Quantitative analyses were done with a computer-assisted analysis system (Stereo Investigator). SIPBs were analyzed in the prelimbic area (PRL), the cingulate gyrus (GC), and in the CA1, CA3 and dentate gyrus (DG) of the hippocampus (1.6 and 0.9 anterior and 2.1 posterior to bregma, respectively). Within the PRL and GC two square boxes were placed within the borders of the intended brain areas. In the hippocampus, two randomly chosen regions per section were analyzed in stratum radiatum of area CA1 (SR), stratum lucidum of area CA3 (SL), inner molecular layer (IML) and outer molecular layer (OML) of the DG (Fig. 1). Brain regions were based on the mouse brain atlas of Franklin and Paxinos (1997). All images taken were then processed with ImageJ (National Institutes of Health) for quantification

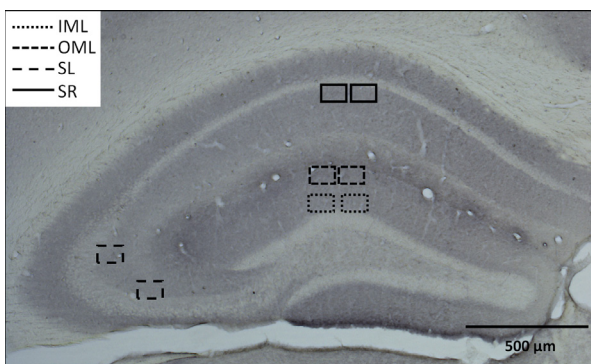


Fig. 1 Placement of contours for the analysis of the number of synaptophysin-immunoreactive presynaptic boutons in the hippocampus. The squares indicate the randomly chosen areas in the inner (IML) and outer molecular layer (OML) of the dentate gyrus, the stratum lucidum (SL) of the CA3, and the stratum radiatum (SR) of the CA1.

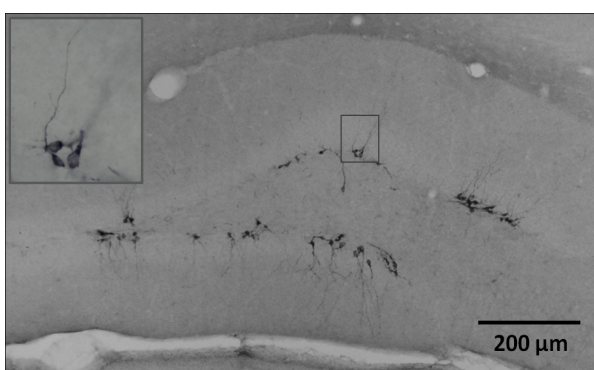


Fig. 2 Representative doublecortin-immuno-stained neurons in the dentate gyrus of hippocampus. Coronal section.

of the SIPBs. Images were first converted to 8-bit gray scale, then to 16-bit and finally contrast was enhanced. Threshold was set at 26471-33153 for the males, and at 27242-30840 for the females. Thresholds were inevitably different due to different staining sessions. Particles ranging between 0.1 to $4.5 \mu\text{m}^2$ (circularity 0.0-1.0) were considered to be normal sized SIPBs and included in the analysis.

2.4.2 Doublecortin

Appropriate sections were digitized and quantified, using a Zeiss Axioskop microscope equipped with hardware and software of Microbrightfield (Williston, VT, USA). Quantitative analyses were done with a computer-assisted analysis system (Stereo Investigator). For every mouse doublecortin positive cells (Fig. 2) were counted in the entire hippocampus in 3 different sections (at 2.1, 2.4, and 2.7 posterior to bregma). Brain regions were based on the mouse brain atlas of Franklin and Paxinos (1997). Contours of the hippocampi were drawn at 5 \times magnification, cells were counted at 20 \times magnification. Mean number of doublecortin

positive newly formed neurons was used in the analysis. Inter-rater reliability, as measured by intraclass correlation coefficient, was $> .90$.

2.5 Statistical analysis

All statistical analyses were performed with SPSS 16.0. Data were analyzed with univariate ANOVAs with genotype as independent factor, followed by post-hoc Tukey's HSD. Statistical significance was set at $p < .05$.

3. Results

3.1 Decreased amount of SIPBs in female apoE4 mice

In female apoE4 mice a significant decrease in the amount of synaptophysin-immunoreactive presynaptic boutons (SIPBs) in the inner molecular layer (IML) of the dentate gyrus in the hippocampus was found compared to female wild type (WT) mice (WT: $M = 100$, SEM = 4.67; apoE4: $M = 79.28$, SEM = 2.91; $p < .01$, Fig. 3). There were no significant differences in the amount of SIPBs in the cortex (prelimbic area and cingulate gyrus) or in the other regions of the hippocampus (outer molecular layer, stratum radiatum and stratum lucidum). In male mice there were no significant differences between the genotypes in the amount of SIPBs in any of the investigated brain regions.

3.2 Increased neurogenesis in female apoE ko mice

A trend was observed in the number of doublecortin positive newly formed neurons between genotypes in female mice ($F = 3.53$, $p = .052$, Fig. 4). There is a strong indication that neurogenesis is increased in female apoE ko mice compared to female WT mice. In male mice there were no significant differences in neurogenesis between the genotypes.

4. Discussion

In this study we investigated the sex differences in aging focusing on parameters related to cognitive functioning. We looked at synaptic density and neurogenesis in different models for Alzheimer's disease (AD) and vascular disease in both male and female mice. In middle-aged female apoE mice we found decreased synaptic density and increased

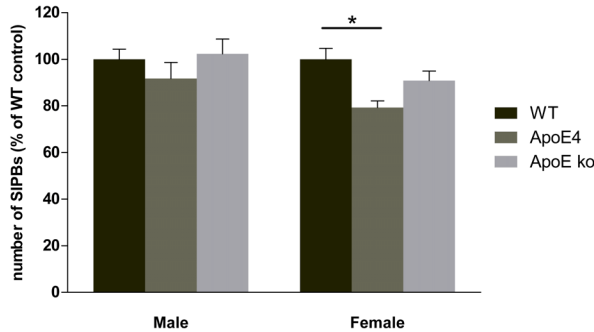


Fig. 3 Number of synaptophysin-immunoreactive presynaptic boutons (SIPBs) in the inner molecular layer (IML) of the dentate gyrus in the hippocampus. In female mice there is a significant effect of genotype on the number of SIPBs in the IML ($n = 7/\text{group}$, $*p < .01$). ApoE4 female mice have less SIPBs than wild type female mice ($*p < .01$). In male mice there are no significant effects ($n = 7-8/\text{group}$, $p > .05$). Error bars show mean \pm SEM.

neurogenesis compared to wild type (WT) mice. In male mice no differences between genotypes could be detected.

In female apoE4 mice we found a decrease in the number of synaptophysin immunoreactive presynaptic boutons (SIPBs) in the inner molecular layer (IML) of the dentate gyrus compared to controls. To our knowledge there are no other studies that investigated synaptic density in female apoE4 or apoE knock out (apoE ko) mice. Studies in male apoE mice either found no difference between apoE4, apoE ko and WT mice or demonstrated a decrease in synaptic density in aged apoE ko mice (Levi, Jongen-Relo, Feldon, & Michaelson, 2005; Veinbergs et al., 1999). The decrease in SIPBs in our female apoE4 mice is in line with Rutten et al. (2005) who found an age related loss of the number of SIPBs in the hippocampus in females of an APP/PS1 transgenic AD mouse model and with autopsy studies in which a decrease in synaptic proteins or synaptic density was found in male and female patients with mild cognitive impairment (MCI) or AD compared to controls (Reddy et al., 2005; Scheff, Price, Schmitt, DeKosky, & Mufson, 2007; Scheff, Price, Schmitt, & Mufson, 2006). However, Scheff et al. (2007; 2006) did not find a relationship with apoE genotype (E2, E3, E4).

In our female mice we found a trend in the number of doublecortin positive newly formed neurons, indicating that neurogenesis is increased in female apoE ko mice compared to controls. This result contrasts with Li et al. (2009) who found a decrease in neurogenesis in female apoE ko mice. However, their mice are aged 6-7 months, which is much younger than our 12-15 months old mice. Possibly a compensatory mechanism, where synaptic

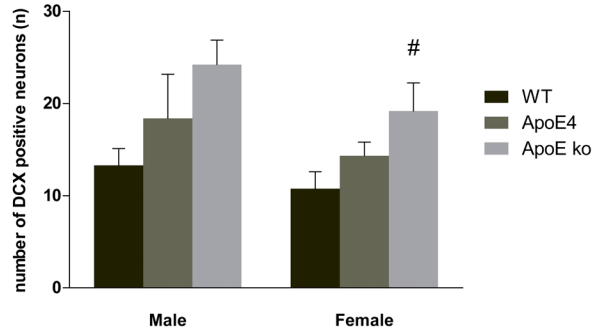


Fig. 4 Neurogenesis in the dentate gyrus of the hippocampus. In female mice a trend was observed in the number of doublecortin positive newly formed neurons between genotypes ($n = 6-7 \text{ mice/group}$, $\#p = .052$). The data strongly indicate that neurogenesis is increased in female apoE knockout mice compared to female wild type mice. In males no differences in neurogenesis are found ($n = 5-7 \text{ mice/group}$, $p > .05$). Error bars show mean \pm SEM.

contacts are and/or neurogenesis is increased in response to synaptic failure (Jansen et al, submitted) or insults to the brain (Jin, Peel et al., 2004; Levi & Michaelson, 2007), is established only at an older age.

We did not find any differences in synaptic density or in neurogenesis between male apoE4, apoE ko and WT mice. The absence of an effect of genotype on the number of SIPBs is in line with Levi et al. (2005), who did not observe differences in pre-synaptic density in the hippocampus of male apoE3, apoE4, apoE ko and WT mice. Also, Liraz, Haas and Michaelson (2011) could not detect differences between male apoE3 and apoE4 in hippocampal synaptophysin levels, as determined by western blot. However, Veinbergs et al. (1999) did find a decrease in pre-synaptic density in the hippocampus and frontoparietal cortex of aged male apoE ko mice. In human autopsy studies male and female patients with AD or MCI are also often found to have synaptic loss compared to controls (Reddy et al., 2005; Scheff et al., 2007; Scheff et al., 2006).

Regarding neurogenesis in AD patients and AD and apoE mouse models conflicting results have been found. Most studies on AD found a decrease in neurogenesis both in humans (Boekhoorn, Joels, & Lucassen, 2006) and in APP and PS1 mouse models (Donovan et al., 2006; Wen et al., 2004). The exceptions are Jin et al. (2004) who found an increase in neurogenesis in male AD patients and Jin et al. (2004) who found increased neurogenesis in AD transgenic mice. However, the first study suffers from some serious methodological issues concerning differences between the AD and control group in age, sex and postmortem interval. In apoE mouse

models only one study reports on male mice. Levi and Michaelson (2007) found that neurogenesis, as measured immunohistochemically by doublecortin staining, is increased in 6 months old male apoE ko mice and even more in apoE4 mice. In contrast, we did not find any differences in neurogenesis in our male mice. Possibly this discrepancy results from the age difference (6 vs. 11 months) between the mice in these studies.

The present findings support previously found gender differences in AD and between apoE genotypes. Possibly estrogen can explain these differences, as it has many effects on the vasculature and is protective against the development of atherosclerosis, as demonstrated for example by the lower incidence in pre-menopausal women (Mendelsohn & Karas, 1999; Vaccarino et al., 2011). Estrogen is vasodilating, anti-inflammatory and acts as an antioxidant (Kublickiene & Luksha, 2008; Villablanca et al., 2010). Additionally it can regulate gene expression by binding its nuclear estrogen receptor that acts as a transcription factor (Yamamoto, 1985). It also decreases plasma LDL levels and increases HDL levels (Hulley et al., 1998). Possibly the beneficial effects of estrogen explain the difference in incidence and age of onset of vascular disease between sexes. However, the higher incidence of AD in women suggests an interaction between estrogen, AD risk factors and pathology.

ApoE is also involved in the cardiovascular system via its role as a cholesterol transporter and its involvement in cerebral amyloid angiopathy (Greenberg et al., 1995; Hauser, Narayanaswami, & Ryan, 2011; Trembath et al., 2007). Women are particularly affected by the adverse affects of the APOE4 genotype with regard to AD incidence and cognitive deficits (Bartres-Faz et al., 2002; Bretsky et al., 1999; Mortensen & Hogh, 2001).

The interplay of estrogen and apoE is not a simple one with the various effects both have on the vasculature. However, a specific interaction seems to exist between the apoE4 isoform and estrogen. For example, although hormone replacement therapy (HRT) can lower the incidence of AD when initiated perimenopausal (Kawas et al., 1997; Tang et al., 1996) and it can be effective in reducing cognitive decline in women not carrying the e4 allele, it is not beneficial in apoE4 women (Yaffe, Haan, Byers, Tangen, & Kuller, 2000). In addition, apoE4 women with an increased reproductive period, and therefore a longer lifetime exposure to estrogen, have an increased risk for dementia and AD (Geerlings et al., 2001). Furthermore, Lambert et al. (2004) have shown in vitro that regulation of APOE by

estrogen is allele dependent. The harmful effect of estrogen in the apoE4 genotype could also explain the stronger association of APOE4 with AD in women and the increased susceptibility of female apoE4 mice to spatial memory deficits. In contrast, androgens have been shown to protect against apoE4-induced cognitive deficits. Androgen treated female apoE4 mice improved their performance on a spatial memory test. Male apoE4 mice, on the other hand, which first did not show any deficits, were impaired in spatial memory after blockade of androgen receptors (Raber, Bongers, LeFevour, Buttini, & Mucke, 2002). A combined effect of apoE4 and sex has been found in other diseases as well, such as ocular herpes simplex virus type 1 (Hill, Lhattacharjee, & Neumann, 2007). Here, again female apoE4 mice are most susceptible to infection as well as to a higher neuroinvasiveness of the virus. The current result, where only female apoE4 mice show a loss of synapses, is also in line with this view of a specific female susceptibility to the negative effect of apoE4.

In our apoE mouse models several mechanisms are involved producing in one case a decrease in synapses in female apoE4 mice and in another case increased neurogenesis in female apoE ko mice. Whereas the severely compromised vasculature in apoE ko mice results in a compensatory effect by increased neurogenesis, the specific interaction of apoE4 with estrogen, even though their vasculature is less affected than that of apoE ko mice, results in a deleterious effect in the form of a loss of synapses. In addition, male apoE4 mice could possibly be benefiting from protection by androgens to the effects of apoE4. The fact that a compensatory mechanism can be observed in female apoE ko mice, in contrast to male apoE ko mice, could be due to their difference in estrogen exposure.

We find a different effect in females compared to males concerning the amount of presynaptic boutons and neurogenesis. Although the slightly higher age of the female group should be kept in mind, we do not expect a large influence due to this age difference of only two months. Since our female mice can be considered pre-menopausal, large hormonal fluctuations are absent. Therefore both our male and female mice belong to the same stable age range.

Several studies have shown that sex differences exist in the neurodegenerative processes after cerebral ischemia (Du et al., 2004; McCullough, Zeng, Blizzard, Debchoudhury, & Hurn, 2005; Siegel, Turtzo, & McCullough, 2010). For example the apoptosis-initiating pathway that is activated

as a result of ischemia is different in men and women. While in men ischemic cell death occurs mainly via caspase-independent mechanisms, by activation of poly-ADP-ribose polymerase (PARP) and apoptosis-inducing factor, in women caspase-mediated mechanisms are mainly responsible, via apoptosome formation and caspase activation (Lang & McCullough, 2008; McCullough et al., 2005; Siegel et al., 2010). Inhibiting the PARP pathway has protective effects in male animals but in females it worsens outcomes after ischemic injury (McCullough et al., 2005). In contrast, inhibiting the caspase pathway is only neuroprotective in females and not in males (Liu et al., 2009). This highlights the importance of considering sex when designing new therapeutic agents, as the effects can be very different in men and women. This can already be seen for example in aspirin treatment in the primary prevention of CVD. Though both men and women benefit from aspirin treatment, the effect in men is through a reduced risk of myocardial infarction, while in women it reduces the risk of ischemic stroke (Berger et al., 2006). And in stroke patients treated with tissue plasminogen activator, functional outcomes are nearly three times higher in men than in women (Elkind et al., 2007). However, the current practice is still to study mainly young male animals, which can pose a risk to women when translating the results to clinical trials in both sexes, as well as possible discarding novel therapeutic agents that fail to work in males but are never tested on their efficacy in females.

HRT and statins are two therapy options that have been suggested for the treatment or prevention of CVD (Brugts & Deckers, 2010; Ravn, Rosenberg, & Bostofte, 1994), as well as AD (Sparks et al., 2008; Tang et al., 1996). Timing of HRT is likely a crucial factor in the efficacy of this treatment, where starting perimenopausal leads to largely beneficial effects but starting postmenopausal can be harmful (Manson et al., 2006; Phillips & Langer, 2005). However, from the above conclusion that estrogen specifically interacts with the APOE4 genotype in a harmful way it follows that HRT possibly should be avoided in apoE4 women. Yaffe et al. (2000) have indeed shown that ε4 carriers do not benefit cognitively from HRT as do non-ε4 carriers. At a minimum an even more careful consideration of the possible advantages (cardiovascular) and disadvantages (cognitive) should be made when considering initiating HRT in apoE4 women.

Many studies revealed that statins (3-hydroxy-3-methylglutaryl coenzyme A reductase inhibitors) decrease the prevalence of AD (Rockwood et

al., 2002; Sparks et al., 2008; Wolozin, Kellman, Rousseau, Celesia, & Siegel, 2000) (but see (Arvanitakis et al., 2006)). A study by Sparks et al. (2006) indicates that statins are specifically beneficial for ε4 allele carriers, although this effect might be partly or entirely driven by their higher cholesterol levels. Still, statins could provide a viable treatment option to slow or prevent AD in either carriers of an ε4 allele and/or those with high, or moderately high, plasma cholesterol levels.

Both sex and apoE allele status should be more carefully considered in the search for and development of new therapeutic agents, as any one of these can significantly influence the outcome.

5. Conclusion

To our knowledge, we are the first to investigate synaptic density in female apoE4 and apoE ko mice. We found a decrease in synaptic density in the hippocampus of middle-aged female apoE4 mice compared to WT mice. This could be the result of a specific harmful interaction of estrogen with apoE4 as we did not observe any differences in male mice. In addition we found neurogenesis to be increased in middle-aged female apoE ko mice. Previous studies have suggested a compensatory mechanism for synaptic failure by temporarily increasing the amount of synaptic contacts and/or neurogenesis. The increased neurogenesis found in female apoE ko mice supports this hypothesis. Our results support previously found sex specific differences between apoE genotypes, that could account for some of the sex differences in AD and CVD. Sex differences should be taken into account in any research concerning CVD, AD or apoE.

Acknowledgements

The research leading to these results have received funding from the European Community's Seventh Framework Programme (FP7/2007-2013) under grant agreement no202167. The authors report no actual or potential conflicts of interest.

References

- Abbey, M., Owen, A., Suzakawa, M., Roach, P., & Nestel, P. J. (1999). Effects of menopause and hormone replacement therapy on plasma lipids, lipoproteins and LDL-receptor activity. *Maturitas*, 33 (3), 259-269.
- Arvanitakis, Z., Leurgans, S. E., Wang, Z. X., Wilson, R. S., Bennett, D. A., & Schneider, J. A. (2011). Cerebral

- Amyloid Angiopathy Pathology and Cognitive Domains in Older Persons. *Annals of Neurology*, 69 (2), 320-327.
- Arvanitakis, Z., Schneider, J. A., Wilson, R. S., Bienias, J. L., Kelly, J. F., & Bennett, D. A. (2006). Statins, Alzheimer's disease, change in cognitive function, and neuropathology. *Neurology*, 66 (5), 310-310.
- Attems, J., Quass, M., Jellinger, K. A., & Lintner, F. (2007). Topographical distribution of cerebral amyloid angiopathy and its effect on cognitive decline are influenced by Alzheimer disease pathology. *Journal of the Neurological Sciences*, 257 (1-2), 49-55.
- Bartres-Faz, D., Junque, C., Moral, P., Lopez-Alomar, A., Sanchez-Aldeguer, J., & Clemente, I. C. (2002). Apolipoprotein E gender effects on cognitive performance in age-associated memory impairment. *Journal of Neuropsychiatry and Clinical Neurosciences*, 14 (1), 80-83.
- Bell, R. D., Sagare, A. P., Friedman, A. E., Bedi, G. S., Holtzman, D. M., Deane, R. et al. (2007). Transport pathways for clearance of human Alzheimer's amyloid beta-peptide and apolipoproteins E and J in the mouse central nervous system. *Journal of Cerebral Blood Flow and Metabolism*, 27 (5), 909-918.
- Bell, R. D., & Zlokovic, B. V. (2009). Neurovascular mechanisms and blood-brain barrier disorder in Alzheimer's disease. *Acta Neuropathologica*, 118 (1), 103-113.
- Berger, J. S., Roncaglioni, M. C., Avanzini, F., Pangrazzi, I., Tognoni, G., & Brown, D. L. (2006). Aspirin for the primary prevention of cardiovascular events in women and men - A sex-specific meta-analysis of randomized controlled trials. *Journal of the American Medical Association*, 295 (3), 306-313.
- Boekhoorn, K., Joels, M., & Lucassen, P. J. (2006). Increased proliferation reflects glial and vascular-associated changes, but not neurogenesis in the presenile Alzheimer hippocampus. *Neurobiology of Disease*, 24 (1), 1-14.
- Bondi, M. W., Salmon, D. P., Monsch, A. U., Galasko, D., Butters, N., Klauber, M. R. et al. (1995). Episodic memory changes are associated with the APOE-epsilon 4 allele in nondemented older adults. *Neurology*, 45 (12), 2203-2206.
- Bour, A., Grootendorst, J., Vogel, E., Kelche, C., Dodart, J. C., Bales, K. et al. (2008). Middle-aged human apoE4 targeted-replacement mice show retention deficits on a wide range of spatial memory tasks. *Behavioural Brain Research*, 193 (2), 174-182.
- Bretsky, P. M., Buckwalter, J. G., Seeman, T. E., Miller, C. A., Poirier, J., Schellenberg, G. D. et al. (1999). Evidence for an interaction between apolipoprotein E genotype, gender, and Alzheimer disease. *Alzheimer Disease and Associated Disorders*, 13 (4), 216-221.
- Brugts, J. J., & Deckers, J. W. (2010). Statin prescription in men and women at cardiovascular risk: to whom and when? *Current Opinion in Cardiology*, 25 (5), 484-489.
- Brun, A., & Englund, E. (1986). A White Matter Disorder in Dementia of the Alzheimer Type - a Pathoanatomical Study. *Annals of Neurology*, 19 (3), 253-262.
- Corder, E. H., Saunders, A. M., Strittmatter, W. J., Schmeichel, D. E., Gaskell, P. C., Small, G. W. et al. (1993). Gene dose of apolipoprotein E type 4 allele and the risk of Alzheimer's disease in late onset families. *Science*, 261 (5123), 921-923.
- DaRocha-Souto, B., Scotton, T. C., Coma, M., Serrano-Pozo, A., Hashimoto, T., Sereno, L. et al. (2011). Brain Oligomeric beta-Amyloid but Not Total Amyloid Plaque Burden Correlates With Neuronal Loss and Astrocyte Inflammatory Response in Amyloid Precursor Protein/Tau Transgenic Mice. *Journal of Neuropathology and Experimental Neurology*, 70 (5), 360-376.
- Davignon, J. (2005). Apolipoprotein E and atherosclerosis beyond lipid effect. *Arteriosclerosis, Thrombosis, and Vascular Biology*, 25 (2), 267-269.
- Davis, D. G., Schmitt, F. A., Wekstein, D. R., & Markesberry, W. R. (1999). Alzheimer neuropathologic alterations in aged cognitively normal subjects. *Journal of Neuropathology and Experimental Neurology*, 58 (4), 376-388.
- de la Torre, J. C. (2004). Is Alzheimer's disease a neurodegenerative or a vascular disorder? Data, dogma, and dialectics. *Lancet Neurology*, 3 (3), 184-190.
- Deane, R., Sagare, A., Hamm, K., Parisi, M., Lane, S., Finn, M. B. et al. (2008). apoE isoform-specific disruption of amyloid beta peptide clearance from mouse brain. *Journal of Clinical Investigation*, 118 (12), 4002-4013.
- Donovan, M. H., Yazdani, U., Norris, R. D., Games, D., German, D. C., & Eisch, A. J. (2006). Decreased adult hippocampal neurogenesis in the PDAPP mouse model of Alzheimer's disease. *Journal of Comparative Neurology*, 495 (1), 70-83.
- Du, L. N., Bayir, H., Lai, Y. C., Zhang, X. P., Kochanek, P. M., Watkins, S. C. et al. (2004). Innate gender-based proclivity in response to cytotoxicity and programmed cell death pathway. *Journal of Biological Chemistry*, 279 (37), 38563-38570.
- Elkind, M. S. V., Prabhakaran, S., Pittman, J., Koroshetz, W., Jacoby, M., & Johnston, K. C. (2007). Sex as a predictor of outcomes in patients treated with thrombolysis for acute stroke. *Neurology*, 68 (11), 842-848.
- Farrer, L. A., Cupples, L. A., Haines, J. L., Hyman, B., Kukull, W. A., Mayeux, R. et al. (1997). Effects of age, sex, and ethnicity on the association between apolipoprotein E genotype and Alzheimer disease - A meta-analysis. *Journal of the American Medical Association*, 278 (16), 1349-1356.
- Fernando, M. S., & Ince, P. G. (2004). Vascular pathologies and cognition in a population-based cohort of elderly people. *Journal of the Neurological Sciences*, 226 (1-2), 13-17.
- Flory, J. D., Manuck, S. B., Ferrell, R. E., Ryan, C. M., & Muldoon, M. F. (2000). Memory performance and the apolipoprotein E polymorphism in a community

- sample of middle-aged adults. *American Journal of Medical Genetics*, 96 (6), 707-711.
- Franklin, K., & Paxinos, G. (1997). *The Mouse Brain in Stereotaxic Coordinates*. San Diego: Academic press.
- Geerlings, M. I., Ruitenberg, A., Witteman, J. C. M., van Swieten, J. C., Hofman, A., van Duijn, C. M. et al. (2001). Reproductive period and risk of dementia in postmenopausal women. *Journal of the American Medical Association*, 285 (11), 1475-1481.
- Gong, J. S., Kobayashi, M., Hayashi, H., Zou, K., Sawamura, N., Fujita, S. C. et al. (2002). Apolipoprotein E (ApoE) isoform-dependent lipid release from astrocytes prepared from human ApoE3 and ApoE4 knock-in mice. *Journal of Biological Chemistry*, 277 (33), 29919-29926.
- Greenberg, S. M., Rebeck, G. W., Vonsattel, J. P. G., Gomez-Isla, T., & Hyman, B. T. (1995). Apolipoprotein E ε4 and cerebral hemorrhage associated with amyloid angiopathy. *Annals of Neurology*, 38 (2), 254-259.
- Hardy, J. A., & Higgins, G. A. (1992). Alzheimer's disease: The amyloid cascade hypothesis. *Science*, 256 (5054), 184-185.
- Hauser, P. S., Narayanaswami, V., & Ryan, R. O. (2011). Apolipoprotein E: From lipid transport to neurobiology. *Progress in Lipid Research*, 50 (1), 62-74.
- Hill, J. M., Lhattacharjee, P. S., & Neumann, D. A. (2007). Apolipoprotein E alleles can contribute to the pathogenesis of numerous clinical conditions including HSV-1 corneal disease. *Experimental Eye Research*, 84 (5), 801-811.
- Hirao, K., Ohnishi, T., Hirata, Y., Yamashita, F., Mori, T., Moriguchi, Y. et al. (2005). The prediction of rapid conversion to Alzheimer's disease in mild cognitive impairment using regional cerebral blood flow SPECT. *Neuroimage*, 28 (4), 1014-1021.
- Hooijmans, C. R., Van der Zee, C. E. E. M., Dederen, P. J., Brouwer, K. M., Reijmer, Y. D., van Groen, T. et al. (2009). DHA and cholesterol containing diets influence Alzheimer-like pathology, cognition and cerebral vasculature in APPswe/PS1dE9 mice. *Neurobiology of Disease*, 33 (3), 482-498.
- Huang, Y. D. (2010). Mechanisms linking apolipoprotein E isoforms with cardiovascular and neurological diseases. *Current Opinion in Lipidology*, 21 (4), 337-345.
- Hulley, S., Grady, D., Bush, T., Furberg, C., Herrington, D., Riggs, B. et al. (1998). Randomized trial of estrogen plus progestin for secondary prevention of coronary heart disease in postmenopausal women. *Journal of the American Medical Association*, 280 (7), 605-613.
- Iadecola, C. (2004). Neurovascular regulation in the normal brain and in Alzheimer's disease. *Nature Reviews Neuroscience*, 5 (5), 347-360.
- Iadecola, C., Park, L., & Capone, C. (2009). Threats to the Mind Aging, Amyloid, and Hypertension. *Stroke*, 40 (3), S40-S44.
- Jellinger, K. A. (2002). Alzheimer disease and cerebrovascular pathology: An update. *Journal of Neural Transmission*, 109 (5-6), 813-836.
- Jin, K., Galvan, V., Xie, L., Mao, X. O., Gorostiza, O. F., Bredesen, D. E. et al. (2004). Enhanced neurogenesis in Alzheimer's disease transgenic (PDGF-APP Sw,Ind) mice. *Proceedings of the National Academy of Sciences of the United States of America*, 101 (36), 13363-13367.
- Jin, K., Peel, A. L., Mao, X. O., Xie, L., Cottrell, B. A., Henshall, D. C. et al. (2004). Increased hippocampal neurogenesis in Alzheimer's disease. *Proceedings of the National Academy of Sciences of the United States of America*, 101 (1), 343-347.
- Johnson, N. A., Jahng, G. H., Weiner, M. W., Miller, B. L., Chui, H. C., Jagust, W. J. et al. (2005). Pattern of cerebral hypoperfusion in Alzheimer disease and mild cognitive impairment measured with arterial spin-labeling MR imaging: Initial experience. *Radiology*, 234 (3), 851-859.
- Kalaria, R. N. (2000). The role of cerebral ischemia in Alzheimer's disease. *Neurobiology of Aging*, 21 (2), 321-330.
- Kawas, C. M., Resnick, S. P., Morrison, A. M. R. C., Brookmeyer, R. P., Corrada, M. S., Zonderman, A. P. et al. (1997). A prospective study of estrogen replacement therapy and the risk of developing Alzheimer's disease: *The Baltimore Longitudinal Study of Aging*. *Neurology*, 48 (6), 1517-1521.
- Kim, J., Basak, J. M., & Holtzman, D. M. (2009). The Role of Apolipoprotein E in Alzheimer's Disease. *Neuron*, 63 (3), 287-303.
- Klann, E., & Dever, T. E. (2004). Biochemical mechanisms for translational regulation in synaptic plasticity. *Nature Reviews Neuroscience*, 5 (12), 931-942.
- Klunk, W. E., Engler, H., Nordberg, A., Wang, Y. M., Blomqvist, G., Holt, D. P. et al. (2004). Imaging brain amyloid in Alzheimer's disease with Pittsburgh Compound-B. *Annals of Neurology*, 55 (3), 306-319.
- Kublickiene, K., & Luksha, L. (2008). Gender and the endothelium. *Pharmacological Reports*, 60 (1), 49-60.
- Lambert, J. C., Coyle, N., & Lendon, C. (2004). The allelic modulation of apolipoprotein E expression by oestrogen: potential relevance for Alzheimer's disease. *Journal of Medical Genetics*, 41 (2), 104-112.
- Lang, J. T., & McCullough, L. D. (2008). Pathways to ischemic neuronal cell death: are sex differences relevant? *Journal of Translational Medicine*, 6 (33).
- Launer, L. J., Andersen, K., Dewey, M. E., Letenneur, L., Ott, A., Amaducci, L. A. et al. (1999). Rates and risk factors for dementia and Alzheimer's disease - Results from EURODEM pooled analyses. *Neurology*, 52 (1), 78-84.
- Levi, O., Jongen-Relo, A. L., Feldon, J., & Michaelson, D. M. (2005). Brain area- and isoform-specific inhibition of synaptic plasticity by apoE4. *Journal of the Neurological Sciences*, 229, 241-248.
- Levi, O., & Michaelson, D. M. (2007). Environmental enrichment stimulates neurogenesis in apolipoprotein E3 and neuronal apoptosis in apolipoprotein E4 transgenic mice. *Journal of Neurochemistry*, 100 (1), 202-210.
- Li, G., Bien-Ly, N., Andrews-Zwilling, Y., Xu, Q., Bernardo, A., Ring, K. et al. (2009). GABAergic interneuron

- dysfunction impairs hippocampal neurogenesis in adult apolipoprotein E4 knockin mice. *Cell Stem Cell*, 5 (6), 634-645.
- Liu, F. D., Li, Z., Li, J., Siegel, C., Yuan, R. W., & McCullough, L. D. (2009). Sex Differences in Caspase Activation After Stroke. *Stroke*, 40 (5), 1842-1848.
- Lynch, J. R., Morgan, D., Mance, J., Matthew, W. D., & Laskowitz, D. T. (2001). Apolipoprotein E modulates glial activation and the endogenous central nervous system inflammatory response. *Journal of Neuroimmunology*, 114 (1-2), 107-113.
- Maas, A. H. E. M., & Appelman, Y. E. A. (2010). Gender differences in coronary heart disease. *Netherlands Heart Journal*, 18 (12), 598-603.
- Maas, A. H. E. M., Van Der Schouw, Y. T., Regitz-Zagrosek, V., Swahn, E., Appelman, Y. E., Pasterkamp, G. et al. (2011). Red alert for womens heart: The urgent need for more research and knowledge on cardiovascular disease in women. *European Heart Journal*, 32 (11), 1362-1368d.
- Mahley, R. W. (1988). Apolipoprotein-E - Cholesterol Transport Protein with Expanding Role in Cell Biology. *Science*, 240 (4852), 622-630.
- Manson, J. E., Bassuk, S. S., Harman, S. M., Brinton, E. A., Cedars, M. I., Lobo, R. et al. (2006). Postmenopausal hormone therapy: new questions and the case for new clinical trials. *Menopause-the Journal of the North American Menopause Society*, 13 (1), 139-147.
- McCullough, L. D., Zeng, Z. Y., Blizzard, K. K., Debczochdury, I., & Hurn, P. D. (2005). Ischemic nitric oxide and poly (ADP-ribose) polymerase-1 in cerebral ischemia: male toxicity, female protection. *Journal of Cerebral Blood Flow and Metabolism*, 25 (4), 502-512.
- Mendelsohn, M. E., & Karas, R. H. (1999). The protective effects of estrogen on the cardiovascular system. *New England Journal of Medicine*, 340 (23), 1801-1811.
- Miyata, M., & Smith, J. D. (1996). Apolipoprotein E allele-specific antioxidant activity and effects on cytotoxicity by oxidative insults and beta-amyloid peptides. *Nature Genetics*, 14 (1), 55-61.
- Moreira, P. I., Zhu, X., Smith, M. A., Perry, G., & Larry, R. S. (2009). *Alzheimer's Disease: An Overview Encyclopedia of Neuroscience* (pp. 259-263). Oxford: Academic Press.
- Mortensen, E. L., & Hogh, P. (2001). A gender difference in the association between APOE genotype and age-related cognitive decline. *Neurology*, 57 (1), 89-95.
- Packard, C. J., Westendorp, R. G. J., Stott, D. J., Caslake, M. J., Murray, H. M., Shepherd, J. et al. (2007). Association between apolipoprotein E-4 and cognitive decline in elderly adults. *Journal of the American Geriatrics Society*, 55 (11), 1777-1785.
- Phillips, L. S., & Langer, R. D. (2005). Postmenopausal hormone therapy: critical reappraisal and a unified hypothesis. *Fertility and Sterility*, 83 (3), 558-566.
- Pilote, L., Dasgupta, K., Guru, V., Humphries, K. H., McGrath, J., Norris, C. et al. (2007). A comprehensive view of sex-specific issues related to cardiovascular disease. *Canadian Medical Association Journal*, 176 (6), S1-S44.
- Raber, J., Bongers, G., LeFevour, A., Buttini, M., & Mucke, L. (2002). Androgens protect against apolipoprotein E4-induced cognitive deficits. *Journal of Neuroscience*, 22 (12), 5204-5209.
- Raber, J., Wong, D., Buttini, M., Orth, M., Bellobusta, S., Pitas, R. E. et al. (1998). Isoform-specific effects of human apolipoprotein E on brain function revealed in ApoE knockout mice: Increased susceptibility of females. *Proceedings of the National Academy of Sciences of the United States of America*, 95 (18), 10914-10919.
- Ravn, S. H., Rosenberg, J., & Bostofte, E. (1994). Postmenopausal Hormone Replacement Therapy - Clinical Implications. *European Journal of Obstetrics Gynecology and Reproductive Biology*, 53 (2), 81-93.
- Reddy, P. H., Mani, G., Park, B. S., Jacques, J., Murdoch, G., Whetsell, W. et al. (2005). Differential loss of synaptic proteins in Alzheimer's disease: Implications for synaptic dysfunction. *Journal of Alzheimers Disease*, 7 (2), 103-117.
- Reed, T., Carmelli, D., Swan, G. E., Breitner, J. C. S., Welsh, K. A., Jarvik, G. P. et al. (1994). Lower Cognitive Performance in Normal Older Adult Male Twins Carrying the Apolipoprotein-E Epsilon-4 Allele. *Archives of Neurology*, 51 (12), 1189-1192.
- Rockwood, K., Kirkland, S., Hogan, D. B., MacKnight, C., Merry, H., Verreault, R. et al. (2002). Use of lipid-lowering agents, indication bias, and the risk of dementia in community-dwelling elderly people. *Archives of Neurology*, 59 (2), 223-227.
- Rutten, B. P. F., Van der Kolk, N. M., Schafer, S., van Zandvoort, M., Bayer, T. A., Steinbusch, H. W. M. et al. (2005). Age-related loss of synaptophysin immunoreactive presynaptic boutons within the hippocampus of APP751(SL)/PS1(M146L) and APP751(SL)/PS1(M146L) transgenic mice. *American Journal of Pathology*, 167 (1), 161-173.
- Scheff, S. W., Price, D. A., Schmitt, F. A., DeKosky, S. T., & Mufson, E. J. (2007). Synaptic alterations in CA1 in mild Alzheimer disease and mild cognitive impairment. *Neurology*, 68 (18), 1501-1508.
- Scheff, S. W., Price, D. A., Schmitt, F. A., & Mufson, E. J. (2006). Hippocampal synaptic loss in early Alzheimer's disease and mild cognitive impairment. *Neurobiology of Aging*, 27 (10), 1372-1384.
- Selkoe, D. J. (1991). The molecular pathology of Alzheimer's disease. *Neuron*, 6 (4), 487-498.
- Shankar, G. M., Leisring, M. A., Adame, A., Sun, X. Y., Spooner, E., Masliah, E. et al. (2009). Biochemical and immunohistochemical analysis of an Alzheimer's disease mouse model reveals the presence of multiple cerebral A beta assembly forms throughout life. *Neurobiology of Disease*, 36 (2), 293-302.
- Siegel, C., Turtzo, C., & McCullough, L. D. (2010). Sex Differences in Cerebral Ischemia: Possible Molecular Mechanisms. *Journal of Neuroscience Research*, 88 (13), 2765-2774.
- Smith, D. D., Tan, X., Tawfik, O., Milne, G., Stechschulte, D. J., & Dileepan, K. N. (2010). Increased aortic

- atherosclerotic plaque development in female apolipoprotein E-null mice is associated with elevated thromboxane A2 and decreased prostacyclin production. *Journal of Physiology and Pharmacology*, 61 (3), 309-316.
- Sparks, D. L., Connor, D. J., Sabbagh, M. N., Petersen, R. B., Lopez, J., & Browne, P. (2006). Circulating cholesterol levels, apolipoprotein E genotype and dementia severity influence the benefit of atorvastatin treatment in Alzheimer's disease: results of the Alzheimer's disease cholesterol-lowering treatment (ADCLT) trial. *Acta Neurologica Scandinavica*, 114, 3-7.
- Sparks, D. L., Kryscio, R. J., Sabbagh, M. N., Connor, D. J., Sparks, L. M., & Liebsack, C. (2008). Reduced risk of incident AD with elective statin use in a clinical trial cohort. *Current Alzheimer Research*, 5 (4), 416-421.
- Strittmatter, W. J., Saunders, A. M., Schmechel, D., Pericakvance, M., Enghild, J., Salvesen, G. S. et al. (1993). Apolipoprotein-E - High-Avidity Binding to Beta-Amyloid and Increased Frequency of Type-4 Allele in Late-Onset Familial Alzheimer-Disease. *Proceedings of the National Academy of Sciences of the United States of America*, 90 (5), 1977-1981.
- Strittmatter, W. J., Weisgraber, K. H., Huang, D. Y., Dong, L. M., Salvesen, G. S., Pericak-Vance, M. et al. (1993). Binding of human apolipoprotein E to synthetic amyloid β peptide: Isoform-specific effects and implications for late-onset Alzheimer disease. *Proceedings of the National Academy of Sciences of the United States of America*, 90 (17), 8098-8102.
- Tang, M.-X., Jacobs, D., Stern, Y., Marder, K., Schofield, P., Gurland, B. et al. (1996). Effect of oestrogen during menopause on risk and age at onset of Alzheimer's disease. *The Lancet*, 348 (9025), 429-432.
- Terry, R. D., Masliah, E., Salmon, D. P., Butters, N., Deteresa, R., Hill, R. et al. (1991). Physical basis of cognitive alterations in Alzheimer's-disease - synapse loss is the major correlate of cognitive impairment. *Annals of Neurology*, 30 (4), 572-580.
- Trembath, D., Ervin, J., Broom, L., Szymanski, M., Welsh-Bohmer, K., Pieper, C. et al. (2007). The distribution of cerebrovascular amyloid in Alzheimer's disease varies with ApoE genotype. *Acta Neuropathologica*, 113 (1), 23-31-31.
- Vaccarino, V., Badimon, L., Corti, R., de Wit, C., Dorobantu, M., Hall, A. et al. (2011). Ischaemic heart disease in women: are there sex differences in pathophysiology and risk factors? Position Paper from the Working Group on Coronary Pathophysiology and Microcirculation of the European Society of Cardiology. *Cardiovascular Research*, 90 (1), 9-17.
- Veinbergs, I., Mallory, M., Mante, M., Rockenstein, E., Gilbert, J. R., & Masliah, E. (1999). Differential neurotrophic effects of apolipoprotein E in aged transgenic mice. *Neuroscience Letters*, 265 (3), 218-222.
- Villablanca, A. C., Jayachandran, M., & Banka, C. (2010). Atherosclerosis and sex hormones: current concepts. *Clinical Science*, 119 (11-12), 493-513.
- Wen, P. H., Hof, P. R., Chen, X., Gluck, K., Austin, G., Younkin, S. G. et al. (2004). The presenilin-1 familial Alzheimer disease mutant P117L impairs neurogenesis in the hippocampus of adult mice. *Experimental Neurology*, 188 (2), 224-237.
- Wolozin, B., Kellman, W., Ruosseau, P., Celesia, G. G., & Siegel, G. (2000). Decreased prevalence of Alzheimer disease associated with 3-hydroxy-3-methylglutaryl coenzyme A reductase inhibitors. *Archives of Neurology*, 57 (10), 1439-1443.
- Yaffe, K., Haan, M., Byers, A., Tangen, C., & Kuller, L. (2000). Estrogen use, APOE, and cognitive decline - Evidence of gene-environment interaction. *Neurology*, 54 (10), 1949-1953.
- Yamamoto, K. R. (1985). Steroid receptor regulated transcription of specific genes and gene networks. *Annual Review of Genetics*, 19, 209-252.
- Zhong, N., & Weisgraber, K. H. (2009). Understanding the Association of Apolipoprotein E4 with Alzheimer Disease: Clues from Its Structure. *Journal of Biological Chemistry*, 284 (10), 6027-6031.

Preverbal Infants' Use of Others' Communicative Signals Depends on Culture

Rocio Silva Zunino¹
Supervisor: Ulf Liszkowski¹

¹Max Planck Institute for Psycholinguistics, Nijmegen, The Netherlands

This study explored preverbal infants' understanding of communicative signals across two cultures with different interactional structure. 29 Dutch and 18 Peruvian 10-month-old infants participated in this study in which they were filmed in natural-interaction with caretakers and given two tests (the A-not-B error and Point Comprehension) used to measure communicative understanding in young infants. The results of the natural recording revealed the trend that Peruvian infants are less exposed to communicative cues than are Dutch infants. The results of the A-not-B task show that Peruvian infants made less perseveration errors than Dutch infants. This is in line with a recently proposed account of performance in this task, in which communicative context affects perseveration. The Point Comprehension task shows that both Peruvian and Dutch infants performed similarly, searching for the toy at the pointed to target location. These findings suggest that there are communicative skills that are shared across cultures (e.g. the ability to understand pointing signals) while cognitive bias in acting upon such communicative signals may develop through the social interaction that infants are exposed to in their culture.

Keywords: preverbal cognition, social interaction, cross-cultural

Corresponding author: Rocio Silva Zunino; E-mail: rocio81sz@hotmail.com

1. Introduction

Human communication is achieved not only through the use of linguistic terms, but also involves the use of non-linguistic signals such as pointing and eye-contact. Infants must learn from early on to comprehend and produce these signals during childhood for effective communication in society. A major source from which infants acquire knowledge of communicative signals and develop their communication skills is from infant-caretaker interactions. Interestingly, it is known that such infant-caretaker interactions are structured differently across cultures and that the input that infants receive from caretakers varies (Salomo & Liszkowski, submitted). Cross-cultural studies of natural everyday infant-caretaker interaction done with Mayan, Dutch and Chinese by Salomo and Liszkowski revealed differences across cultural settings in infants' triadic social interaction. Across all cultural settings infants engaged in joint action formats and used the same type of deictic gestures. However, the frequency of joint action and deictic gestures differed. Yucatec Mayan infants spent half as much time in triadic interactions as compared to Dutch infants, who again spent half as much time as Shanghai infants. Furthermore, pre-linguistic gestural communication was best predicted by time spent in joint action. The gestures emerged earlier and were used more depending on the amount of joint action and gestures infants were exposed to. This leads to the hypothesis that also infants' understanding of communicative signals might be influenced by culture and the amount of input exposed to. To address this issue, we conducted a cross-cultural study comparing two cultures in which the interaction is differently structured (Peru/The Netherlands). We recorded 10-month-old-infant-caretaker natural interaction and infants' performance in two tasks that are used to assess infant's understanding of communicative signals (the A-not-B Error and the Point Comprehension).

The A-not-B task (Piaget, 1954) is one of the classic tests of human cognitive development in the first year of life. In this task the experimenter hides a small, attractive toy in the hiding location A. After a delay of about five seconds, infants typically search correctly on the A-trials, recovering the toy. After a number of repeated A hidings and recoveries, there is a shift trial where the infant observes as the experimenter hides the toy in the second location, B. In the B-trials, infants younger than 12 months of age typically show a perseverative response, reaching back to the original A location. At least

three different explanations have been proposed to account for this error. Interestingly, these accounts give different predictions as to the influence of culture, and will therefore be further discussed with respect to this.

According to Piaget, the perseveration error observed is due to the lack of object permanence in young infants. Adults easily know that objects continue to exist even when they cannot longer be seen or touched. Piaget held that this is acquired by infants between the ages of 9 and 12 months and develops through the infants' sensorimotor experience of individual actions on the environment. Infants construct an understanding of the world from the experience of the physical actions they perform on it. The lack of object permanence in younger infants leads to the errors in the A-not-B task. Piaget's account does not predict an influence of culture on the A-not-B task.

Although Piaget's observations of object permanence have been confirmed by a number of studies (Gratch, 1975; Harris, 1987) his interpretations of these observations have been questioned. For example, Baillargeon (1987) suggests that infant's failure in the search task is not because of lack of object permanence but rather due to infant's inability to perform coordinated actions at this age. In her study, she showed that during tasks that do not require coordinated actions, 4½ month-old infants demonstrate that they understand that an object continues to exist when it is occluded. Others have argued that the perseveration in the A-not-B task might be due to a lack of executive functions and the maturation of dorsolateral prefrontal cortex. The A-not-B task is very similar to the classic test for frontal lobe function in nonhuman primates (delay response; DR). In the DR task, the experimenter places food in one of the two containers and covers them with identical items (e.g., cardboard) in full view of the subject, then, blocks the monkey's view for a delay period of about four seconds after which the monkey is allowed to choose a container. Performance of monkeys in the DR task depends on dorsolateral prefrontal cortex. Moreover, performance of macaque monkeys with dorsolateral prefrontal lesions is comparable to that of 7-9-month-old infants in the A-not-B task (Diamond, 1991); both infants and monkeys fail to perform the task correctly. Maturation of prefrontal cortex is considered of biological origin, and as such again culture is expected to have little influence.

Most recently Topal, Gergely, Miklosi, Erdöhegyi and Csibra (2008) have given an alternative explanation of infant's errors in the A-not-B task.

They have explained the error by looking at the role of the communicative demonstration context of the task. The A-not-B task normally involves face-to-face interaction and the experimenter's use of ostensive and referential signals, such as eye-contact, infant directed speech and looking back and forth between the object and the infant. In their study, Topal et al. varied the presence or absence of the social communicative context of the hiding event. Their results revealed that the magnitude of the A-not-B error was considerably smaller in the non-communicative than in the traditional ostensive-communicative context, indicating that depending on the communicative context the number of B-trial errors varied. It is possible that infants who understand and pay more attention to other's communication signals are as a result thereof more susceptible to the A-not-B error. Thus, we would expect that in cultures in which infants are less exposed to communicative input, infants should perform better (i.e. make less perseverations on the B-trials) on the A-not-B task than those infants exposed more to communicative cues.

Another task used to measure infant's understanding of communication is the Point Comprehension task. This task is a hiding-search game in which the experimenter hides a toy in one of two locations, then points to the correct location to see if the infant follows the pointing gesture and retrieves the toy. Between the ages of 3 and 6 months infants begin to follow the gaze direction of others to nearby objects (D'Entremont, Hains, & Muir, 1997). At the age of 12 months they are able to do so to more distal targets (Corkum & Moore, 1995). And they are also able to follow pointing gestures to objects (Carpenter, Nagell, & Tomasello, 1998; Tomasello, Carpenter, & Liszkowski, 2007). Following the direction of the gaze/pointing gesture itself, however, is generally not considered evidence for communicative understanding since this could be learned through association without being aware of the other person's intentions with the gestures (Behne, Liszkowksi, Carpenter, & Tomasello, 2011).

Communicative understanding can, however, be inferred when infants not only have to follow the pointing but also use it, as for example to retrieve a toy at the hidden but pointed to location (Behne, Carpenter, & Tomasello, 2005). This has been shown to occur for infants as young as 14 (Behne et al., 2005) and even 12 (Behne et al., 2011) months. Interestingly it is this latter feature (intention understanding) that is specific to humans, as monkeys are only capable of following direction, without inferring intention (Call & Tomasello, 2005). Importantly, it is at present

unclear how this understanding emerges in young infants; whether infants as young as 10 months are already able to understand communicative signals, and if so, whether it is influenced by socialization. If it emerges under social influence, then there is the possibility of cultural differences. In this case, we may expect that in cultures in which infants are less exposed to social-interactional input infants should have a poorer performance on the Point Comprehension task than infants exposed to more social-interactional input.

An important aspect in which cultures differ is the structure of interactions. For example, whereas children are expected to be mainly independent of the families in some cultures, they are mainly dependent in others (Kagitcibasi, 2005). Such differences can be related to different styles of dyadic face-to-face interactions in the first few months of life (Keller, Otto, Lamm, Yovsi, & Kartner, 2008). Mayan infants, for example, are reported to be socially less engaged as a result of their parents interacting less with them, as they believe that communicative development is maturational, rather than culturally acquired (Gaskins, 1999, 2006; Salomo & Liszkowski, submitted). Although culture has been shown to influence the production of communicative signals, little is known about the influence of culture on infant's understanding of such signals. It is this issue that we aim to address in the current study. Specifically, we aimed to address whether social input and experiences that infants receive from their caretakers shape their understanding of communicative signals. To this end, we conducted a cross-cultural study comparing two cultures in which the interaction is differently structured (Peru/The Netherlands). We took measures of natural infant-caretaker interaction in Peru to compare it to the data of natural interactions in The Netherlands, used in Salomo and Liszkowski's (submitted) study, and we looked at 10-month-old Peruvian and Dutch infants' performance in both the A-not-B Error and the Point Comprehension tasks.

The Peruvian infants were recruited from the surrounding rural areas of the city of Puno located in the southeastern part of Peru and were tested in their own homes. The infants from this region spend great part of the day carried in the back of their mothers by means of a 'manta' or 'awayo' which is a large woven fabric folded in half and tied in a knot at the mother's chest so that the infant can be carried on the mother's back. This means that most of the time during the day the mother does not have direct eye-contact with her infant. The Dutch infants were recruited from the medium-

sized city of Nijmegen in the southeastern part of The Netherlands and were tested at the Baby Research Center in Nijmegen. Dutch infants spend great part of the day in situations that allow face-to-face-interactions with caretakers. At home or in daycares they spend time in floor mats and cradles.

2. Natural observation

2.1 Methods

2.1.1 Participants

Eleven Peruvian infants (7 boys, 4 girls) with a mean age of 9 months and 24 days (range = 7 months, 1 day to 12 months, 23 days) and their families participated in the natural observation recordings. Four additional infants and their families took part in the natural recordings but were not included in our analysis. This was because although they had been asked to continue with their daily activities and ignore the cameras they did not do so but rather sat down and played with the infant in front of the camera. Three additional families chose not to be filmed in the natural recordings although the infants did participate in the two tasks, thus, we have no data for the natural recordings of these three infants but we did use their results in both tasks. The Peruvian infants and their families were contacted through the social program 'El vaso de leche' which consists of bringing support in feeding young infants and providing them with the appropriate nutrition. These were compared to age-matched Dutch infants who participated in Salomo and Liszkowski (submitted) study. These were 8 Dutch infants (3 boys and 5 girls) with a mean age of 9 months and 25 days (range = 8 months, 1 day to 11 months, 19 days) and their families, contacted via the Nijmegen Baby Research Center's data base and were video-taped at home while interacting with their caretakers.

2.1.2 Design and procedure

Peruvian infants were visited at home for 45 minutes of video recording while the Dutch infants in Salomo and Liszkowski (submitted) study were video-taped for 60 minutes. Two cameras were used for the recordings. One was placed on a tripod in a corner of the room to get a wide shot of the infant and the environment. The other camera was hand-used by the experimenter hidden in another corner of the room taking a closer shot of the infant and

caretaker. This camera was also used to follow both the infant and caretaker from a distance whenever they decided to leave the room. Before starting the natural observation sessions, families were asked to continue with their daily activities even if this meant they had to leave the room at any moment. They were also asked to ignore the cameras at all times.

2.1.3 Data coding

Infant-caretaker interactions of 45 minutes were then coded for infant's and caretaker's gestures using ELAN, a software program developed by The Max Planck Institute for Psycholinguistics. Only gestures that infants produced or that caretakers produced for the infants were coded for further analysis. The gestures coded were the following:

Index Point: Arm extended and index finger stretched out towards an object without an attempt to reach or touch it.

Show: Brings an object into focus by holding it up or in front of the other in order to direct the other's attention to the object.

Place: Places an object in front of the other with the intention to direct the other's attention towards the object.

Reach: Extends a hand towards an object, indicating desire for help from the other. Sometimes it is accompanied by the moving of the hands or torso towards the front.

Request: Holds out hands (usually palms up) in order to request an object.

Give: Transfer or attempt to transfer an object from one person to another. If the object is pulled out of another's hand it was not coded as GIVE.

The gestures were coded by a second person for inter-rater-reliability and a Cohen's kappa of 0.89 was obtained. Caretaker's gestures were also coded for whether they were accompanied by ostensive cues. Ostensive cues referring to the use of motherese (infant directed speech), eye gaze, calling the infant's name, tapping on someone, clapping and attention getters such as, "hey look!". For the inter-rater-reliability, a Cohen's kappa of 0.75 was obtained.

2.2 Results

We predicted that there were differences between Peruvian and Dutch interactional structures and amount of input of ostensive communicative cues that infants received as had previously been found across other cultures (Salomo and Liszkowski,

submitted). We tested our predictions with a one-tailed independent samples t-test on the use of gestures with ostensive cues by the caretakers: $t(17) = 1.72$, $p = 0.057$ (see Fig. 1). Our results show the trend that Dutch infants ($M = .68$) receive more input of gestures with ostensive communicative cues than Peruvian infants ($M = .45$).

2.3 Discussion

The results reveal the trend for Dutch infants to receive more input of ostensive communicative cues from caretakers than Peruvian infants but of course these statistics were based on a small group size. These results support the view that there are cultural differences in infant-caretaker interactions and that this difference occurs particularly in the use of ostensive communicative cues. However, further analysis should be done with a larger number of participants. Next we look at infants' performance in the A-not-B task to see whether such differences might also impact on the preverbal understanding of communicative signals.

3. A-not-B task

3.1 Methods

3.1.1 Participants

Participants were 14 Peruvian infants (6 boys, 8 girls) with a mean age of 9 months and 29 days (range = 7 months, 1 day to 12 months, 22 days). Nine of these infants had also participated in the natural recordings. Fourteen Dutch infants (6 boys, 8 girls) with a mean age of 9 months and 22 days (range = 7 months, 11 days to 12 months, 26 days) participated in this study, these were different infants than those that participated in the natural observation. Four additional Peruvian infants and 13 Dutch infants took part in the task but were not included because they did not complete the minimum of four required A-trials (see below for details).

3.1.2 Materials

Two identical brown/black flower pots served as hiding containers (15 cm high, 12 cm diameters at top, 17 cm diameters at bottom), these were placed on a cardboard sheet (80 cm x 20 cm) so that they could easily be slid back and forth towards the infant. The containers were placed 40 cm apart from each other so that they could both be in reach of

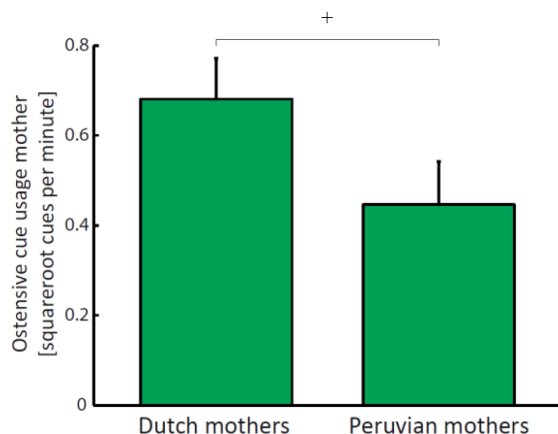


Fig. 1 Square root of gestures with ostensive cues used per minute by Dutch and Peruvian mothers.

the infant. A blue toy (about 6 cm x 9 cm) which made a honking sound and produced a small red light used to get the child's attention, was used as the target object being hidden. Three cameras were used to video tape the tasks, one facing the infant, a second one facing the experimenter (E) and a third one providing a side view.

3.1.3 Design and procedure

After a play period to familiarize the infant with E, the infant was seated on the parent's lap facing the testing table (120 cm x 60 cm) and opposite to E. All infants first participated in a warm-up task to familiarize them with the containers used for hiding. E showed the infant a toy, then placed it in the middle of the table and semi-covered it with a container encouraging the infant to retrieve it. Once the infant retrieved the toy or touched the container, the toy was given to him/her and the experimental trials began. The experimental trials began with E calling the infant's name and establishing eye-contact, then hiding the target toy (blue toy) under container A (container at the left-hand side of E and right-hand side of the infant) while shifting her gaze back and forth between the infant and the container to direct the child's attention to location A (see Fig. 2). The toy was hidden four times at the first location (A-trials) and three times at the other location (B-trials- right hand-side of E and left-hand side of the infants). To be included in the study infants had to have at least four correct searches in the A-trials, if one search error was made the infant received a total of six A-trials. All infants received three B-trials where their name was called, eye-contact was established and the toy was hidden. In the B-trials, the gaze going back and forth from the infant to the hiding location was omitted (step 2; see Fig. 2), following standard procedures (e.g.



Fig. 2 Steps in the A-not-B task.

Topal et al., 2008). For all A and B-trials there was a four second delay between the hiding of the toy and the sliding of the cardboard towards the infant for the search response to be made. In addition to this, in the B-trials a distractor was introduced (noise of a pen being dropped on the floor) in the middle of the four second delay to avoid the infant's fixation on the B-container. When the infants grasped the target container the experimenter gave the toy and slid the cardboard back. The trial ended if no search occurred within approximately 20 seconds, point at which E proceeded to the next trial.

3.1.4 Data coding

Infant's responses in all trials (A and B trials) were examined for initial reach location. Infants' responses were coded as correct, when the infants touched first the container where the toy had been hidden, incorrect, when they touched the opposite container and no choice, when they touched neither of the containers. A second person coded the data for inter-rater-reliability and a Cohen's kappa of 0.92 was obtained. Proportions of correct responses in the A and B trials were then calculated for each infant in both cultures.

3.2 Results

In accordance with previous studies using the A-not-B task, we observed that infants made more errors in B as compared to A trials (see Fig. 3). This was confirmed by a 2×2 (group x trial-type) repeated measures ANOVA with a statistically significant main effect of trial-type: $F(1, 26) = 36.37$, $p < .001$. Importantly, we observed that this difference between A and B trials was significantly

greater for Dutch as compared to Peruvian infants, interaction between trial-type and culture: $F(1, 26) = 5.25$, $p < .05$. In particular, while infants in both cultures performed correctly in approximately 80% of the A-trials (Dutch $M = .89$; Peru: $M = .81$), in the B trials the Peruvian infants ($M = .55$) made more correct responses than the Dutch ($M = .31$). Thus, Dutch infants are more inclined to make a perseveration error than are Peruvian infants.

We also looked at infants' performance in the A-not-B task in relation to their data of natural interaction with caretakers (see Fig. 4). This was done for the nine children that had participated in both the A-not-B task and the natural recordings. We found a negative correlation between the number of gestures that the caretakers used with ostensive cues and the results of Peruvian infants performance in the A-not-B task, $r = -.80$, $p < .05$. The higher the number of gestures that parents used with ostensive cues the lower the proportion of correct responses in the B-trials.

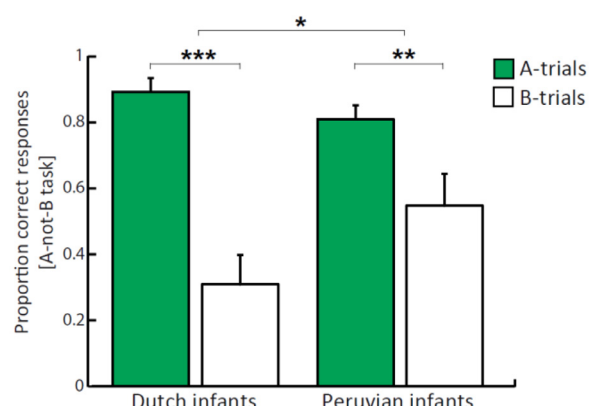


Fig. 3 Proportion correct responses (mean + SE) in A- and B-trials as a function of infants' culture (Dutch, Peruvian). *** $p < 0.001$, ** $p < 0.01$, * $p < 0.05$.

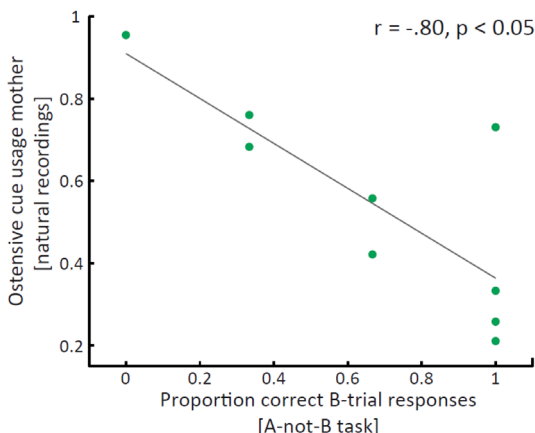


Fig. 4 Correlation between number of gestures with ostensive cues used by mother and proportion of Peruvian infants' correct responses in the B-trials of A-not-B error task.

3.3 Discussion

These results show that Peruvian infants responded differently from Dutch infants in the A-not-B task. In particular we observed that whereas in the A-trials infants from both cultures perform similarly, in the B-trials Dutch infants made more perseveration errors than Peruvian infants. The negative correlation that we find in the Peruvian data reveals that infants' performance in the A-not-B task is influenced by the amount of input of ostensive communicative signals that they receive from caretakers. This shows that not only differences between cultures, but also variations within a culture in the amount of communicative signals infants are exposed to can influence their understanding of such signals.

4. Point comprehension task

4.1 Methods

4.1.1 Participants

Participants were 18 Peruvian infants (10 boys, 8 girls) with a mean age of 9 months and 29 days (range = 7 months, 1 day to 12 months, 23 days) and 29 Dutch infants (16 boys, 13 girls) with a mean age of 9 months and 21 days (range = 7 months, 11 days to 12 months, 26 days). One additional Dutch infant took part in the Point Comprehension task but was not included in the study because he became too tired during the warm-up trials to continue with the task. Some of the Peruvian infants had also participated in the A-not-B task and natural recordings. Some of the Dutch infants had participated in the A-not-B task but none in the natural recordings.

4.1.2 Materials

Two flat boxes (12 cm x 15 cm) were used as hiding locations. These were placed on a cardboard (80 cm x 20 cm) forming an apparatus that could easily be slid back and forth towards the infant. The flat boxes were covered with same color paired cloths in each trial and were enclosed on three sides meaning that when they were covered on the top by the cloths, the experimenter (E) could easily slide her hands with a toy through the open side of the box. The objects used were very small toys that could easily be hidden in E's hands (about 4-5 cm) without being seen by the infant.

4.1.3 Design and procedure

The infants sat on the parent's lap facing the testing table and opposite to E. All infants first participated in three warm-up trials to familiarize them with the set-up of the task. In warm-up 1, E took a small toy from underneath the table called the infant's attention to it and placed it on the table in front of the infant encouraging him to take it. In warm-up 2, E placed a small toy in one of the boxes of the apparatus (counterbalanced across infants) and slid the apparatus towards the infant encouraging him to grab the toy. In warm-up 3, E covered the boxes with a pair of cloth, took a toy from underneath the table, played with it, called the infant's attention to it and then placed it in one of the boxes under the cloth (counterbalanced across infants). E then slid the apparatus over to the infant encouraging him to take it. In the warm-up trials, E visibly hid the toys, so that the infants could see the toy's hiding location.

After the 3 warm-up trials the 8 test trials began. The hiding boxes were covered with a pair of same color cloth. E took a toy from under the table, played with it and called the infant's attention to it. Then, the following 4 steps (see Fig. 5) took place:

1. E held the toy up high with both hands.
2. Quickly transferred it into one hand.
3. Placed each hand in the hiding boxes and deposited the toy in one of the boxes.
4. Took hands out of the boxes and placed them palms/up showing the infant that she no longer had the toy.

These steps were done in 4 seconds in order to maintain the infants' attention on the task and memory of the object. E then called the infant's



Fig. 5 Steps in the Point Comprehension task.

name, established eye-contact and pointed to the box where the toy was hidden (step 5; see Fig. 5) with the hand at the opposite side while pushing the apparatus towards the infant with the other hand and her gaze going back and forth from the infant to the hidden location. If the infant had not searched for the toy within approximately 20 seconds then E removed the cloths making the toy visible. Throughout the 8 testing trials infants always had a chance to play with the toy regardless of whether their search was correct or not. This was done so that unsuccessful infants would not lose interest in the task.

The hiding locations were counterbalanced across trials and infants. Approximately half of the infants received the same hiding location in the last warm-up trial and first test trial, while the other half received it on the other side. Infants either received a sequence of ABABABAB or ABBABAAB where toys were not hidden in the same location more than twice in a row. In each trial different toys, colors and materials of cloth were used to minimize perseveration errors.

4.1.4 Data coding and analysis

Infant's responses in all trials were coded for initial search location. Responses were coded as correct when the infant's search was in the location where the toy was hidden, this meant that the infant

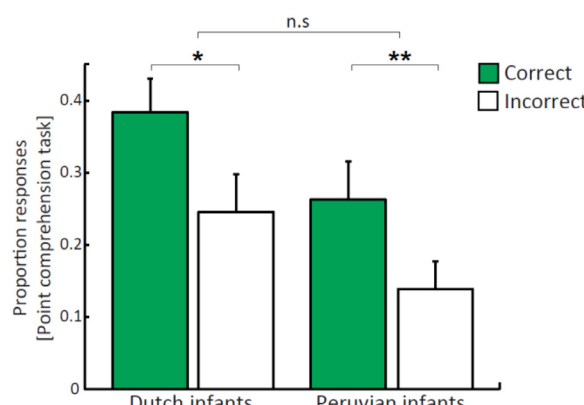


Fig. 6 Proportion of correct and incorrect responses (Mean + SE) as a function of infants' culture (Dutch, Peruvian). ** $p < .01$, * $p < .05$.

had to remove the cloth covering the toy and search for the toy in the hidden location. The response was coded as incorrect if the infant searched in the opposite location to where the toy had been hidden. And no search was coded when the infant did not search at all, or did not remove the cloth in neither side of the apparatus. The inter-rater-reliability obtained was a Cohen's kappa of 0.84. Proportions of correct responses in the task were then calculated for each infant in both cultures.

We also coded for infant's tendency to perseverate in the Point Comprehension task. Here we coded for whether the infant searched in the same location as in the previous trial or in the opposite location. If they had not searched in the previous trial then the trial before that one was taken as the reference point. For the first trial, the last warm-up trial was considered the reference point to same or different location of search.

4.2 Results

We observed that infants in both cultures searched the target location ($M = .34$) (location to which E pointed) more often than the distractor ($M = .20$) (see Fig. 6). This was confirmed by a statistically significant main effect of location of search: $F(1, 44) = 16.83$, $p < .001$.

Importantly, we also observed perseveration in the task. This was confirmed by a statistically significant main effect of perseveration: $F(1, 44) = 19.04$, $p < .001$, indicating that infants search more often at the same location than in the previous trial ($M = .52$) as opposed to searching in the opposite location ($M = .29$) (see Fig. 7). There was no interaction between the location of search and perseveration and also there were no significant interactions with culture.

4.3 Discussion

The results show that infants in both cultures performed similarly in the Point Comprehension task. Infants searched more often in the pointed-to target location (where the toy was hidden) than in

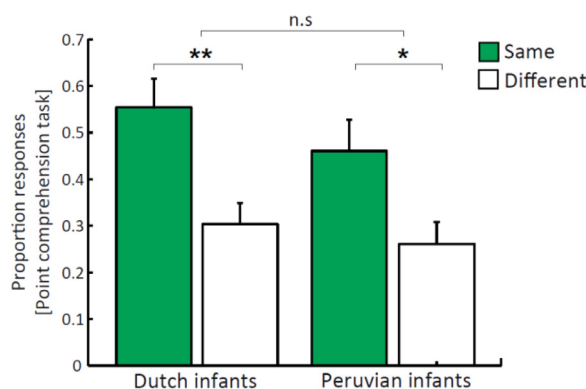


Fig. 7 Proportion same and different responses (Mean + SE) as a function of infant's culture (Dutch, Peruvian). ** $p < .01$, * $p < .05$.

the distractor location (where no toy was hidden). Both groups performed above chance indicating that they understood the task and were able to use the adult's gestures to guide their search for the hidden toy. Previous studies (Behne et al., 2011) have shown that infants as young as 12-month old can perform the Point Comprehension task correctly. Our study was performed with even younger infants and reveals that already at 10 months infants can perform this task.

5. General discussion

We set out to investigate whether culture influences preverbal infants' understanding of communicative signals. The results of our study support the claim that infants' understanding of pre-linguistic communication is influenced by culture. In particular, we observed differences between Dutch and Peruvian infants' responses in the A-not-B task. These differences are potentially due to cultural differences in infant-caretaker interaction, as confirmed by our analyses of natural recordings. In fact we observed that the amount of communicative cues in the infants' environment were predictive of performance in the A-not-B task. At the same time, we did not observe differences in infants' performance in the Point Comprehension task, suggesting that infants in both cultures similarly understand the pointing gesture. Together, these results show that both Peruvian and Dutch infants are able to understand communicative signals (e.g. pointing), while at the same time cognitive biases reflect cultural differences with respect to such signals. In what follows, we first discuss the results of the A-not-B experiment. Thereafter we discuss the results of the Point Comprehension experiment.

Peruvian infants responded differently from

Dutch infants in the A-not-B task. In particular we observed that whereas in the A-trials infants from both cultures perform similarly, in the B-trials Dutch infants made more perseveration errors than Peruvian infants. It is important to point out that the results obtained from the Dutch infants are very similar to results obtained in numerous previous studies using the A-not-B task (Butterworth, 1975, 1976; Bremmer & Bryant, 1977; Bremmer, 1978; Smith, Thelen, Titzler, & McLin, 1999; Diedrich, 2001; Clearfield, Diedrich, Smith, & Thelen, 2006; Lew, 2007; Topal et al., 2008). Strikingly, these previous studies were all conducted in Western countries. Using the same experimental set-up, applied by the same experimenter to age-matched infants in a rural south-eastern area of Peru, we observed that infants' responses in the A-not-B task were different.

Why would there be a reduction in the B-trial error in a different culture? One theory that accounts for the A-not-B error is Piaget's theory of object permanence which claims that infants younger than 12 months of age make the error due to lack of object permanence. For Piaget, sensory-motor experience is needed in infants in order to perform this task correctly and there is no indication that this is different across cultures. If any difference were to be found we might expect the Dutch infants to perform better since, as seen in the videos, they have a bigger number and variety of toys to play with at home and they might be less constrained than Peruvian babies because of the 'manta', which is the cloth used to carry infants in their mother's back. Since in our experiment infants in both cultures were age-matched and on average 10 months old, Piaget's theory of object permanence as a universal stage of development cannot account for the differences we observe.

Another account for the A-not-B error is that of Diamond (1985, 1991) on maturation of prefrontal cortex which considers the error to be caused by an underdeveloped prefrontal cortex. If, however, the error was due to such biological reasons alone, no difference of culture would be expected. Of course we cannot rule out the possibility that prefrontal maturation itself can be dependent on cultural difference in, for example, nutrition. If any, one may expect the Dutch to have optimally balanced nutrition and thus better performance (i.e. more matured prefrontal cortex leading to less B-trial errors). However, we observed the opposite pattern: Peruvian infants performed better. Also, we did not observe maturation (i.e. age) dependency of our results in either culture.

Following Topal et al. (2008), errors in the A-not-B task are induced through ostensive-referential communication. B-trial perseverations are due to the fact that infants rely on the communicative cues given by the experimenter in the A-trials and therefore continue to search at the old (i.e. A) location in the B-trials. In line with this notion, one would expect that infants who rely less on ostensive-referential communication perform better on B-trials. This is confirmed by our results and is strengthened by our observed negative correlation between the amount of ostensive cues infants are exposed to and the amount of correct responses in the B-trials. In fact, this shows that not only differences in social-interaction between cultures, but also within cultures can influence the understanding of communicative signals.

One possibility is that communicative biases develop in infancy and depend on the social input infants receive (Csibra & Gergely, 2009). For the Dutch infants the theory would hold that they expect to learn something generalizable in ostensive-referential contexts rather than just become informed about a particular episodic fact obtained in the 'here-and-now'. In this way infants are biased to interpret ostensive-referential communication as conveying information that is kind-relevant and generalizable and therefore make errors in the A-not-B task. The Peruvian infants, on the contrary, have less exposure to ostensive contexts in which referential expectation can develop. The results of the performance of Peruvian infants in this task raise the question whether these infants are not sensitive to ostensive-referential communication or whether they do not make generic conclusions during the A-not-B task. We elaborate on the latter possibility below where we discuss infant's performance in the Point Comprehension task.

As opposed to the differences found in the A-not-B task, infants in both cultures performed similarly in the Point Comprehension task. Infants searched more often in the pointed-to target location (where the toy was hidden) than in the distractor location (where no toy was hidden). Both groups performed above chance indicating that they understood the task and were able to use the adult's gestures to guide their search for the hidden toy. Previous studies (Behne et al., 2011) have shown that infants as young as 12-month old can perform the Point Comprehension task correctly. Our study was performed with even younger infants and reveals that already at 10 months infants can perform this task. Furthermore, not only did infants at this age gaze-follow the experimenter's pointing gesture to

the location of the hidden object, they also manually reached for the cloth covering the toy and searched for the toy at this location. However, although we did not observe any differences between cultures, we cannot conclude that there are no such differences in development. In particular, it will be interesting to investigate whether interactional experience influences the developmental trajectory of gesture understanding.

Contrary to results of the A-not-B task, we did not observe a correlation between natural recording data and the results of the Point Comprehension task. Together with the fact that infants performed differently in the A-not-B task but similarly in the Point Comprehension task supports the view that infants in both cultures comprehend communicative cues at this early age (which does not depend on culture, nor on variations of input within a culture). However, we can see that they make use of communicative signals in a different manner (which does depend on culture and variations of input within a culture). While Dutch infants generalize the information provided to them, the Peruvian infants do not make generalizations.

In sum, our data shows that the understanding of pre-linguistic communication signals, and as such thus preverbal cognition, can be influenced by culture. Our observations from different tasks support the idea that there are communicative skills that are shared across cultures (e.g. the ability to understand pointing signals) while cognitive biases in acting upon such communicative signals might develop through the social interaction that infants are exposed to in their culture. Already at the pre-linguistic stage it can be seen that cognitive development can be influenced by social factors. Our results thus stress the need to take socio-cultural factors into account when considering infants' communicative abilities.

References

- Baillargeon, R. (1987). Object permanence in 3 ½ and 4 ½ month old infants. *Developmental Psychology, 23*, 655-664.
- Behne, T., Carpenter, M., & Tomasello, M. (2005). One-year-olds comprehend the communicative intentions behind gestures in a hiding game. *Developmental Science, 8* (6), 492-499.
- Behne, T., Liszkowski, U., Carpenter, M., & Tomasello, M. (2011). Twelve-month-olds' comprehension and production of pointing. *British Journal of Developmental Psychology*. Advanced online publication.
- Bremner, J. G., & Bryant, P. E. (1977). Place versus response as the basic of spatial errors made by young

- infants. *Journal of Experimental Child Psychology*, 23, 162-171.
- Bremner, J. G. (1978). Spatial errors made by infants: Inadequate spatial cues or evidence of egocentrism? *British Journal of Psychology*, 69 (1), 77-84.
- Butterworth, G. (1975). Object identity in infancy: The interaction of spatial location codes in determining search errors. *Child Development*, 46, 866-870.
- Butterworth, G. (1976). Asymmetrical search errors in infancy. *Child Development*, 47 (3), 864-867.
- Call, J., & Tomasello, M. (2005). What chimpanzees know about seeing revisited: An explanation of the third kind. In N. Eilan, C. Hoerl, T. McCormack & J. Roessler (Eds.). *Joint Attention: Communication and other minds* (pp. 45-64). Oxford: Oxford University Press.
- Carpenter, M., Nagell, K., & Tomasello, M. (1998). Social cognition, joint attention, and communicative competence from 9 to 15 months of age. *Monographs of the Society for Research in Child Development*, 63 (4), serial no. 255.
- Clearfield, M. W., Diedrich, F. J., Smith, L. B., & Thelen, E. (2006). Young infants reach correctly in A-not-B tasks: On the development of stability and perseveration. *Infant Behavior & Development*, 29, 435-444.
- Corkum, V., & Moore, C. (1995). Development of joint visual attention in infants. In C. Moore & P. J. Dunham (Eds.), *Joint attention: Its origins and role in development* (pp. 61-83). Hillsdale, NJ: Erlbaum.
- Csibra, G., & Gergely, G. (2009). Natural Pedagogy. *Trends in Cognitive Science*, 13 (4), 148-153.
- D'Entremont, B., Hains, S. M. J., & Muir, D.W. (1997). A demonstration of gaze following in 3- to 6-month-olds. *Infant Behavior and Development*, 20 (4), 569-572.
- Diamond, A. (1985). Development of the ability to use recall to guide action, as indicated by infants' performance on AB. *Child Development*, 56 (4), 868-883.
- Diamond, A. (1991). Frontal lobe involvement in cognitive changes during the first year of life. In K.R. Gibson & A.C. Petersen (Eds.), *Brain maturation and cognitive development: Comparative and cross-cultural perspectives* (pp. 127- 180). NY: Aldine de Gruyter.
- Diedrich, F. J., Highlands, T. M., Spahr, K. A., Thelen, E., & Smith, L. B. (2001) The role of target distinctiveness in Infant perseverative reaching. *Journal of Experimental Child Psychology*, 78, 263-290.
- ELAN program, <http://www.lat-mpi.eu/tools/elan/>
- Max Planck Institute for Psycholinguistics, Nijmegen, The Netherlands. Brugman, H., Russel, A. (2004). Annotating Multimedia/Multi-modal resources with ELAN. In: Proceedings of LREC 2004, Fourth International Conference on Language Resources and Evaluation.
- Gaskins, S. (1999). Children's daily lives in a Mayan village: A case study of culturally constructed roles and activities. In A. Göncü (Ed.), *Children's engagement in the world*. Cambridge University Press.
- Gaskins, S. (2006). Cultural perspectives on infant-caregiver interaction. In N.J. Enfield & S.C. Levinson (Eds.), *Roots of Human Sociability*. Oxford: Berg.
- Gratch, G. (1975). Recent studies based on Piaget's view of object concept development. In L. B. Cohen & P. Salapatek (Eds.), *Infant perception: From sensation to cognition*. New York: Academic Press, 1975.
- Harris, P. L. (1987). The Development of Search. In P. Salapatek & L.B. Cohen (Eds.) *Handbook of Infant Perception*. Vol. 2. New York NY, Academic Press.
- Kagitcibasi, C. (2005). Autonomy and relatedness in cultural context. *Journal of Cross-Cultural Psychology*, 36 (4), 403-422.
- Keller, H. Otto, H., Lamm, B., Yovsi, R. D., & Kartner, J. (2008). The timing of verbal/vocal communications between mothers and their infants: A longitudinal cross-cultural comparison. *Infant Behavior & Development*, 31, 217-226.
- Lew, A. R. (2007). Postural change effects on infants' AB task performance: Visual, postural or spatial? *Journal of Experimental Child Psychology*, 97, 1-13.
- Piaget, J. (1954). The construction of reality in the child. New York: Basic Books.
- Salomo, D. & Liszkowski, U. (2011) Natural observations of joint action and deictic gestures in infancy: a cross-cultural study. *Manuscript submitted for publication*.
- Smith, L.B., Thelen, E., Titzer, R., McLin, D. (1999). Knowing in the context of acting: the task dynamics of the A-not-B error. *Psychological Review*, 106 (2), 235-260.
- Tomasello, M., Carpenter, M., & Liszkowski, U. (2007). A new look at infant pointing. *Child Development*, 78, 705-722.
- Topal, J., Gergely, G., Miklosi, A., Erdöhegyi, A., & Csibra, G. (2008). Infant perseverative errors are induced by pragmatic misinterpretation. *Science*, 321, 1831-1834.

Abstracts

Proceedings of the Master's Programme of Cognitive Neuroscience is committed to publishing all submitted theses. Given the number of submissions we select certain articles under the recommendation of the editors for our printed edition. To interested readers, we have provided the abstracts of all other articles of which the full versions are available on our website: www.ru.nl/master/cns/journal.

Do Neuronal Oscillations Reflect Semantic Coherence in Short Discourses?

Christian Hoffmann, Marcel C. M. Bastiaansen, Herbert Schriefers

There is growing consensus that modulation of event-related oscillatory activity in the EEG or MEG provides an index of the coupling and uncoupling of brain areas into functional networks subserving cognition. According to the MUC (Memory-Unification-Control) model of language comprehension, lexical semantic and syntactic information are continuously retrieved and immediately integrated into a coherent representation of an utterance. Previous research indicated that the functional distinction between syntactic and semantic unification is reflected in oscillatory activity as well: syntactic unification co-occurs with beta power modulation, whereas gamma power levels are sensitive to semantic unification processes.

However, unification studies so far relied on paradigms using isolated sentences. We predict that semantic information is unified across sentence boundaries, whereas syntactic information is only unified within sentence boundaries. This study explores whether a modulation of semantic coherence across multiple sentences is reflected by modulations of gamma and/or beta power. We compare oscillatory responses to the visual presentation of short discourses across three conditions: sentences forming coherent stories, random sentences and syntactic prose sentences.

Our results indicate that the beta band (16-20 Hz) is reliably modulated across those conditions, with beta power values being highest for coherent stories and lowest for syntactic prose. Gamma power (45-55 Hz, 70-75 Hz and 90-100 Hz) only differed significantly between random sentences and syntactic prose. Our results stand in contrast to previous findings, while showing at the same time that unification operations work across sentence boundaries. Our data suggest that beta-power a) either does not solely index syntactic unification or b) that syntactic unification is very much influenced by semantic context. The role of gamma power in unification within the discourse context remains somewhat unclear. We suggest that hypotheses about a functional distinction between beta- and gamma-power, as suggested by previous research, have to be revisited.

Event-Related Potentials (ERP) and Pain Rating in Response to Noxious Stimuli Induced Before and After High Frequency Stimulation

Fedde Sappelli, Emanuel N. van den Broeke, Clementina M. van Rijn, Oliver H.G. Wilder-Smith

Long Term Potentiation is an important mechanism for chronic pain. High frequency stimulation is inducing LTP of the nociceptive system in the spinal cord and higher cortical structures. In this study HFS is applied to the skin of humans, and it is tested whether this causes LTP-like sensitization in heterotopic areas of stimulation. This is tested using blocks of double pulses and stimulation with a von Frey filament. These test-stimuli are measured with ERP (N1 and P300) and Visual Analogue Scales. We were not able to find LTP-like sensitization. This effect could indicate that HFS to the skin is not capable of inducing heterotopic LTP of which correlates can be measured with EEG or behavioural assessment. Alternatively, the design specification were possibly not optimal. In the experiment we were able to find Long Term Habituation in N1 and P300 peaks, but not in behavioural scales. Also some non-LTP-like sensitization effects were observed in ERP but not in VAS. Finally there were intergroup differences before HFS.

The Effect of Semantic Context on Embodied Language Representations

Margriet van Dijk, Wessel van Dam, Shirley-Ann Rueschemeyer, Harold Bekkering

The embodied view implies that language comprehension depends on perceptual and motor representations, and that lexical-semantic representations rely on information acquired from interaction with the world. Evidence for this comes from both behavioral and neuroimaging studies. However, the results from several studies indicate that the activation of information in sensory-motor brain areas is not a purely automatic process, but instead is a rather flexible process (Raposo et al., 2009; Rueschemeyer et al., 2007). A crucial factor for observing activity in motor and premotor regions during action word processing seems to be that the context in which the word is presented, supports a motor interpretation and that the word form as a whole, conveys a motor meaning. In these studies, flexibility is characterized by the relative presence or absence of activation in motor and perceptual brain areas. These studies show that the context in which a word is presented, can allow for or undermine a motor interpretation. In addition to this, also the degree to which motor or sensory regions contribute to a representation, could be determined by the context in which conceptual features are retrieved. In the present study, we investigated precisely this issue by presenting word stimuli for which either motor properties (e.g., doorbell), visual properties (e.g., pyramid) or both motor and visual properties (e.g., tennis ball) were important in constituting the concept. Conform with the idea that language representations are flexible and context dependent, we demonstrated that for words associated with both action and color, the degree to which a motor-related region contributes to a representation considerably changes as a function of context. This is one of the first neuroimaging studies to show that embodied lexical-semantic representations are flexible and context-dependent.

Institutes associated with the Master's Programme in Cognitive Neuroscience



Donders Institute for Brain, Cognition
and Behaviour:

Centre for Cognitive Neuroimaging
Kapittelweg 29
6525 EN Nijmegen

P.O. Box 9101
6500 HB Nijmegen
www.ru.nl/neuroimaging/

Donders Institute for Brain, Cognition
and Behaviour:
Centre for Neuroscience
Geert Grooteplein Noord 21, hp 126
6525 EZ Nijmegen

P.O. Box 9101
6500 HE Nijmegen
www.ru.nl/neuroscience

Donders Institute for Brain, Cognition
and Behaviour:
Centre for Cognition
Montessorilaan 3
6525 HR Nijmegen

P.O. Box 9104
6500 HB Nijmegen
www.ru.nl/cognition/



MAX-PLANCK-GESELLSCHAFT

Max Planck Institute for Psycholinguistics
Wundtlaan 1
6525 XD Nijmegen

P.O. Box 310
6500 AH Nijmegen
<http://www.mpi.nl>



Universitair Medisch Centrum St Radboud
Geert Grooteplein-Zuid 10
6525 GA Nijmegen

P.O. Box 9101
6500 HB Nijmegen
<http://www.umcn.nl/>

Nijmegen Centre for Molecular Life Sciences
Geert Grooteplein 28
6525 GA Nijmegen

P.O. Box 9101
6500 HB Nijmegen
<http://www.ncmls.nl>

Baby Research Center
Montessorilaan 10
6525 HD Nijmegen

P.O. Box 9101
6500 HB Nijmegen
<http://babystudycenter.nl>

